



Green nanotechnology-An innovative pathway towards biocompatible and medically relevant gold nanoparticles

Velaphi Thipe, Alice Karikachery, Pinar Çakilkaya, Umer Farooq, Hussein Genedy, Norraseth Kaeokhamloed, Dieu-Hien Phan, Refaya Rezwan, Gözde Tezcan, Emilie Roger, et al.

► To cite this version:

Velaphi Thipe, Alice Karikachery, Pinar Çakilkaya, Umer Farooq, Hussein Genedy, et al.. Green nanotechnology-An innovative pathway towards biocompatible and medically relevant gold nanoparticles. Journal of Drug Delivery Science and Technology, 2022, 70, 10.1016/j.jddst.2022.103256 . hal-03615301

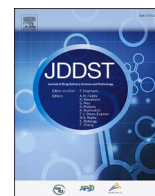
HAL Id: hal-03615301

<https://hal.science/hal-03615301>

Submitted on 21 Mar 2022

HAL is a multi-disciplinary open access archive for the deposit and dissemination of scientific research documents, whether they are published or not. The documents may come from teaching and research institutions in France or abroad, or from public or private research centers.

L'archive ouverte pluridisciplinaire **HAL**, est destinée au dépôt et à la diffusion de documents scientifiques de niveau recherche, publiés ou non, émanant des établissements d'enseignement et de recherche français ou étrangers, des laboratoires publics ou privés.



Green nanotechnology—An innovative pathway towards biocompatible and medically relevant gold nanoparticles

Velaphi C. Thipe^a, Alice Raphael Karikachery^a, Pınar Çakılkeya^b, Umer Farooq^b, Hussein H. Genedy^b, Norraseth Kaeokhamloed^b, Dieu-Hien Phan^b, Refaya Rezwan^b, Gözde Tezcan^b, Emilie Roger^{b,c}, Kattesh V. Katti^{a,*}

^a Institute of Green Nanotechnology, Department of Radiology, School of Medicine, University of Missouri, Columbia, 65212, USA

^b EMJMD NANOMED, Pharmacy School, Faculty of Health, UNIV Angers, France

^c Micro et Nanomédecines Translationnelles, MINT, UNIV Angers, UMR INSERM 1066, UMR CNRS 6021, Angers, France

ARTICLE INFO

Keywords:

Diagnostics
Imaging
Nanomedicine
Phytochemicals
Therapy
Theranostics
Green nanotechnology

ABSTRACT

In this review, we focus on recent advances in green nanotechnology, providing details on reliable synthetic pathways towards biocompatible and medically relevant gold and radioactive gold nanoparticles. We cover a wide plethora of synthetic protocols that utilize green nanotechnology with in-depth understanding of what makes a green process green. In section 2, we provide full details on the intervention of green nanotechnology for the production of various functionalized gold nanoparticles (AuNPs). Section 3 focuses on various characterization tools to be used for the complete physicochemical, size and *in vitro* characterization of gold nanoparticles before translating them into potential *in vivo* applications. Section 4 focuses on the science and applications of gold nanoparticles in diagnostic imaging. Specifically, we have highlighted the importance of the chemistry and physics of gold nanoparticles for applications in a myriad of diagnostic imaging including X-ray contrast agents, in single photon emission computed tomography (SPECT) imaging, positron-emission tomography (PET) imaging, optical coherence tomography (OCT), fluorescence imaging, magnetic resonance imaging (MRI), in surface enhanced Raman spectroscopy (SERS), and in ultrasound (US) imaging. Section 5 discusses latest advances on gold nanoparticles in drug delivery, gold nanoparticles in photothermal therapy and radioactive gold nanoparticles in cancer therapy. In particular, we discuss green nanotechnological interventions on how the electron rich phytochemicals including epigallocatechin gallate (EGCG) from tea, mangiferin (MGF) from mango and allied phytochemicals can be utilized in their dual roles, as reducing agents as well as rendering tumor specificity due to their strong tumor cell receptor avidity—to produce tumor specific molecular imaging and therapy agents. We also discuss latest advances on the importance of gold nanoparticles in X-ray Therapy. Important aspects relating to systemic toxicity of gold nanoparticles and ways to mitigate toxicity issues for their effective implementation in biomedical sciences are also discussed in section 6. The topics covered are intended to answer questions including why we should use green processes and what is the role of nanomedicine in the domain of human health and hygiene. Most importantly, we provide critical analysis on the ubiquitous role of gold nanoparticles in nanomedicine.

1. Introduction

One may ask “What is so appealing about green processes?” The answer lies in our surroundings. With the changes brought about by the industrial revolution of the 1760s came a plethora of environmental issues [1]. We are currently at the gateway to a ‘nanorevolution’—bound to define all endeavors of life on our planet. Nanoparticles are

microscopic molecular assemblies, with at least one dimension of size from 1 to 100 nm, that can bring about great advances to many sectors of modern civilization, including: medicine, transport, electronics and telecommunications [2,3]. However, nanomaterials are also poised to bring about measurable changes to our environment as a result of their long-term applications, exposure, and environmental accumulation in the air and water. This puts us at crossroads between choosing various

* Corresponding author.

E-mail address: KattiK@health.missouri.edu (K.V. Katti).

<https://doi.org/10.1016/j.jddst.2022.103256>

Received 29 September 2021; Received in revised form 24 February 2022; Accepted 8 March 2022

Available online 11 March 2022

1773-2247/© 2022 The Authors. Published by Elsevier B.V. This is an open access article under the CC BY-NC-ND license (<http://creativecommons.org/licenses/by-nc-nd/4.0/>).

nanoparticles/nanomaterials embedded products for a safe, sustainable future and one filled with environmental pollution that various different types of nanomaterials might cause in the near and long term. In this context, green processes with capabilities to minimize or eliminate negative carbon footprints on our environment become highly imperative in the production and utility of nanoparticles embedded materials for use in a myriad of sectors.

Green processes including green chemistry and green nanotechnology, utilize nontoxic precursors and environmentally-benign solvents throughout the synthetic scheme. Such processes aim at complete elimination of toxic substances in reaction media as well as aim to eliminate toxic byproducts that destroy our environment [4]. Green nanotechnology aims to eliminate all toxic substances in the entire manufacturing processes [5–12]. A remarkable feature of green nanotechnology is the utilization of phytochemicals derived from plants to serve as reducing and stabilizing agents for the transformation of metal ions into metallic nanoparticles [13]. There are 12 well-accepted principles that govern green chemistry which provide a framework for designing or improving materials, processes, products and systems: (i) prevention of toxic waste, (ii) atom economy of the synthetic route to maximize the final product, (iii) no hazardous chemicals within the synthetic routes, (iv) designing biocompatible and safe materials, (v) application of environmentally-benign solvents such as water, (vi) application of minimum energy to achieve high yields with minimized environmental and economic impacts, (vii) use of renewable raw materials or feedstock for sustainability, (viii) reduce derivatives to limit additional steps, (ix) application of catalyst as opposed to less efficient stoichiometric reactions (x) design resulting into innocuous degradation products, (xi) life cycle analysis toward reduction and prevention of environmental pollution, and (xii) increased effectiveness in the production, storage and transportation processes [14].

Nanotechnology is still in its infancy but continues to grow rapidly with implications in energy, electronics, food, medicine, and allied sectors. Globally, the market for nanodevices and nanomachines is forecast to increase from \$736.1 million in 2018 to \$2.7 billion in 2028 [15]. The global market for nanocomposites is poised to rise to \$7.3 billion by the year 2022, increasing at a Compound Annual Growth Rate (CAGR) of 29.5% for the 2017–2022 period [16]. Consequently, it is imperative that we develop nanotechnology in a sustainable and eco-friendly manner to support this growth while addressing the current and future impacts of the nano-revolution on our environment. The concept of ‘Green Nanotechnology’ embraces this idea of environmentally-benign and sustainable technology [6,10,12,17,18].

Green nanotechnology can assist in wastewater treatment, site remediation [19], reduction of waste and byproducts [20] and air purification [21]. It is important to recognize that a vast majority of synthetic processes for the manufacture of nanoparticles often utilize toxic and environmentally-harsh chemicals. Various toxic chemical reducing agents including hydrazine, sodium citrate, and sodium borohydride are used in the production of metallic nanoparticles [22–24]. Several harsh physical processes, including pyrolysis and attrition, employed for the production of a myriad of nanomaterials also create a negative environmental impact both in the short and long term [25]. It is therefore imperative to develop nanoparticles production processes that utilize minimal/no toxic chemicals and develop engineering tools to minimize/eliminate toxic undetectable nanoparticulate pollutants in the overall production scheme.

Katti's group has pioneered a new paradigm in green nanotechnology towards the development of zero carbon emission and zero pollution nanotechnologies. According to Katti's definition, a green nanotechnology approach encompasses the use of plant-based phytochemicals as electron rich chemical reducing agents for the conversion of metal precursors into a myriad of functionalized nanoparticles [26, 27]. Green nanotechnology processes, generally, do not employ any toxic human-made chemical-based reducing agents for the manufacturing of nanoparticles. This approach has significant

superiority compared to other non-chemical based approaches including the application of bacteria, fungi [28], and algae [29] for the production of nanoparticles. Pioneering work by Katti et al. demonstrated that phytochemicals from soy, tea, cumin, cinnamon, grapes and mango can be used to produce well-defined tumor specific gold nanoparticles through 100% nontoxic methods [6–11,17,30–40]. Green nanotechnology processes combine all the advantages of traditional green synthetic processes and often enjoy additional benefits of being fast, low cost as they utilize byproducts from the agricultural produce and ensure environmentally friendly features as well [41–52].

Nanotechnology is bringing about a profound effect across several scientific, technological, and medical sectors. There is global recognition that nanotechnology is already bringing about a paradigm shift in the way diseases are diagnosed and treated. For example, in recent years, metal nanoparticles have gained immense importance in the field of drug discovery due to their surface, charge and size-dependent properties. Nanoparticles-based drugs (both metallic and non-metallic) are being used as drug candidates for designing disease targeting, highly selective, and sustained drug delivery systems [43–52]. Among all the metallic nanoparticles explored so far, gold nanoparticles are the most promising for pharmaceutical and biomedical applications for the following reasons: (i) surface atoms of gold nanoparticles allow incorporation of various targeting moieties (such as peptides, proteins or other biomolecules) as well as drug molecules, (ii) the sizes of gold nanoparticles can be engineered to allow efficient penetration across specific types of cells including cancer cells allowing interrogation, diagnosis and treatment of diseases at cellular levels, (iii) functionalized gold nanoparticles are non-immunogenic and are often non-toxic, and (iv) the photophysical, magnetic and radioactive properties of gold nanoparticles allow for the development of a plethora of diagnostic, therapeutic and theranostic agents for treating various diseases [9,38, 53–55].

Gold, within the realms of nanotechnology, is unique. It is the only element in the periodic table that is inert to oxidation even at the nanoparticulate level [38]. Its characteristic surface plasmon resonance (SPR) produces strong electromagnetic fields on the surface of the particles and enhances light absorption and scattering causing a strong red color [56–58]. Availability of surface atoms for rapid reactions with target specific molecules such as tumor/disease specific proteins, peptides and biomolecules—individually and collectively, make nanoparticles of gold ubiquitous in nanomedicine for molecular imaging and therapy applications [24,32,59–62].

Blood vessel endothelial lining in the tumor tissues range from 100 nm to 2 μ m in size and is significantly larger than normal capillaries; this allows carefully designed gold nanoparticles, in the size range 15–30 nm, to penetrate across capillaries into the tumor tissues [63]. Therefore, a host of chemotherapeutic agents loaded onto gold nanoparticles can be targeted for active or passive internalization into tumor cells to achieve optimum diagnostic and therapeutic payloads [64].

Early efforts on the application of green nanotechnology to nanomedicine have come from the creation of tumor specific gold nanoparticles through encapsulation of tea and cinnamon phytochemicals onto gold nanoparticles (T-AuNPs and Cin-AuNPs) [39,65]. These nanoparticles have been used as computed tomographic X-ray imaging/optical contrast-enhancement agents for diagnostic imaging of tumors [39]. A first example of the application of green nanotechnology in precision medicine has come from mangiferin functionalized gold nanoparticles (MGF-AuNPs). These nanoparticles have been shown to be immunomodulatory by targeting pro-tumor macrophages and thus treat tumors through an immunomodulatory mechanism [9,11].

Functionalized gold nanoparticles have found significant applications in the design and development of dual diagnostic and therapeutic agents (theranostics agents). Such types of medical approaches are gaining considerable prominence in medicine because of their extraordinary ability to perform both diagnosis and therapy simultaneously (Fig. 1) [66]. Recent investigations have shown a variety of effective

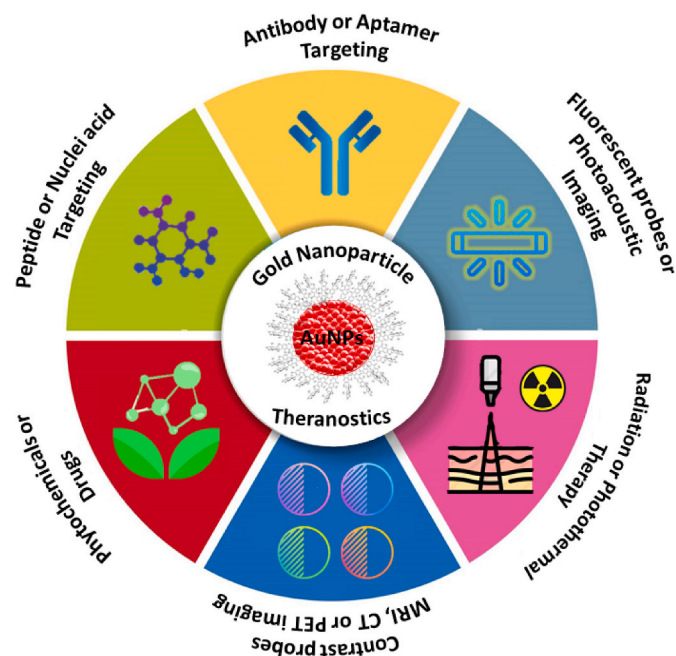


Fig. 1. Gold nanoparticles for theranostics: Gold nanoparticles (AuNPs) that have been functionalized with contrast agents/dyes and drugs for imaging/therapy, among other applications. Tumors can be targeted selectively using intelligent AuNPs systems decorated with targeting moieties. AuNPs can also act as phototherapeutic agents by adhering to specific targets for tumor cell death while remaining non-toxic to healthy cells. (For interpretation of the references to color in this figure legend, the reader is referred to the Web version of this article.)

multiplexed theranostic agents, including epigallocatechin gallate (EGCG) functionalized radiolabeled gold-198 (^{198}Au) nanoparticles (EGCG- ^{198}Au NPs), which provide excellent dual imaging and therapy applications through single photon emission computed tomography (SPECT) as well as through radiation therapy [67].

This review presents latest overview on the importance of green nanotechnological processes and their applications comprising of: (i) myriad of synthetic pathways for the production of functionalized nanoparticles with a focus on green nanotechnology of gold, (ii) their applications in the field of drug delivery for diagnosis, including computed tomography (CT), single photon emission computed tomography (SPECT), photoacoustic imaging, optical coherence tomography (OCT), X-ray and fluorescence imaging, magnetic resonance imaging (MRI), and surface enhanced Raman spectroscopy (SERS), and finally (iii) therapeutic applications through photothermal/photodynamic therapy, chemotherapy, X-ray therapy, and radiotherapy (using radioactive gold nanoparticles). Concluding remarks will highlight realistic scope of green nanotechnology in oncology for the care and treatment of cancer patients.

2. Green nanotechnology

2.1. Synthesis of gold nanoparticles (AuNPs) using green nanotechnology

The method to synthesize AuNPs, aka colloidal gold, by reduction of gold salt first appeared in a publication dating back to 1857 by Michel Faraday. He described that reduction of chloroauric acid solution (HAuCl_4) by phosphorus in carbon disulfide created a “ruby color” colloidal gold solution [68]. In 1951, Turkevich et al. proposed a synthetic method for colloidal gold using trisodium citrate ($\text{Na}_3\text{C}_6\text{H}_5\text{O}_7$) to reduce boiling chloroauric acid solution. The method can produce AuNPs with sizes in the 15–20 nm range [69]. Frens G., subsequently investigated further on the Turkevich’s procedure and discovered that

the decrease in the concentration of the trisodium citrate salt resulted in increasing size of AuNPs (10–150 nm range) [70]. This later became a standard synthetic method for the production of AuNPs and is generally known today as the Turkevich-Frens method. The procedure starts with heating chloroauric acid solution up to 100 °C followed by the addition of trisodium citrate solution with stirring until the color of the solution turns ruby red depending on the size of the particles (Fig. 2a–b).

Emergence of nanomedicine with a greater focus on biocompatibility of AuNPs resulted in rapid progress in the discovery of a variety of biocompatible AuNPs. This rapid advance in the synthesis of AuNPs may be attributed to the widespread use of AuNPs in diagnosis and treatment of various cancers and diseases [71,72]. Various synthetic techniques for stabilizing or regulating the shape and size of AuNPs have been developed. These techniques are still based on the reduction reactions of gold chloride proposed by Turkevich; with minimal modifications of the standard Turkevich-Frens method [73–75].

In recent years, three key factors have gained considerable importance in the context of new synthetic methodologies to produce AuNPs: (1) various types of reducing agents used; (2) nature of chemical entities used for stabilizing surface atoms and (3) input of energy (heat, electricity, etc.) and finally (5) nature of solvents, aqueous vs organic (Fig. 2a–f). For example, in the original Turkevich-Frens method, trisodium citrate was the reducing agent and heat was used as a source of input energy to initiate the chemical reaction without the use of any stabilizers [76]. AuNPs produced using this method were unstable due to the susceptibility of surface atoms on AuNPs for agglomeration. In order to circumvent this problem, recent methods are focused on finding ways to stabilize AuNPs through surface encapsulation with a variety of chemicals and proteins. In the Brust-Schiffrin method, introduced in 1994, surfactant tetraoctylammonium bromide (TOAB) and stabilizing agents (dodecanethiol) are added to prevent the agglomeration by corona coating layers around the AuNPs, while stronger reducing agent sodium borohydride (NaBH_4) is used for complete conversion of gold precursor(s) into the corresponding AuNPs (Fig. 2c) [73].

As the nano-revolution continues to unfold and unleash its tremendous potential on the human population, a focal point of scientific debate is concerned on the large amount of toxic chemical substances that are currently used as chemical reducing agents in the fabrication of nanoparticles. The duality of this concern is also focused on the environmentally toxic byproducts generated at the nanoscale. Sodium borohydride, dodecanethiol, and TOAB are used in the transformation of gold salts to their corresponding nanoparticles [73,77–81]. All these substances pose serious health and environmental risks as they leave negative carbon footprints in the near and long term. Therefore, it is scientifically prudent to focus on developing ecologically friendly and biocompatible synthetic technologies for the large-scale production of nanoparticles, which ultimately make their way into a myriad of products for various applications.

2.2. Moving toward green nanotechnology

Katti’s group have pioneered the development of innovative synthetic techniques based on the principles of green technology over the past two decades [7,27,30,31,34–37,40,65,82–84]. Their overarching objective for introducing the concept of ‘Green Nanotechnology’ has been to minimize or eliminate the application of toxic chemicals as reducing/stabilizing agents for the transformation of metallic precursors to their corresponding nanoparticles. Green nanotechnology, a body of new knowledge developed by Katti et al., utilizes electron rich phytochemicals as effective chemical reducing agents, thus eliminating the use of toxic chemicals as reducing agents.

The biodiversity of our planet provides an abundance of phytochemicals with biocompatible properties that can be used to develop novel green nanotechnologies for the synthesis, stabilization, and subsequent utilization of nanomaterials in a variety of product formulations. Other non-chemical reduction processes include biosynthesis of

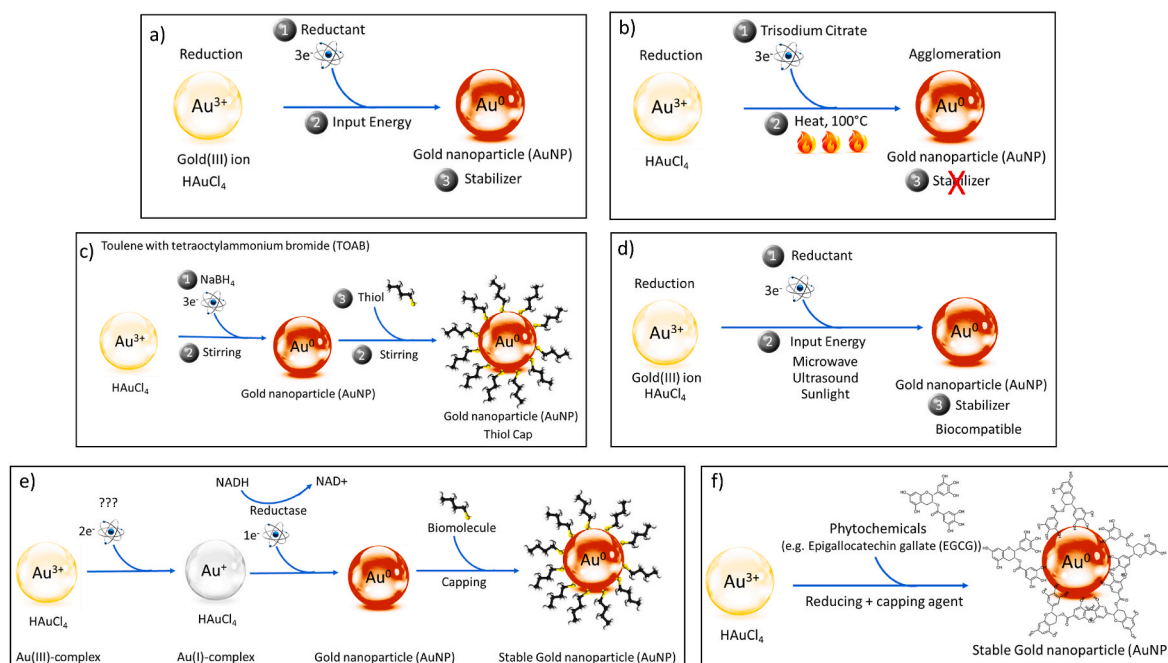


Fig. 2. Methods for the synthesis of gold nanoparticles (AuNPs): a) Key factors in synthesis of AuNPs consist of (1) suitable reductant (2) input of energy and (3) stabilizer, b) Turkevich-Frens method and its key factors consists of (1) trisodium citrate as the reductant (2) heat as the input of energy and (3) no presence of stabilizer, c) Brust-Schiffrin method involves (1) sodium borohydride as the reductant (2) constant stirring as the input of energy and (3) thiol in toluene and TOAB phase as the stabilizer, d) Various methodologies for the ecofriendly synthesis of gold nanoparticles, e) Intracellular NADH-dependent reductase mechanism for the synthesis of gold nanoparticles, and f) Phytochemicals-based reduction of gold ions into gold atoms. (For interpretation of the references to color in this figure legend, the reader is referred to the Web version of this article.)

nanoparticles using microorganisms [85–88]. Various species of bacteria, fungi, yeast, algae etc. are also reported for their ability to synthesize AuNPs via biological processes [89]. Irradiation of metal precursors using various radiation sources including ultrasound [75], microwave, and sunlight have been demonstrated for nanoparticle production as well (Fig. 2d).

2.3. Biosynthesis of gold nanoparticles by microorganisms

Microorganisms possess innate ability to transform Au^{3+} ions into AuNPs. However, the specifics of this process of reduction are complicated and not completely understood. Recent studies have shown that the reduction mechanisms involve the intervention of electron-rich biomolecules characteristic of microorganisms. These mechanisms are rather unique to each organism as shown in Table 1 and Table 2.

One of the most common mechanisms is the reduction via NADH-dependent reductase enzyme. Investigations in bacteria *Cupriavidus metallidurans*; fungi *Fusarium oxysporum*, *Helminthosporium solani*, *Sclerotium rolfii* and *Aspergillus foetidus* [87,90,91] have suggested that the mechanism appears to involve both intracellular and extracellular pathways. In the extracellular mechanism, microorganisms secrete reductase enzymes, that works in tandem with NADH or NADPH to transform gold(III) (Au^{3+}) ions into their equivalent gold(0) (Au^0) nanoparticles. In the case of the intracellular mechanism, studies in *Deinococcus radiodurans* [92] and *Verticillium* spp [93], have revealed that there is formation of a gold(I) complex intermediate and the mechanism of nanoparticle formation occurs in multiple steps: (1) gold (III) will first form a complex to become a negatively charged ion; (2) this complex will then absorb onto the microbial cell wall and the cytoplasmic membrane, which are positively charged, and ultimately reduced to the gold(I)-complex by the unknown mechanism. The gold(I) complex is toxic to the microbe; therefore, it will trigger the detoxification mechanism; (3) gold(I) complex can either be absorbed into the cytoplasm or remain on the membrane depending on the physiology of

the organism, to get reduced to AuNPs by reductase enzyme or other unidentified biomolecules; and finally (4) the AuNPs are capped (or coated) by microbial biomolecule and then secreted out of the microbial cell; because of this the AuNPs are also stabilized against aggregation as outlined in Fig. 2e. Many other biomolecules can also act as reducing and stabilizing agents both intracellularly and extracellularly. Examples include laccase in *Protosphaerion variabile*; prodigiosin and cytochrome in *Serratia marcescens* [94] or polyphenols in *Cladosporium cladosporioides* (Tables 1 and 2) [95].

2.3.1. Biosynthesis production method

The production process mainly involves 2 pathways through biosynthesis: (1) direct biomass pathway using active biomass as reactants and (2) cell product pathway which uses cell products as reactants. For the procedure following the use of active biomass, first, microbes are cultured in a suspension medium. When it has grown to an appropriate amount, it is extracted from the medium and repeatedly washed with deionized water. Then, the biomass is resuspended and mixed with chloroauric acid. After several hours or days of incubation, the biomass is separated out to obtain AuNPs in solution (Table 1). For the technique using cell products, the only difference is that the biomass is extracted or filtered out before mixing it with the chloroauric acid solution (Table 2 and Fig. 3).

2.3.2. Reusability of the biomass

Sustainability of various processes used to produce AuNPs plays a paramount role in the overall success of zero carbon emission green manufacturing technologies. Reusability of the biomass reduces waste and makes the process sustainable and “greener”. Investigations using *Escherichia coli* and *Verticillium* spp [93], showed that the microbial biomass could tolerate and survive the reduction via the use of chloroauric acid. This process did not appear to be toxic to the live biomass. Hence, it can be separated from the AuNPs after the reaction and can be used again and again. However, this was not always practical. With the

Table 1
Gold nanoparticles biosynthesis using live biomass as reductants.

Species	Reaction site	Mechanism/ Reductant	Complete reduction time (h)	NP Shape	NP size (nm)	Stability	Clinical application	Year	Citation
Bacteria									
<i>Rhodococcus</i> spp.	Intracellular (mycelia surface)	No data	24	Sphere	12	–	–	2003	[238]
<i>Thermomonospora</i> spp.	Extracellular	Unknown enzyme	120	Sphere	8	>6 mo.	–	2003	[239]
<i>Escherichia coli</i> DH5 α	Intracellular (cell surface)	No data	120	Sphere, Triangle, Quasi-hexagon	25	–	Biosensors	2007	[240]
<i>Rhodopseudomonas</i> <i>capsulata</i>	Extracellular	Unknown enzyme	48	Triangle, Sphere, Quasi-hexagon	10–400	3 mo.	–	2007	[241]
<i>Stenotrophomonas</i> <i>maltophilia</i>	Intracellular	Unknown enzyme on cytoplasmic membrane	–	Sphere	40	>2 Wk. (4 °C)	–	2009	[242]
<i>Brevibacterium casei</i>	Cell wall	Unknown protein	–	Sphere	10–50	24 h (in blood)	<i>in vitro</i> anticoagulant	2010	[243]
<i>Deinococcus</i> <i>radiodurans</i>	Intracellular and Extracellular	Antioxidants and proteins	8	Sphere, Pseudo- sphere, Truncated triangle	40	>3 mo.	<i>in vitro</i> antibacterial	2016	[92]
<i>Serratia marcescens</i>	Intracellular and Extracellular	Prodigiosin, other antioxidants	144	Sphere	20–120	–	–	2017	[94]
Fungi									
<i>Verticillium</i> spp.	Cytoplasmic membrane, cell wall	Unknown enzyme	–	Sphere, Triangle, Quasi-hexagon	20	–	–	2001	[93]
<i>Fusarium oxysporum</i>	Extracellular	NADH-dependent reductase	48	Sphere, Triangle	8–40	>1 mo.	–	2002	[244]
<i>Trichothecium</i> spp.	Intracellular, cell wall, cell membrane	Unknown protein or enzyme	72	Sphere	10–25	–	–	2005	[245]
<i>Trichothecium</i> spp.	Extracellular	Unknown protein or enzyme	48	Triangle, Hexagon, Sphere, Rod	5–200	>1 mo.	–	2005	[245]
<i>Helminthosporium</i> <i>solani</i>	Extracellular	NADH-dependent reductase	72	Sphere, Triangle, Rod, Hexagon, Star-shaped	2–70	–	<i>in vitro</i> anticancer (doxorubicin conjugated)	2008	[98]
<i>Penicillium</i> <i>brevicompectum</i>	Intracellular and Extracellular	Unknown biomolecules	12	Sphere, Triangle, Hexagon	20–80	>3 mo (2–8 °C)	<i>in vitro</i> anticancer	2011	[246]
Yeasts									
<i>Magnusiomyces</i> <i>intense</i> LH-F1	Extracellular	NADH-independent enzyme and other unknown biomolecules	24	Sphere, Triangle, Pentagon, Hexagon	16–420	–	–	2016	[247]

NP = Nanoparticles.

intracellular synthesis using the direct biomass technique, the live biomass has to be killed and disintegrated usually by ultrasound for the collection of the AuNPs. This is how it works in the case of *Brevibacterium casei* and *Trichothecium* spp. In the cell product technique, the biomass has to be killed for extracting the cell products. Various methods encompassing investigations using *Protosphaerion variabile* [96], *Serratia marcescens* [94], *Candida albicans*, *Rhizopus oryzae*, and *Streptomyces platensis* have been reported [97].

Although, reusability of biomass is critical, most of the publications do not mention proper or uniform techniques to separate and reuse the biomass. Limited details are provided on methods to separate the live biomass after the formation of AuNPs in various reactions [92,98]. Besides, in the biosynthesis using the cell product technique, as in the studies with bacteria *S. marcescens* [94], *S. griseoruber* [99]; and fungi *A. niger* [100], *P. brevicompactum* *S. rolfii* [90], *A. foetidus* [91] and *C. cladosporioides* [95] (Table 2), only the cell-free filtrate or supernatant broth is required for the reactions. Therefore, the live biomass is not destroyed. It is centrifuged, washed, or filtered out and can still be reused. Although the intention to maintain live biomass has not been clearly stated, the cell product technique can be considered to be the most sustainable biosynthesis process for the production of AuNPs. For full sustainability and scalability of these biosynthesis methods, it is imperative to develop proper separation and purification procedures.

2.3.3. The best nano-biosynthesis process

AuNPs produced by fungi are generally smaller and more uniform in size than those synthesized from bacteria (Tables 1 and 2). The synthesis using the cell product technique is also relatively much faster. It requires from 10 min to as long as up to 48 h for complete reduction of gold salts into the corresponding AuNPs. On the other hand, with the biomass technique, it may take as long as 144 h or 6 days for complete reduction. As discussed previously, the cell product technique is the most sustainable biosynthetic process and is superior to the biomass technique in terms of efficacy and sustainability.

2.4. Synthesis of gold nanoparticles by phytochemicals

Before the emergence of modern medicine, plants have long been used as primary medicinal agents. Traditional Chinese and Indian medicinal systems have been using crude plant extracts with metals for treating ailments. One of the primary issues about the use of phytochemicals in the production of nanoparticles is the lack of reproducibility. But green synthesis of AuNPs provides a robust and reproducible synthetic process utilizing plants and their derivatives. The biosynthetic production of AuNPs without using any harmful chemicals, has received phenomenal attention over the past few years because of concerns relating to human and environment safety [11,101].

Table 2
Gold nanoparticles biosynthesis using cell products as reductants.

Species	Cell products	Mechanism/ Reductant	Complete reduction time	NP Shape	NP size (nm)	Stability	Clinical application	Year	Citation
Bacteria									
<i>Paraconiothorium variabile</i>	Enzyme extract	Laccase	20 min (70 °C)	Sphere	71–266	–	–	2011	[96]
<i>Serratia marcescens</i>	Cell-free filtrate	Prodigiosin, cytochrome oxidase, porphyrin	24 h	Sphere, Prism, Hexagon	21–30 (pH 4)	–	–	2017	[94]
<i>Serratia marcescens</i>	Prodigiosin extract	Prodigiosin	10 min	Hexagon	40–50	–	–	2017	[94]
<i>Streptomyces griseoruber</i>	Supernatant	Unknown biomolecules	30 min	Sphere, Triangle, Hexagon	5–50	–	–	2017	[99]
Fungi									
<i>Aspergillus niger</i> NCIM 616	Cell-free filtrate	Unknown proteins and aromatic amino acids	24 h	Sphere, Ellipse	12	–	–	2009	[100]
<i>Penicillium brevicompactum</i>	Supernatant broth (Cell-free filtrate)	Unknown biomolecules	9 h	Sphere, Triangle, Hexagon	20–50	–	<i>in vitro</i> anticancer	2011	[246]
<i>Sclerotium rolsii</i>	Cell-free filtrate	NADPH-dependent reductase	10–15 min (80 °C)	Triangle, Hexagon, Decahedron, Rod	25	2 mo.	–	2011	[90]
<i>Aspergillus foetidus</i>	Cell-free filtrate	NADH-dependent reductase	4 h	Sphere	30–50	>3 mo.	<i>in vitro</i> anticancer	2016	[91]
<i>Cladosporium cladosporioides</i>	Cell-free filtrate	NADH-independent reductase and unknown polyphenols	2 h	Sphere, Irregular	30–60	6 mo.	<i>in vitro</i> antimicrobial <i>in vitro</i> antioxidant	2017	[95]
Yeasts									
<i>Candida albicans</i>	Cytosolic extract	Unknown biomolecules	–	Sphere, Triangle, Hexagon	20–40	–	<i>in vivo</i> anticancer in mice (LCCS antibody conjugated)	2011	[248]
<i>Rhizopus oryzae</i>	Protein extract	Unknown phosphate protein	24 h	Sphere	5–65	>3 mo.	–	2012	[249]
Algae									
<i>Spirulina platensis</i>	Protein extract	Unknown proteins	48 h	Sphere	2–8	>2 mo.	<i>in vitro</i> antibacterial	2014	[97]
<i>Prasiola crista</i>	Dry powder	Unknown proteins	9 h	Sphere	5–25	>3 mo.	–	2014	[250]

NP = Nanoparticles.

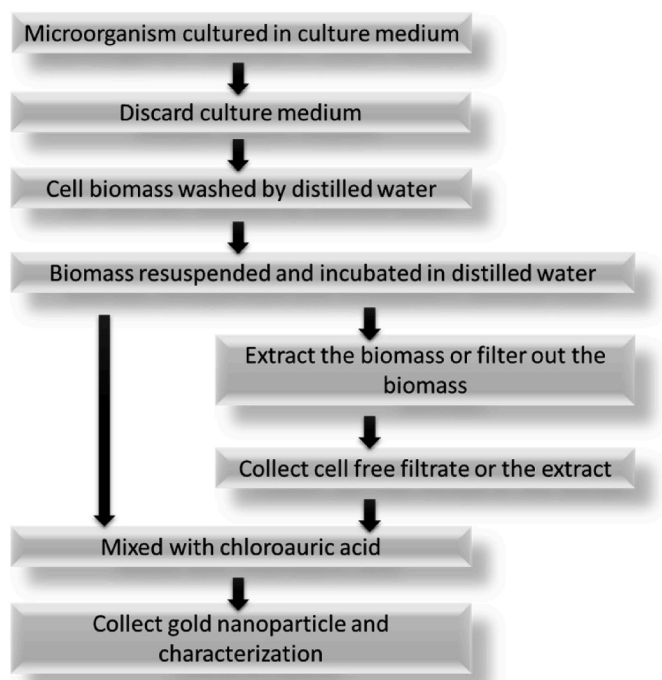


Fig. 3. Techniques for the biosynthesis (1) using active biomass as reactants (left branch) and (2) using cell products as reactants (right branch).

The use of plants in nanoparticle synthesis can be advantageous because it eliminates the need for maintaining microbial cultures and also facilitates the scale up and production of biocompatible nanoparticles. Plant-derived phytochemicals provide a safe, inexpensive, and widely accessible source of reducing agents for the reduction of gold precursors into nanoparticles. An added advantage of using phytochemicals in the overall nanoparticles production scheme is that they serve as dual reducing and stabilizing agent. Proteins, polyphenols, and related multifunctional-electron-rich species, present in various phytochemical cocktails, efficiently encapsulate gold atoms forming a phytochemical corona thereby increasing the stability of nanoparticles. Moreover, the production of AuNPs using phytochemicals is a thermodynamically feasible process. It does not involve huge inputs of energy; no gases are evolved and there are no significant temperature changes during and after the reaction—thus qualifying to be ‘Zero Carbon Emission’ processes. These unique advantages of green nanotechnology appear to define future nanoparticles/nanomaterials productions for industrial applications in the design and development of gold and various other metallic/non-metallic nanoparticles.

Plants are widely used for the green synthesis of AuNPs. Sources of electron-rich phytochemicals include leaf extracts from plants [6–11,17,30–40,102], whole plant extracts, seed extracts, flower extracts, fruit extracts, etc.—all of which are employed as reducing agents to synthesize AuNPs. Furthermore, these nanoparticles can also be stabilized using natural stabilizing agents such as gum arabic—a protein from acacia tree [65]. Synthesis of AuNPs from plants can be divided into 3 major steps: (i) preparation of plant extracts, (ii) reduction of gold ions, and (iii) characterization of AuNPs [6–11,17,30–40,102]. We discuss full details in the following sections:

2.4.1. Preparation of plant extracts

This process can be conceptualized through the preparation of an extract from *Mangifera indica* leaves. The leaves are finely cut and phytochemicals are extracted by boiling in deionized water at 27 °C [11, 103]. In a similar way, aqueous extract of *Achillea wilhelmsii* was prepared by using the flowers of the plant. The flowers are first dried and then cut into small pieces. Boiling the leaves in distilled deionized water for 5 min followed by sterilization of the broth and refrigeration at 4 °C produced reproducible protocol for the extraction of phytochemicals [104]. In other examples, juice of citrus fruits *C. limon*, *C. reticulata* and *C. sinensis* were centrifuged at 10,000 rpm, to remove undesired impurities for the production of AuNPs [105]. Petals of rose (*Rosa hybrida*) are dried and phytochemicals extracted in distilled water at 100 °C [102]. Fruit extract of *Terminalia arjuna* was prepared by washing the fruit with distilled water and then boiling it with double distilled water at 50–60 °C. The extract was then filtered with Whatman No. 1 filter [106]. Dry powder obtained from dried *Gnidia glauca* flower was boiled with distilled water, followed by filtration of the extract with Whatman No. 1 filter and then refrigeration at 4 °C [107].

Finely ground powder of shade dried *Nyctanthes arbortristis* flower was used for extraction. 10 mL ethanol was added to the powder and an ethanolic extract of the phytochemical was obtained after 72 h which was then refrigerated at 4 °C [108]. *Macrotyloma uniflorum* and coriander leaves were boiled with distilled water to obtain the extract [109]. Dried leaves of *Magnolia kobus* and Persimmon (*Diospyros kaki*) were finely cut and put in Erlenmeyer flask and boiled with distilled water for 5 min to obtain leaf extracts [110]. The extract of clove buds (*Syzygium aromaticum*) was obtained by employing the process of maceration. Coarse powder of dried clove buds was allowed to macerate in double distilled water by incubating the maceration flask at 27 °C on an orbital shaker with agitation of 50 rpm for 8 h. The solution obtained was passed through a Whatman filter paper no. 40 and then heated in a china dish to obtain a brown colored solid residue. The solid residue was then solubilized in water and passed through a Whatman filter paper no. 40 to obtain aqueous clove buds solution.

2.4.2. Reduction of gold ions and stabilization

The use of phytochemicals is of great interest to produce nanoparticles as it bridges plant/natural science and nanotechnology. These phytochemicals provide a natural and eco-friendly option. The presence of strong antioxidant activity among the various phytochemicals has encouraged scientists to utilize them for the production of nanoparticles. The synergistic reduction potential of various phytochemicals enable gold salts reduction to AuNPs. Plants rich in polyphenol, flavonoid, amino, thiol and hydroxyl units offer efficient reduction and capping potentials (Table 3). Gold is used in the form of gold(III) chloride trihydrate ($\text{HAuCl}_4 \cdot 3\text{H}_2\text{O}$). Synthesis of Au⁰ is done by the bio-reduction of $[\text{AuCl}_4]^-$ ions using phytochemicals as shown in Fig. 2f. To produce

radioactive AuNPs using epigallocatechin gallate (EGCG-¹⁹⁸AuNPs), radioactive chloroauric acid was used. EGCG has strong reducing properties, resulting in the conversion of gold ions into AuNPs [111]. Extract solution of *Salix alba* was used to reduce gold ions and study how $\text{HAuCl}_4 \cdot 3\text{H}_2\text{O}$ concentration affects synthesis of AuNPs. The chemical structures of different types of phytochemicals from plants used in the synthesis of AuNPs is illustrated in Fig. 4.

The high activity of surface atoms on AuNPs, if not properly stabilized by proteins or thiols or other strongly bonding chemical entities, will result in agglomeration with other gold atoms resulting in the loss of properties attributed to their nano-size. To avoid this phenomenon, a stabilizer or capping agent is used that binds with strong electrostatic/covalent/hydrogen bonding interactions creating corona on the surface of nanoparticles. Stabilization of AuNPs have been reported using various functional groups including thiols, and amines [112] and various proteins including gum arabic as stabilizing agents. Gum arabic (GA) is a highly branched polysaccharide known for its stability, emulsification properties and low viscosity at high temperatures [113], and is frequently used for the stabilization of nanoparticles. Proteins and phytochemicals, obtained from different plant species, provide robust capping for stabilization along with reduction capabilities. This was demonstrated by the use of soybean proteins as a dual reductant and stabilizing agent in the synthesis of AuNPs [27].

3. Characterization of gold nanoparticles

UV-visible spectroscopy a valuable tool for the characterization of AuNPs. It uses the 400–540 nm absorption region to track the formation of AuNPs in solution. The color change, after the formation of AuNPs, is attributed to combined oscillations of free electrons. AuNPs show characteristic optical absorption spectrum with a surface plasmon resonance (SPR) peak between 520 nm and 540 nm [114]. Differential centrifugal sedimentation (DCS) analysis is utilized to investigate the size of nanoparticles by measuring the time required for AuNPs to cross through a sucrose density gradient in a disc centrifuge [27]. The morphology and size of AuNPs are determined using transmission electron microscopy (TEM) technique. TEM and DCS are often used to determine core sizes, whereas dynamic light scattering (DLS) is utilized to determine the hydrodynamic diameter and surface charge of AuNPs. The capping/coating of AuNPs can cause substantial changes in the hydrodynamic diameter. The DLS instrumentation also gives information regarding the zeta potential (surface charge) of particles and is a measure of its stability. The zeta potential is attributed to the presence of attractive and repulsive forces that exists between the surfaces of nanoparticles. The balance between attractive and repulsive forces in nanoparticle dispersions ensure their stability with little or no particles aggregation. Additionally, Fourier transform infrared spectroscopy (FTIR) analysis is performed to determine possible compounds or

Table 3
Various phytochemicals used in the production of gold nanoparticles.

Class	Name	Plant	Core diameter (nm)	Hydrodynamic diameter (nm)	Activity	References
Catechin	Epigallocatechin Gallate	<i>Camellia sinensis</i>	15–45	105–165	Antioxidant, Anti-carcinogenic	[65,251]
Glycosides	Ginsenosides	<i>Panax ginseng</i>	16–20		Antioxidant	[116]
Isoflavone	Genistein, Diadzein	<i>Glycine max</i>		60–62	Antioxidant, Anti-carcinogenic	[27,252]
Polysaccharide	Arabinogalactin	<i>Acacia Senegal</i>	17–25	26.8		[117,253]
Aldehydes	Cuminaldehyde	<i>Cuminum cyminum</i>	9–17	76–78	Anti-tumor, Anti-inflammatory, Neuroprotective	[37,254, 255]
Flavonoid	Resveratrol	<i>Vitis vinifera</i>	35	–	Antioxidant, Anti-carcinogenic	[256,257]
Xanthonoid	Mangiferin	<i>Mangifera indica</i>	17–20	–	Antioxidant, Anti-carcinogenic neuroprotective, anti-inflammatory immunomodulation	[103,258]
Tannins	Tannic acid	<i>Myrica pensylvanica</i>	7.3–14.1	–	Antimicrobial	[259–261]





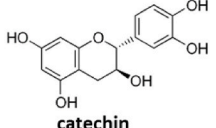
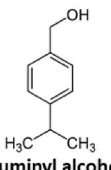
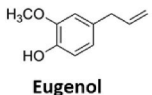
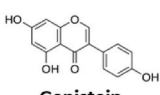

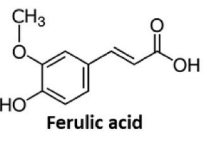
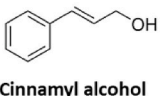
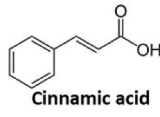
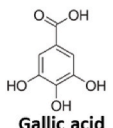

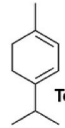
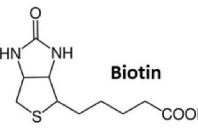
	 Black Tea <i>(Camellia sinensis)</i>	 Cumin <i>(Cuminum cyminum)</i>	 Cinnamon <i>(Cinnamomum verum)</i>	 Soybean <i>(Glycine max)</i>
Active ingredient	 catechin	 Cumyl alcohol	 Eugenol	 Genistein
Antioxidant	 Epigallocatechin gallate	 Ferulic acid	 Cinnamyl alcohol	 Cinnamic acid
Phytochemical	 Gallic acid	 Terpinolene	 Terpinene	 Biotin

Fig. 4. The chemical structure of active ingredient, antioxidant, and phytochemicals found in numerous plants that are utilized to synthesize gold nanoparticles. (For interpretation of the references to color in this figure legend, the reader is referred to the Web version of this article.)

biomolecules involved in the reduction and capping of AuNPs [115].

3.1. Stability tests

Long term and optimum *in vitro* stability are important in the utility of AuNPs in various biomedical applications. *In vitro* stability studies are performed on AuNPs by mixing them with biological media such as human serum albumin, histidine, cysteine, bovine serum albumin and various pH ranges to mimic *in vivo* conditions. The SPR peak is monitored to see the stability of AuNPs upon mixing with various solutions. The peak in the 520–540 nm region confirms the presence of AuNPs as observed in the case of ginseng-AuNPs [116]. The stability of nanoparticles are measured by monitoring the UV–visible absorption spectra. Electrolyte introducing method was also used to study the stability of AuNPs produced using gum arabic [30,117]. Furthermore, zeta potentiometry also provides important stability information because AuNPs with low surface charge tends to agglomerate and gain the stable energy state over a period of time.

4. Applications of gold nanoparticles in diagnosis

4.1. Gold nanoparticles as contrast agents

Iodine based contrast agents currently used in clinical applications are toxic and are rapidly eliminated from the body. Gold is a better contrast agent than iodine due to its higher atomic number, electron density, absorption coefficient and X-ray absorption capacity (Fig. 5). Since gold nanoparticles remain in the target for a longer period, one injection of targeted gold nanoparticles is sufficient for imaging over a longer duration avoiding need for multiple doses. Whereas, iodinated contrast agents, because of their rapid systemic clearance, have to be injected several times to achieve a better contrast [118,119]. Moreover, because of their small size, facile surface and shape modification, optical and fluorescence properties and longer blood circulation, gold nanoparticles are emerging as excellent diagnostic tools for detection of

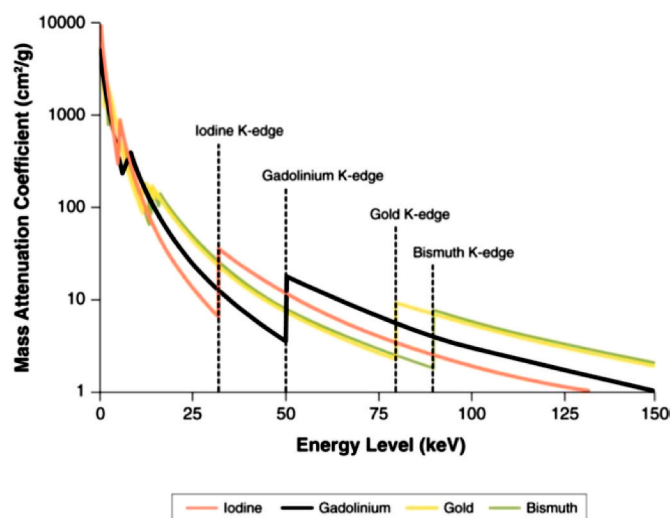


Fig. 5. X-ray attenuation of different substances (Reprinted with permission from Goswami et al.). [121].

diseases.

Strong X-ray absorption and scattering of light makes gold nanoparticles ideal for utilization in various light-based techniques such as photothermal/photodynamic and photoacoustic imaging. In fact, gold nanoparticles can also be used in bio-sensor development for signal amplification and detection of analytes of interest at very low concentrations [120]. Such approaches entail binding of molecules such as antibodies, peptides, enzymes, aptamers etc. to the surface atoms of gold nanoparticles. The optical properties of gold changes upon analyte binding and allows for detection and quantification of analytes [120]. This approach can be used to detect various signature biomarkers that serve as fingerprints in tracking diseases. Gold nanoparticles elastic

light-scattering characteristics makes it feasible to detect individual nanoparticles using a visible light microscope with spatial resolution of ~ 100 nm [121]. Tumor targeted gold nanoparticles exhibit selective tumor affinity and good retention within the tumor microenvironment leading to *in vivo* detection of tumors. Gold nanoparticles because of their small size allows for excellent conductivity and surface plasmon resonance (SPR) absorbance as well [121].

The fundamental aim in molecular imaging is to obtain clinically discernible good quality images with high spatial resolution that pose minimum risk to patients. Consequently, new imaging modalities are emerging in diagnostics. The challenge is to improve the imaging device to obtain better quality images and get a good contrast to distinguish between healthy tissues and tumor cells. In this context, gold nanoparticles are promising candidates as excellent contrast agents for different imaging modalities [30,122–124]. In addition, gold nanoparticles synthesized by phytochemicals have innate ability to recognize cancer cell receptors or other type of receptors over expressed in different tumor cells [11,31,35,82,84,124]. This leads to greater detectability, better imaging capability for various diseases and even early-stage disease detection attributed by the multifunctionality of gold nanoparticles governed by their shape, size, surface coating, and functional moieties as shown in Fig. 6 [125]. Lymph node, brain vasculature, tumor and cardiovascular imaging is possible by utilizing gold nanoparticles in imaging modalities.

It can be envisioned that, in the future, whole body imaging with photoacoustic or surface enhanced Raman spectroscopy (SERS) imaging in real-time, mediated by a patch injected/implanted inside the human body, we may be able to monitor abnormal cell developments, blood glucose levels, etc. A plethora of multiplexed imaging and therapy applications will be possible by exploiting the properties of biocompatible gold nanoparticles. All these applications will lead to personalized medicine which provides better treatments and diagnosis of various diseases for patients. Recently, several gold and silver nanoparticle-based theranostics agents have been developed [6–11,17,30–40,102,123,124,126–133].

4.1.1. Photoacoustic imaging

Photoacoustic (PA) imaging is an imaging technique where the subject is irradiated with laser pulses and some of the delivered energy is absorbed and converted into heat (phototherapy). This causes tissue expansion, which is then picked up as a sound wave for detection of diseases. Ultrasonic frequency sound waves are generated by employing short laser pulses [134]. Early indication of disease state can be obtained through photoacoustic imaging. For instance, in the case of melanoma tumor, pigmentation is very high, hence detection of melanoma with photoacoustic imaging is very efficient [134]. However, tumor cells may not be able to absorb photons as efficiently as red blood cells because of the absence of pigmentation in some tumors; as a result, there is no signal. Gold nanoparticles, internalized into melanoma and other tumor cells, will help to solve this problem due to the surface plasmon characteristics of nanoparticles.

In comparison to various other imaging methods, photoacoustic imaging has many advantages. Ultrasound waves provide greater spatial resolution and are non-ionizing. Because of their strong light absorption, gold nanoparticles-based contrast agents have been investigated for photoacoustic imaging. Also, using light in the near-infrared (NIR) window has an added advantage of light penetrating deep tissue. Deep tissue imaging covering several centimeters range was recently reported with regards to photoacoustic imaging [134]. Gold nanoparticles are good exogenous contrast agents for both diagnosis and image-guided treatment because of tunability of their SPR (by changing shape and size of nanoparticles), biocompatibility and efficient photothermal conversion.

Detection of macrophages with contrast agents is a big challenge due to lower specificity of inflammation sites in the body. A few investigations have been reported on targeting macrophages for imaging purposes. PEGylated gold nanoparticle contrast agent was utilized by Wang et al., in detecting macrophages in atherosclerotic plaques *ex vivo*. As a result of macrophage endocytosis in cells, gold nanoparticles aggregated and resulted in an absorption to red-shift because of plasmon resonance coupling. This enabled in identifying the gold nanoparticles specifically taken up by the macrophages [135].

Ocular imaging is very important for eye disease monitoring,

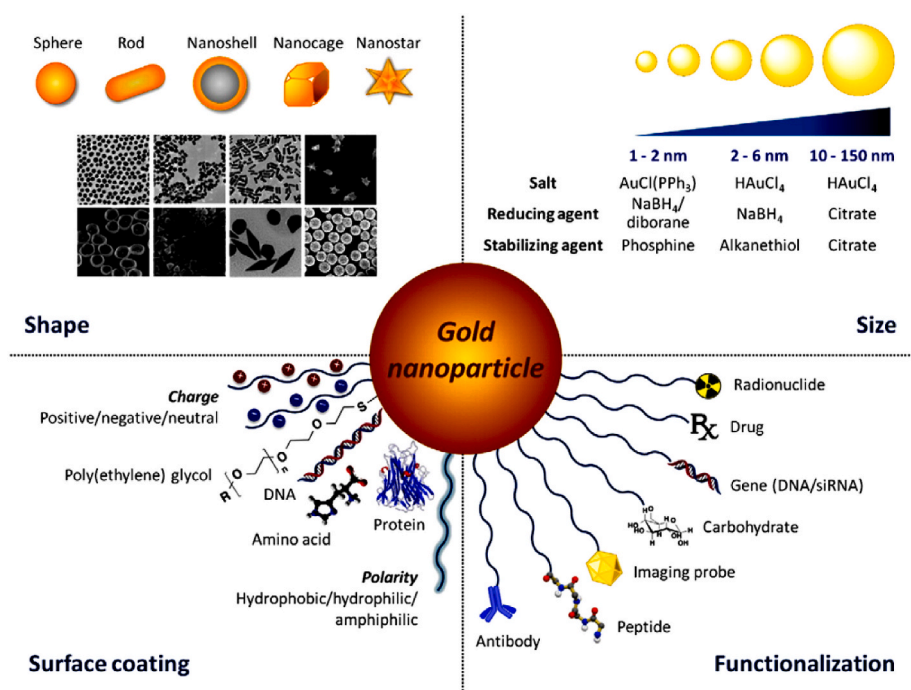


Fig. 6. Multifunctionality of gold nanoparticles governed by their shape, size, surface coating, and functional moieties for imaging and therapy (Reprinted with permission from Her et al.). [126]. (For interpretation of the references to color in this figure legend, the reader is referred to the Web version of this article.)

diagnosis, and therapy. Raveendran et al. have reported the utility of gold nanocages as a photoacoustic contrast agent in ocular imaging. Safe and high-resolution deep tissue imaging of the eye is provided by photoacoustic imaging. For early detection of uveal melanoma, a form of intraocular cancer seen in the choroid, ciliary body and iris, photoacoustic imaging modality is very helpful [136].

Imaging of lymphatic system can be critical for diagnosing metastatic cancer. Gold nanoparticles can be utilized for enhanced photoacoustic imaging of lymph nodes for tracking cancer metastasis [137]. Moreover, gold nanocages, as a new family of lymph node tracers, have been used for noninvasive sentinel lymph node (SLN) photoacoustic imaging with penetration of at least 33 mm beneath the skin surface (rat model) with fine contrast.

Katti et al. tagged melanoma cells with EGCG-conjugated gold nanoparticles (EGCG-AuNPs) to detect circulating tumor cells which are associated with cancer metastasis and are precursors to secondary tumors. In metastasized melanoma diagnosis utilizing photoacoustic imaging, gold nanoparticle tagging provided an improved photoacoustic signal. EGCG-AuNPs at 500 nm demonstrated a photoacoustic effect increase of 41% which was an excellent improvement in photoacoustic systems using a single wavelength [122].

Imaging of cardiovascular diseases is important for understanding progression of atherosclerosis and for determining disease causing factors. For tracking a vascular cell adhesion molecule in mice, Rouleau et al. developed a gold nanoshell (immunonanoshell) photoacoustic molecular probe. In both *in vitro* and *in vivo* experiments, the probe showed good targeting and no acute toxicity [138]. With an increased photoacoustic signal, the molecular probe displayed specific targeting for the aortic arch and the aortas *ex vivo* (Fig. 7a) [138].

For targeting the tumor microenvironment various techniques have been explored. One of these methods is to use stimuli-responsive smart gold nanoparticles. Exploiting the acidic tumor microenvironment

through the design of gold nanoparticles sensitive to mildly acidic environment is one such example. Song et al. designed “smart” gold nanoparticles (SANs) which conjugate in weakly acidic environments. Gold nanoparticles were coated with hydrolysable citraconic amide groups. Due to electrostatic attractions, SANs aggregate rapidly resulting in an absorption to red-shift into the longer wavelength visible and NIR region (Fig. 7b). This shift can be exploited to ‘turn-on’ agents by using NIR excitation. SANs accumulate very efficiently in tumor cells compared to regular cells which results in selective photoacoustic imaging for diagnostic applications [139].

4.1.2. Single photon emission computed tomography (SPECT) imaging

Utilizing a gamma radiation emitting radiopharmaceutical tracer, single-photon emission computed tomography (SPECT), provides 3D imaging capabilities. A gamma camera captures 3D views of anatomical structures. Non-invasive SPECT nuclear imaging is cost-effective and more widely available. Accumulation and biodistribution of gold nanoparticles in tumor region are enabled by targeting tumor specific receptors. For dual SPECT and CT tumor imaging, Li et al. prepared nanoparticles of gold dendrimer conjugated with folic acid (FA) and tagged with ^{99m}Tc for targeted delivery [140]. Generation two dendrimers poly(amidoamine) (PAMAM) with polyethylene glycol (PEG) surface modification and cyclic diethylenetriamine pentaacetic anhydride (cDTPAA) conjugation were utilized. It was then followed by ^{99m}Tc chelation radiolabeling. PAMAM dendrimer was used as a carrier for contrast agent in order to stabilize gold nanoparticles. In addition, stability and cytocompatibility were demonstrated in different systems. In dual-mode SPECT/CT imaging, versatile low-generation dendrimer gold nanoprobe can be used for targeting FA receptors (FAR) which are overexpressed in tumor cells for both *in vitro* and *in vivo* (Fig. 8a) studies [140].

Radioactive gold nanoparticles are very attractive because they

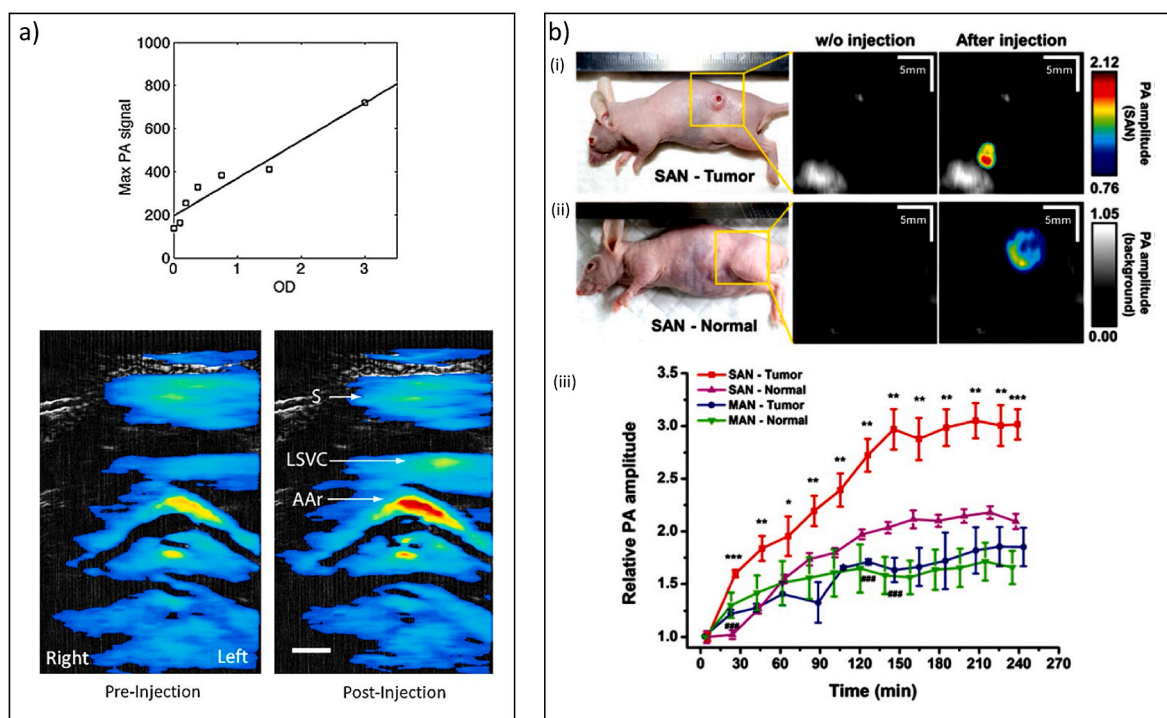


Fig. 7. Photoacoustic Imaging using gold nanoparticles a) Peripheral arterial tone (PAT) signal from AuNS-PEG probe and image of the parasternal short axis and aortic arch region in one animal pre- and post-injection ($t = 3 \text{ min } 20 \text{ s p.i.}$). (S: Sternum, AAr: Aortic arch, LSVC: Left superior vena cava. Bar 1 mm), and b) (i) Photograph (left) and PA MAP images (680 nm laser illumination) of tumor xenograft mice before (center) and after (right) “Smart” AuNPs (SAN) injection. (ii) Photographs (left) and PA MAP pictures of a normal model before to (center) and after (right) SAN injection. (iii) Time evolutions of the PA signals in four possible situations (Reprinted with permission from Rouleau et al. [138] and Song et al.). [139]. (For interpretation of the references to color in this figure legend, the reader is referred to the Web version of this article.)

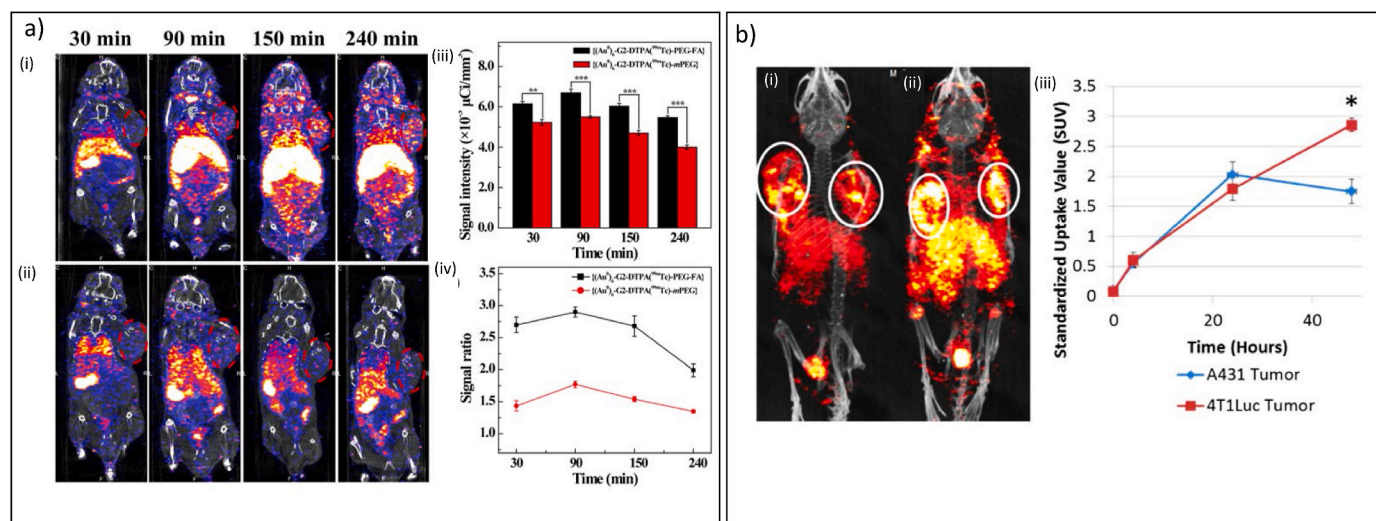


Fig. 8. Single Photon Emission Computed Tomography (SPECT) Imaging using AuNPs a) In vivo SPECT/CT images of tumors expressing folic acid receptors (FAR) (i and ii), tumors SPECT signal intensity (iii), and tumors SPECT signal ratio (tumor/muscle) (iv) after intravenous injection of the $\{(\text{Au}^0)_6\text{-G2-DTPA}^{99\text{mTc}}\text{-PEG-FA}\}$ DENPs (a) or $\{(\text{Au}^0)_6\text{-G2-DTPA}^{99\text{mTc}}\text{-mPEG}\}$ DENPs (ii) ($[\text{Au}^{99\text{mTc}}] = 740 \text{ MBq}\cdot\text{mL}^{-1}$, $[\text{Au}] = 0.08 \text{ M}$, in $100 \mu\text{L}$ PBS) at various post-injection time points, and b) Imaging of tumors using dual-radiolabeled nanoparticles. SPECT/CT pictures of mice 48 h after intravenous injection with bilateral A431 and 4T1Luc tumors (circled). (ii) Tumor-specific uptake values (SUVs) of ^{111}In 48 h after injection ($*p < 8.3 \times 10^{-6}$) (Reprinted with permission from Li et al. [140] and Black et al.). [143].

provide imaging with high resolution and there is no additional need for attaching a diagnostic agent on the surface. In mice with triple negative breast cancer (TNBC) Zhao et al. reported SPECT imaging of tumor utilizing ^{199}Au doped gold nanoparticles. Radiolabel stability was maintained by directly assimilating the ^{199}Au atoms in the gold nanoparticle crystal lattice. ^{199}Au -gold nanoparticles conjugated with receptor targeting moieties displayed better biodistribution and enhanced specificity and sensitivity for SPECT/CT tumor imaging [141,142].

Functionalized gold nanoparticles have application in prevention and monitoring of cardiovascular diseases. For selective tracking of apoptotic macrophages, Li et al. synthesized a SPECT/CT imaging probe,

consisting of amino-PEG coated gold nanoparticles conjugated to Annexin V and tagged with $^{99\text{mTc}}$ radionuclide. Apoptotic macrophage imaging enabled tracking of atherosclerosis plaque buildup. Annexin V, the targeting molecule was very specific and efficient in recognizing the apoptotic macrophages through their phosphatidyl serine moiety. In conclusion, with 30% apoptosis, macrophages showed a $3.52 \pm 0.35\%$ cellular uptake of $^{99\text{mTc}}\text{-AuNPs-Annexin V}$, a $2.41 \pm 0.53\%$ cellular uptake of $^{99\text{mTc}}\text{-AuNPs}$ and a $1.68 \pm 0.36\%$ cellular uptake of $^{99\text{mTc}}\text{-Annexin V}$ post 2 h incubation [140].

With ^{125}I and ^{111}In radiolabeling, Black et al. synthesized gold nanoparticles functionalized with a matrix metalloproteinase 9 (MMP9)

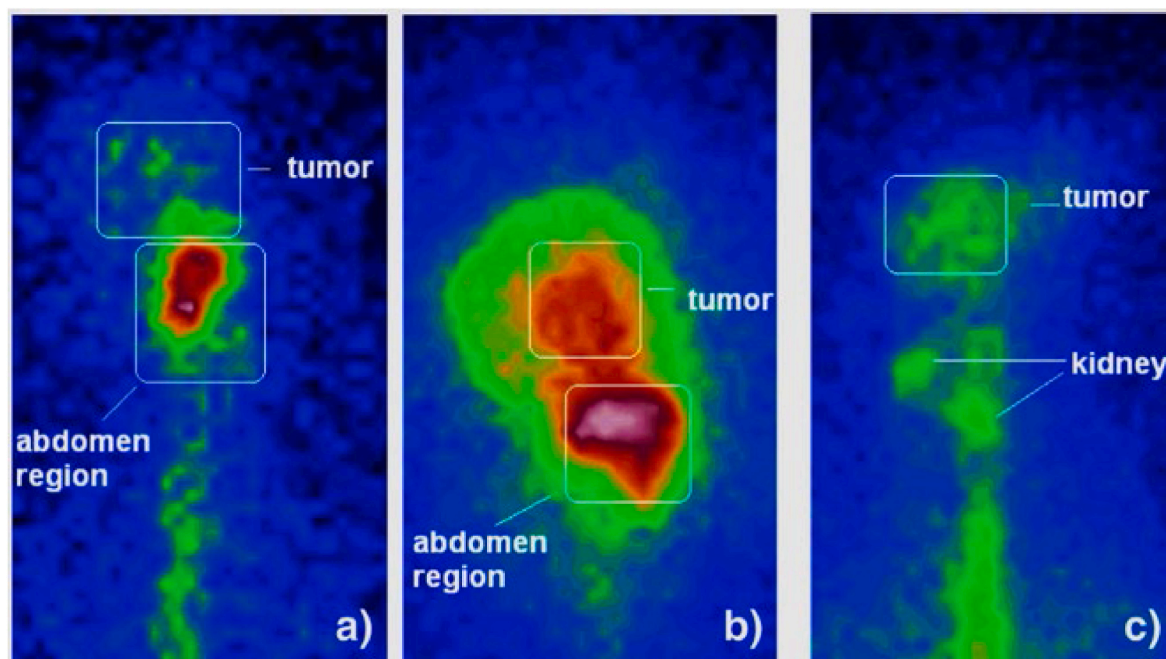


Fig. 9. SPECT images of ^{198}Au , $^{199}\text{Au@AF-GO}$ ($50 \mu\text{g/mL}$, 3.7 MBq , $100 \mu\text{Ci}$) in a rat bearing fibrosarcoma tumor after a) 1, b) 4, and c) 24 h post-injection. (Reprinted with permission from Fazaeli et al.) [144].

to form a multispectral SPECT imaging contrast agent (Fig. 8b) [143]. In this study, following a dual-radiolabeling strategy, MMP9 activity was characterized. The two distinct radionuclides of the imaging agent were separated using a cleavable linker. Enzyme activity imaging using optically-activatable probes was an inspiration for this approach. As a result, tumors with MMP9 expression were differentiated [143].

Aminopropylsilyl functionalized graphene oxide (GO) sheets radiolabeled with ^{199}Au and ^{198}Au nanoparticles were synthesized by Fazaeli et al. for efficient and targeted *in vivo* SPECT tumor imaging. In rats bearing fibrosarcoma tumor, an increased and rapid uptake (tumor to muscle uptake ratio of 167, 4 h post injection) of gold graphene oxide nanocomposites paved way for efficient imaging of tumors as illustrated in Fig. 9 [144].

4.1.3. Positron-emission tomography (PET) imaging

For bioimaging applications, Cheng et al. have developed anisotropic and novel branched gold-tripod nanoarchitectures. With size lower than 20 nm, these Au-tripods are efficient *in vivo* contrast agents for photoacoustic imaging. In biodistribution studies on small animals using positron emission tomography (PET), these Au-tripods functioned favorably. In tumor-bearing mice, after injection with Au-tripods conjugated to a cyclic peptide (Arg-Gly-Asp-D-Phe-Cys), photoacoustic imaging showed a three time increase in contrast in comparison to the control group [145].

Wang et al. investigated gold nanocages PET imaging capabilities and *in vivo* pharmacokinetic properties. Biodistribution studies were carried out with ^{64}Cu radiolabeled gold nanocages of 30 nm and 50 nm size in tumor bearing mice. Gold nanocages showed increased uptake in tumors. By tuning the physicochemical properties of gold nanocages, it is possible to change their biodistribution and intratumoral delivery profile [146].

4.1.4. Optical coherence tomography (OCT)

Optical coherence tomography (OCT) is fast, non-invasive and provides high-resolution 2D and 3D images. Apart from tracking disease progression and early-stage detection of cancer, OCT has enormous applications in ophthalmology and cardiology as well. Utilizing a nonionizing near-infrared optical beam, sub-surface images are captured without requiring any sample preparation. Due to their intense SPR, stimuli-responsive plasmonic gold nanoclusters were developed by Kim et al. as contrast agents for OCT in detecting oral cancer onset. PEG tethered gold nanocapsules were prepared by conjugating gold nanoparticles using acid-cleavable linkers. These nanocapsules deconstructed into individual gold nanoparticles in weakly acidic conditions as shown in Fig. 10. As a result, in dysplastic tissue, OCT imaging showed a weakened scattering intensity and a higher Doppler variance [147].

4.1.5. Contrast agents for X-ray

In X-ray computed tomography (X-ray CT), computer-processed X-ray scans generate tomographic images of specific tissues. Blood vessels

and gastrointestinal organs can be imaged with good contrast due to the excellent X-ray attenuation of various body components. The advantages of X-ray CT imaging are that it is very economical, provides good resolution spatially and also gives precise anatomical features. Thus, 75% of all clinical diagnostic imaging is accounted by X-ray CT, making it one of the most popular diagnosis tools in hospitals.

For improving tissue contrast and signal to noise ratio without radiation dose increment, various types of contrast agents have been explored. Low molecular weight contrast agents (iodinated aromatics), with low toxicity and high-water solubility are currently used in clinics. It may be noted, iodinated contrast agents are rapidly eliminated by kidney due to their short circulation time, thereby not reaching the specific target [148].

AuNPs are well-suited in X-ray imaging because of their biocompatibility and organ selectivity making them highly attractive candidates for diagnosis. Because of gold's high electron density and high Z (atomic number) value, optimal X-ray irradiation absorption has been achieved [123,149]. Due to their high molecular weight, AuNPs clear the blood stream slower than iodinated complexes, exhibiting longer circulation time, thus improving the imaging window [150]. Surface modification can be readily performed with AuNPs, allowing for novel design of AuNPs to increase probe stability and targeting. Investigation of AuNPs in X-ray CT is categorized into 3 main domains: (A) Blood pool (B) Passive targeting and (C) Active targeting. Blood pool requires AuNPs to circulate in the blood vessels for a prolonged time without penetrating through vascular endothelium. Passive targeting utilizes the enhanced permeation retention (EPR) effect in damaged tissues. Tumor vasculature is 'leaky' because of the endothelial blood vessel distortion, and this allows the AuNPs to get into the tumor microenvironment. When contrast agents reach specific tissues/cells of interest, it is called active targeting. It is achieved through nanoparticle surface modification with various ligands or molecules.

The work of Meir et al. reported a CT contrast agent consisting of gold nanoparticles specific for melanoma-specific T-cell receptors [151]. These AuNPs were intravenously injected into mice bearing human melanoma xenografts. CT whole-body imaging revealed the transportation, delivery, and kinetics of T-cells. The transduced T-cells were found at the tumor site compared to the non-transduced cells. Furthermore, labeling with AuNPs did not show any impact on T-cell function *in vitro* and *in vivo* (Fig. 11). This cell tracking technique enabled investigation of the fate of immune cells in cell-based immunotherapy.

Using a new ionic liquid like glucosammonium formate, Iranpour et al. successfully synthesized gold nanoparticles coated with gum arabic (GA-AuNPs). Previously citrate-capped AuNPs were explored as a CT contrast agent, but they were unstable in biological media. Gold nanoparticle synthesized using a novel and green reducing agent like glucosammonium formate, and then capped with gum arabic (GA), a green and nontoxic stabilizing agent displayed greater stability. On HepG2 hepatocyte cells cytotoxicity studies were carried out. Stability studies were carried out in various physiological media like human serum

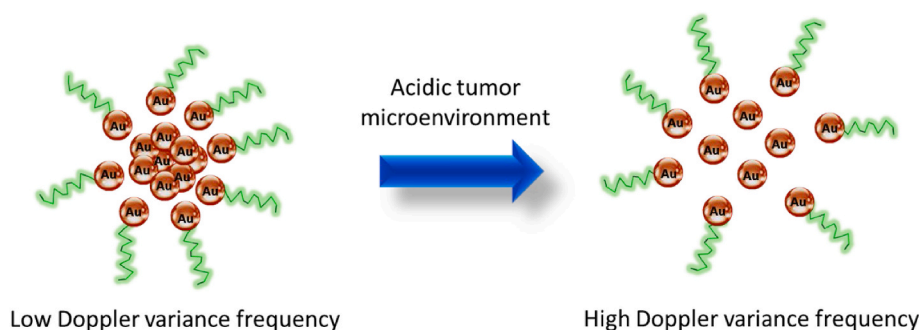


Fig. 10. PEG conjugated gold nanoclusters with acid-cleavable link in tumor microenvironment. (Adapted from Kim et al. [147], distributed under the terms of the Creative Commons CC-BY license). (For interpretation of the references to color in this figure legend, the reader is referred to the Web version of this article.)

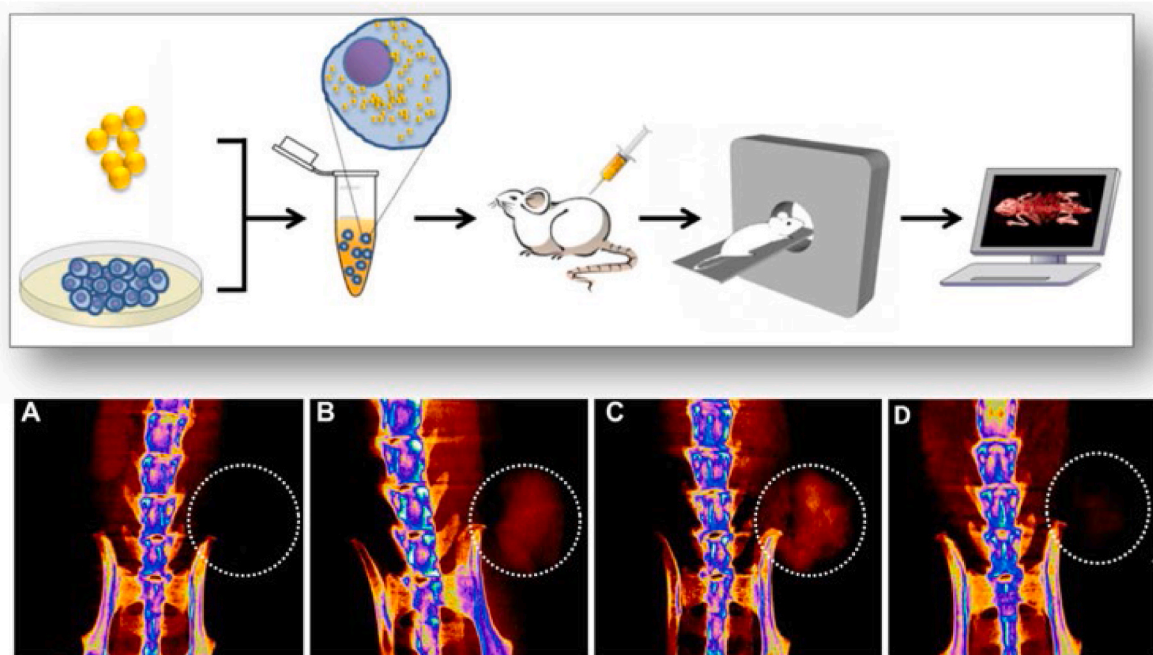


Fig. 11. Top: T-cell tracking process. *In vitro*, T cells were labelled with AuNPs, then injected into mice, and monitored *in vivo* using CT imaging. Bottom: Time-dependent increase of tumor-specific T lymphocytes. Micro-CT scans with maximum intensity projections (A) before to T-cell injection, (B) 24 h after injection, (C) 48 h after injection, and (D) 72 h after injection. The T-cell accumulation is denoted by circles (Reprinted with permission from Meir et al.). [151].

albumin (HSA), bovine serum albumin (BSA) and phosphate-buffer saline (PBS). Conclusively, these GA-AuNPs were highly stable, non-toxic and showed good contrast properties for X-ray CT [152].

In contrast to regular agents, gold nanoparticles owing to their prolonged circulation time, enabled specific imaging of tissues and cells for extended time. Meir and Popovtzer used AuNPs to examine cell trafficking in CT imaging. In cell-based therapy, live cells are transplanted for treating diseases. The observation or monitoring of transplanted cells plays an important role in cell therapy. Using AuNPs; one can label various cell types, including stem cells and immune cells, without disrupting their therapeutic efficacy. Different *in vivo* experiments have demonstrated AuNPs to be non-invasive with longitudinal cell tracking properties and high sensitivity [153]. The injection of biocompatible gold nanoparticle solution facilitates their transport to various organs through blood. AuNPs also showed a very high spatial resolution contrast [154].

Ease of surface functionalization and unique X-ray attenuation characteristics of AuNPs makes them excellent candidates for future generation contrast agents. Gold nanoparticles contrast agents stabilized by dendrimers (Au-DSNPs) were designed for CT imaging applications. For enhanced CT imaging function, 5th generation amine-terminated PAMAM dendrimers reshaped by diatrizoic acid (G5.NH₂-DTA) were used as stabilizers. At room temperature, G5.NH₂-DTA dendrimers were mixed with aqueous gold salt solution, to spontaneously entrap AuNPs in dendrimers. DTA-containing Au-DSNPs display increased attenuation, in comparison to omnipaque, considering the same active element (gold or iodine) molar concentration in both. Au-DSNPs are stable in aqueous solutions, exhibit good hemocompatibility and are non-cytotoxic. Hence, for both *in vitro* cancer cell CT imaging and mice *in vivo* blood pool CT imaging they can be used.

Cai et al. designed gold nanocrystals conjugated with sulfhydrylated PEG for examining their X-ray CT imaging efficacy as an intravascular contrast agent. For toxicity evaluation, histopathologic tests and cytotoxicity studies were carried out. The PEG coated colloidal AuNPs showed no toxicity in mice and were biocompatible. Stable imaging was achieved immediately 24 h post injection. Good microcomputed tomography imaging of tumor vasculature was achieved utilizing AuNP-

PEG [155]. Kattumuri et al. demonstrated that gum arabic (GA) can be utilized as a natural phytochemical in the synthesis of AuNPs. The nontoxic water-soluble phosphine amino acid conjugate, P[CH₂NHCH(CH₃)COOH]₃ (Katti Peptide) was used as a reducing agent in 0.2% GA to produce GA-AuNPs with more than 98% yield. Contrast imaging studies were implemented using phantoms prepared from GA-AuNPs. Boote and Katti et al. work has shown that Phantom images can be captured at 80 kVp and 140 kVp (Fig. 12). GA-AuNPs are stable for several months in aqueous and phosphate-buffered saline solutions as well as in their solid state, allowing for various diagnostic and therapeutic applications [30,123].

For specifically targeting gastrin-releasing peptide (GRP) receptors which are overly expressed in tumors, a novel bombesin (BBN) peptide gold nanoparticle conjugate was developed. These tumor specific BBN conjugated AuNPs, selectively target prostate, breast and lung tumor sites providing tremendous applications for diagnosis and treatment of cancer. The BBN-AuNP size range (115–155 nm) was optimal for entering tumor vasculatures which have a porosity range of 150–300 nm. Endocytosis of BBN-AuNPs within PC-3 cells is significant for cell-specific diagnosis and therapy applications. Gold nanoparticle stabilized by starch (S-AuNPs) and thioctic-acid linked bombesin peptides are synthons for future generation BBN-AuNPs conjugates [156].

For targeted and contrast enhanced CT imaging of head and neck cancers, Popovtzer et al. utilized gold nanorods (AuNRs) conjugated with *anti*-integrin β -4 (UM-A9) antibodies. Following the seed mediated growth technique these AuNRs were synthesized. The mean length and the mean diameter of the AuNR was 45 nm and 15 nm respectively. Gold nanoprobes with tumor specific antigen-targeting capabilities offer unique and selective *in vivo* CT molecular imaging. On cancer cells, these gold nanoprobes aggregate to provide a uniquely identifiable X-ray attenuation (Fig. 13) [157].

Gold nanoparticles afforded better imaging of the previously indistinguishable abdominal renal and aorta arteries in mice with enhanced contrast and 24 h retention time [158]. In contrast, iodine-based vasculature contrast agent persisted for only up to 6 h. Sodium citrate reduced gold(III) chloride trihydrate at 85 °C under vigorous stirring. Color change from yellow to dark purple and then eventually to red

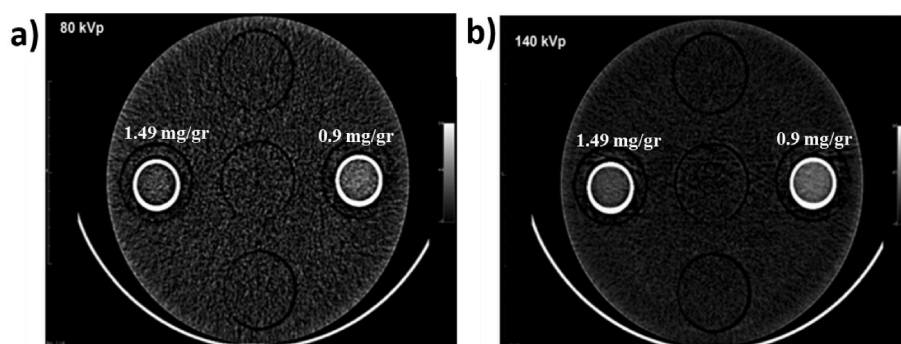


Fig. 12. CT contrast images of GA-AuNPs at 80 kVp (a) and 140 kVp (b) (Reprinted with permission from Katti and Kattumuri et al.). [76].

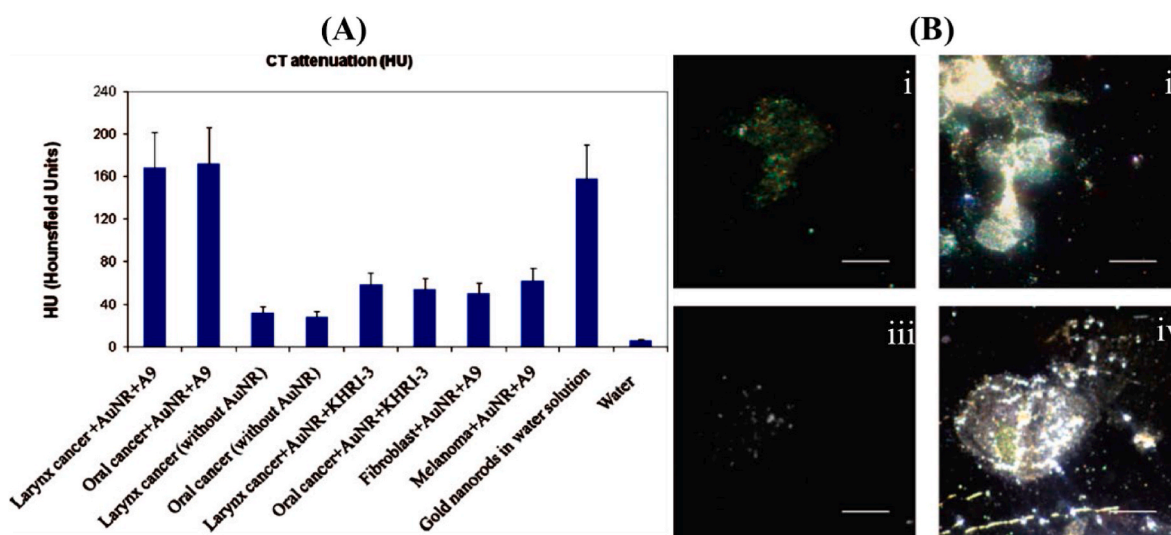


Fig. 13. (A) CT attenuation (HU) of SCC head and neck cancer cells, with positive and negative controls. Bar graph with standard deviation of three samples: larynx and oral cancer cells targeted with A9 antibody-coated gold nanorods (AuNR), larynx and oral cancer cells targeted with nonmatching antibody-coated nanorods (KHRI-3); normal fibroblast and melanoma cells targeted with A9 antibodies, bare gold nanorods in water solution (B) Images of SCC head and neck cancer cells acquired using a dark field microscope. i) & ii) Oral cancer; iii) & iv) larynx cancer: following incubation with i) & iii) nonmatching antibody-coated gold nanorods; ii) & iv) matching UM-A9 antibody-coated gold nanorods. Scale bar: 10 μ m (Reprinted with permission from Popovtzer et al.). [157]. (For interpretation of the references to color in this figure legend, the reader is referred to the Web version of this article.)

indicated successful gold nanoparticle synthesis [158].

In a juvenile swine animal model, Boote and Katti et al. demonstrated the use of AuNPs as a contrast agent for clinical CT systems by utilizing a phantom. Katti Peptide, $P[CH_2NHCH(CH_3)COOH]_3$ was used as a

reducing agent in 0.2% GA to produce GA-AuNPs with more than 98% yield. A tissue-mimicking spherical phantom having known concentrations of Au was used for CT scan. Gold nanoparticles stabilized with gum arabic (GA-AuNPs) were injected in swine. CT scans were taken pre- and



Fig. 14. Change in brightness of liver (A) and spleen (B). Liver: The mean region of interest value in the pre-dose CT image is 69 Hounsfield units; the mean region of interest value in the post-dose CT image is 76 Hounsfield units. Spleen: The mean computed tomography value in the region of interest is 48.5 in the pre-dose image and 57.8 in the post-dose image (Reprinted with permission from Katti and Boote et al.). [159].

post-injection and Hounsfield unit (Δ HU) values measured. This was then compared with gold uptake after autopsy (Fig. 14) [159].

4.1.6. Fluorescence imaging

Fluorophores excitable in the near-infrared (NIR, 650–950 nm) or visible region are utilized as specific probes in fluorescence imaging (FI) [160]. It is not a commonly utilized clinical modality, but real-time and noninvasive imaging is feasible. The limitations of FI that hinders their clinical applications include photobleaching and low penetration into deep tissues. For imaging thin tissue sections, visible region fluorescence is sufficient whereas fluorophores excitable in the near-infrared region are required for deeper penetration. AuNPs do not cause photobleaching or blinking, which is common among many other fluorophores. Under high excitation power, gold nanoparticles display an enhanced native fluorescence despite of a low quantum yields. FI of cells has also been reported through additional modification with certain targeting ligands and fluorescent dyes conjugated to AuNPs.

Zhou et al. loaded gold nanoclusters (AuNCs) in silica for FI in mice. Initially silica coated AuNCs were synthesized. Further, the gold nanoclusters were conjugated to folic acid (FA) covalently to form FA-conjugated AuNCs-SiO₂ nanoprobe. The cytotoxicity of these nanoprobe were estimated using the 3-(4,5-dimethylthiazol-2-yl)-2,5-diphenyltetrazolium bromide (MTT) assay. Their targeting ability for folate receptor positive human gastric mucosal cancer cells (MGC803) and folate receptor negative normal gastric mucous cells (GES-1) was also investigated. Using tail vein injection, nanoprobe were administered to nude mice with human gastric carcinoma for X-ray CT and fluorescence imaging. With red-emitting fluorescence characteristic gold nanoclusters (AuNCs), a collection of gold atoms in the sub-nanometer range displayed background autofluorescence minimizing ability and minimal cytotoxicity [161]. Fluorescence imaging in combination with other techniques provided good spatial resolution for deep tissues. X-ray fluorescence exhibits a high sensitivity for AuNPs, enabling greater penetration depth compared to other optical imaging modalities. AuNPs-loaded phantoms have been successfully imaged utilizing K-X-ray fluorescence (K-XRF) (67.0 keV and 68.8 keV gold emission energies). The L-X-ray fluorescence (L-XRF) imaging using gold nanoparticles was effective in three-dimensional *in vitro* cell and small animal models. Whereas, their effectiveness decreased for imaging deep-seated tumors [162].

Dual imaging integrates fluorescence imaging and computed

tomography (CT) that can be performed using targeted AuNPs. In the synthesis of glycol chitosan gold nanoparticles (GC-AuNPs), glycol chitosan serves both as a reducing as well as a stabilizing reagent. The primary amines on GC polymers have strong affinity for gold nanoparticles. For optical imaging, peptide probes sensitive to matrix metalloproteinase (MMP) were conjugated chemically to GC-AuNPs amino groups. With strong x-ray absorption of gold nanoparticles, optimal tumor imaging was obtained after the *in vivo* nanoparticle accumulation. Metalloproteinases selectively degrade substrates displaying recovery of fluorescence in tumor areas. Employing both CT and optical modalities, tumor imaging was successfully carried out exploiting gold nanoparticles CT contrast and fluorescent properties (Fig. 15) [163].

4.1.7. Magnetic resonance imaging (MRI)

Magnetic resonance imaging (MRI) is an excellent technique for obtaining real time non-invasive cellular and molecular level three dimensional maps. MRI is an ideal platform for imaging of organs and detection of emerging tumors *in vivo* [164]. Under an applied magnetic field, hydrogen atom polarization induces a variety of proton relaxivities, thus producing magnetic resonance contrast images. Hydrogen atoms are abundant in water and fat. Heterogeneous distribution of water and fat in biological organism paves way for MRI imaging applications. With a large spatial resolution of ~ 50 μ m, MRI offers better contrast images of soft and deep tissues in comparison to X-ray CT.

MRI requires exogenous contrast agents to increase sensitivity and they can be categorized into two groups: positive contrast agent (bright) which show T1 signal increment in T1-weighted images and negative contrast agent (dark) which show T2 signal decrease in T2-weighted images. Mn(II) and Gd(III) T1 agents generate strong signals. Cells take up Mn(II) agents easily because of their similarity to Ca²⁺ ions. Yet, un-chelated manganese is toxic to cells [165]. Chelated Gd(III) compounds should have good thermodynamic and kinetic stability to have low cytotoxicity. Macromolecule or protein conjugated Gd(III) are restricted in movement and can increase the relaxivity. Diethylenetriamine pentaacetic acid (DTPA) ligand is kinetically stable, and immobilizes Gd(III) to form stable Gd(III)-DTPA chelates [166].

Gold nanoparticles are excellent contrast agents because of their facile synthesis, non-toxicity, oxidation resistance and solubility feature tunability. Alric et al. suggested multilayers of gadolinium chelates encapsulated with AuNPs to form Au-DTPA-Gd. These AuNPs were synthesized by chloroauric acid (HAuCl₄·3H₂O) reduction utilizing

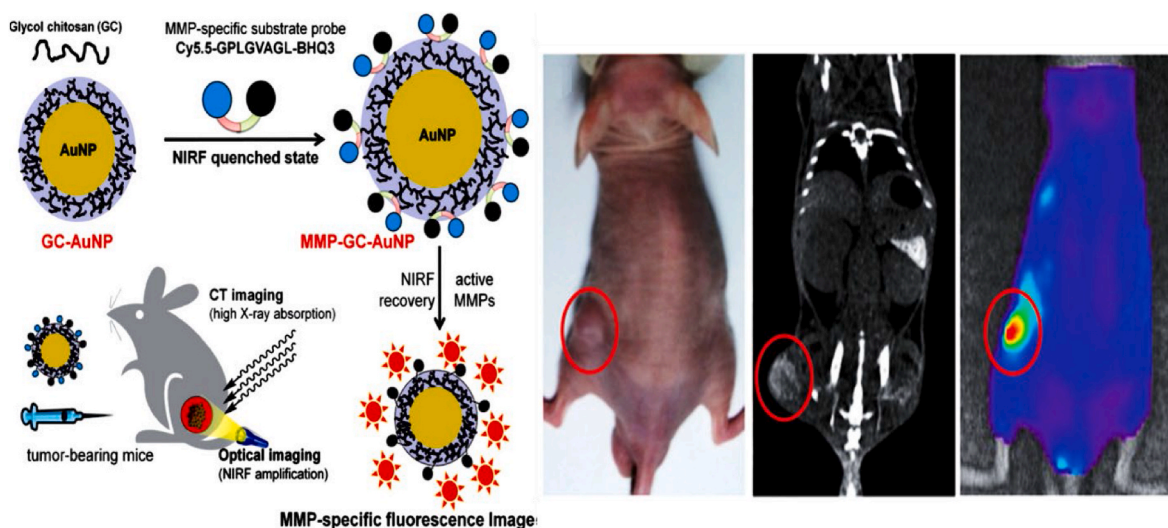


Fig. 15. Dual Computed Tomography/Optical Cancer Imaging using AuNPs (A) matrix metalloproteinase (MMP) peptide conjugated glycol chitosan (GC) gold nanoparticles (MMP-GC-AuNPs) probe as multimodal CT/optical imaging probe, and (B) 24 h post-injection, dual CT/optical imaging of the HT29 tumor-bearing mouse model (Reprinted with permission from Sun et al.). [163]. (For interpretation of the references to color in this figure legend, the reader is referred to the Web version of this article.)

sodium borohydride (NaBH_4) in the presence of dithiolated derivatives of diethylenetriamine pentaacetic acid (DTDTPA). Au-DTDTPA-Gd nanoparticles showed good *in vivo* contrast agent properties for MRI and synchrotron radiation CT (SRCT) dual imaging modalities. Lung, liver, spleen, and heart uptake was lower than kidney and bladder uptake. Therapy or theranostics could be done by covalently grafting bio-targeting groups on multilayers of Au-DTDTPA-Gd nanoparticles. Three carboxylic acid (COOH) moieties in each DTDTPA ligand serve as sites for anchoring (Fig. 16) [167].

For imaging human neural stem cells transplanted *in vivo*, Nicholls et al. utilized gold nanoparticles conjugated to a oligonucleotide containing a Gd(III) chelate and a cyanine dye (Cy3, fluorescent red). These AuNPs showed good cellular uptake and increased T1 relaxivity, providing new avenues for imaging transplanted cells and exploring cellular MRI applications as shown in Fig. 17 [168].

4.1.8. Surface Enhanced Raman Spectroscopy (SERS)

Light passing through metallic nanoparticles can be absorbed or scattered. Light absorption occurs when light is absorbed by the nanomaterials. Light scattering is achieved when photons induce electron oscillations on the surface, and the absorbed photons can be re-emitted as scattered light with a lower frequency (Raman scattering) than the incident light. The frequency shift causes vibration of the molecules [58]. By studying Raman scattering or spectrum, we are able to investigate molecular motions, vibrations and rotations. Raman spectra can provide the chemical composition of a sample [169] and also the “finger print” of molecules. However, Raman spectra are generally weak, since only 1 in 10^8 photons is scattered. Therefore, this technique has not gained popularity in experimental settings, despite the tremendous potential for future development as a reliable medical imaging tool.

The recent development of surface enhanced Raman spectroscopy (SERS) has the advantage of bringing Raman-based imaging into wider use [170]. SERS generates cellular delivery images created by acquisition of hundreds and thousands of Raman spectra from noble metal nanoparticles [171]. The imaging method offers many advantages over conventional modalities due to better sensitivity, high levels of multiplexing and robustness. Gold and silver nanoparticles have emerged as potential SERS substrates owing to their strong surface plasmon resonance and thus can enhance Raman spectra. Silver nanoparticles (AgNPs) are more widely used due to their higher Raman enhancement factor (100–1000 times more than AuNPs). However, AgNPs have lower stability and not very biocompatible. These limitations are resolved with

the utilization of Au nanoshells [172] and hollow gold nanospheres (HGNs) [173]. These particles show strong amplification due to their electromagnetic field localization capability on the surface via the pinhole of their hollow particle structures. The conjugation of Raman active molecules onto AuNPs show an improved Raman spectra of these Raman active reporters (Fig. 18a) [174]. Tunability of the surface plasmon resonance by changing the shape and aspect ratio of the gold nanorods (AuNRs) is very advantageous for SERS imaging [175]. It also affords of up 100,000 times increased Raman scattering of the AuNRs. This enables application of AuNRs for photothermal therapy and SERS imaging for tumor cell detection [175].

Nanoplex™ biotag manufactured by Oxonica Inc. is a SERS nanoparticle which is composed of a gold core and a Raman-active molecule encapsulated in a silica layer (Fig. 18b) [176,177]. The silica encapsulation can ensure the SERS nanoparticle to be physically robust and inert in various environments. Facile surface modifications can also be performed via silica chemistry. By changing the Raman active reporters' various types of biotags can be created. These biotags stimulated by NIR light can be detected with low-cost equipment. Nanoplex™ biotag can be detected at 785 nm in the whole blood.

Chen et al. developed a three-dimensional (3D) polymer film conjugated gold nanoparticle SERS-active substrate. Hexamethylene adipamide (Nylon66) film was immobilized on an organic filter film and used as a template to produce a SERS-active substrate. This substrate showed a significantly enhanced Raman spectra, since 3D porous polymer induced a homogeneous distribution of AuNPs resulting in high-quality SERS [178].

Multilayers of gold nanoparticles were imprinted on silicon substrates in a layer wise fashion, using a gold etchant, for formation of consistent and effective SERS substrates. The layers of nanoparticles and the etching time influenced the performance of the SERS substrates. The substrates showed improved uniformity and excellent reproducibility as well. The ease of access of high density “hot-spots” by probe molecules also facilitated an enhancement factor (EF) increase and a lower detection limit [179].

SERS substrates have been produced based on capillarity-assisted assembly employing AuNPs. Intense electromagnetic field coupling from neighboring gold nanoparticles resulted in a sizeable increase in Raman enhancement factor (3×10^{10}) and very good reproducibility. The relative standard deviation (RSD) of the Rhodamine 6G Raman vibration modes ($1310, 1361, 1509, 1650 \text{ cm}^{-1}$) obtained through the SERS spot-to-spot signal tracking, were consistently lower than 20%, displaying

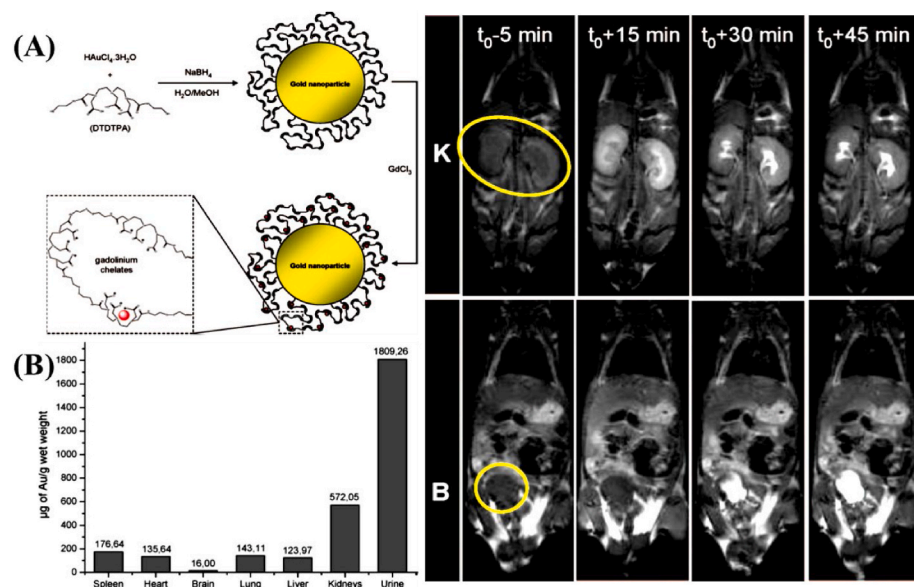


Fig. 16. Gadolinium Chelate Coated Gold Nanoparticles (Au-DTDTPA-Gd50) for dual CT and MRI imaging. (A) Structure of Au-DTDTPA-Gd50 and (B) biodistribution of Au-DTDTPA-Gd50. Right - T1-weighted images of a mouse 5, 15, 30, and 45 min after IV injection of Au-DTDTPA-Gd50 (K for kidneys and B for bladder) (Reprinted with permission from Alric et al.). [167]. (For interpretation of the references to color in this figure legend, the reader is referred to the Web version of this article.)

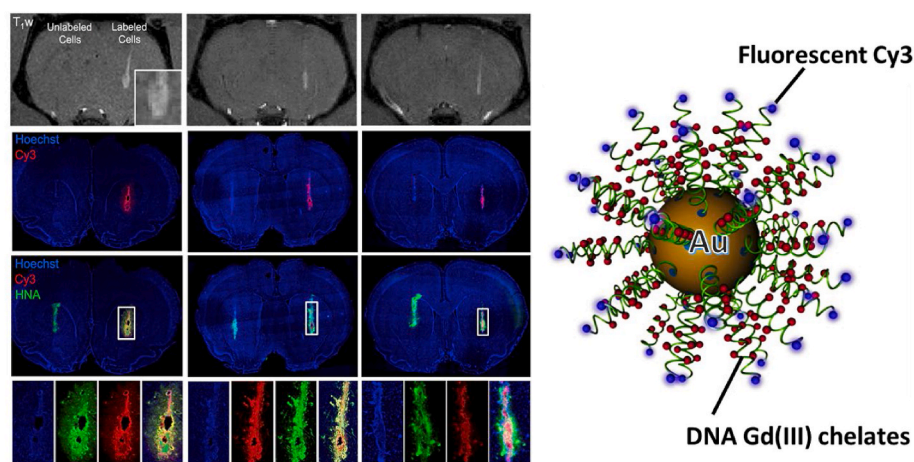


Fig. 17. DNA-Gadolinium-Gold nanoparticles (DNA-GdAuNPs) *in vivo* T1 MR imaging of transplanted human neural stem cells with histological verification. Three animals had one hemisphere transplanted with labelled cells and the other with unlabeled cells. On T1-weighted (T1w) MR images, DNA-GdAuNPs labelled cells were clearly apparent. Fluorescent histology demonstrates that transplanted cells were present in both hemispheres [human nuclei antigen (HNA), in green], however that only cells harboring DNA-GdAuNPs nanoparticles (as identified by the red Cy3 moiety) induced a T1 effect on MR images. (Reprinted with permission from Nicholls et al. [168], distributed under the terms of the Creative Commons CC-BY license). (For interpretation of the references to color in this figure legend, the reader is referred to the Web version of this article.)

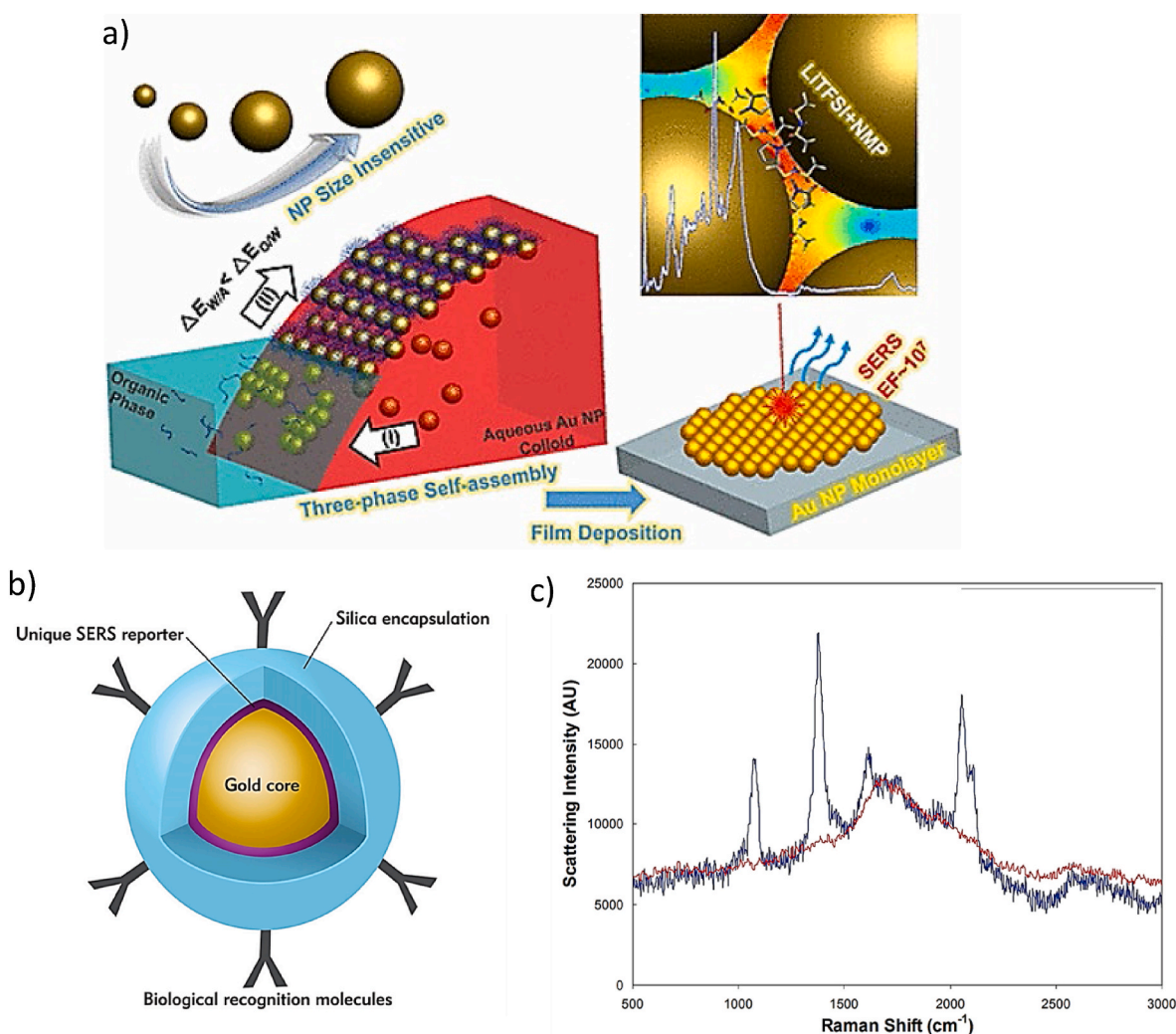


Fig. 18. Gold Nanoparticles for Surface-Enhanced Raman Spectroscopy a) Self-Assembly of gold nanoparticles into ordered monolayers for enhancing Raman intensity, b) Schematic structure of Nanoplex™ Biotag. Au Core has a size of 50 nm, and silica layers coating added an extra 20 nm. A SERS reporter was inserted in between, and c) Raman scattering intensity of whole blood. Red line: Raman scattering of whole blood; Blue line: Raman scattering of Nanoplex™ Biotag in whole blood. (Reprinted with permission from Yang et al. (ACS Appl. Mater. Interfaces 2017, 9, 13,457–13,470). Copyright (2017) American Chemical Society. [174], and Penn et al.) [176]. (For interpretation of the references to color in this figure legend, the reader is referred to the Web version of this article.)

good spatial uniformity and experimental reproducibility. Sudan dye at a concentration of 1×10^{-8} M, also displayed good reproducibility and a low RSD. The gold nanoparticle synthesis via the capillarity-assisted assembly was cost effective and uniform [179].

An efficient SERS substrate based on PEG modified AuNPs was introduced by Leopold et al. [180]. SERS active gold colloids were synthesized utilizing short and long chain PEG. The average size of gold nanoparticles can be adjusted between 15 nm and 60 nm based on the mixing rate during synthesis. Using UV-Vis, SERS and TEM, various gold nanoparticles were characterized. TEM indicated spherical nanoparticles of 15 nm size and polygonal particles of 60 nm size with UV-Vis absorption peaks at 520 nm and 562 nm respectively. These PEG modified gold colloids produced strong Raman scattering similar to that of standard gold colloids synthesized following the citrate reduction method. This is revealed from the various analytes from SERS spectra utilizing the 633-laser line.

For SERS image mapping, Lee et al. proposed hollow gold nanospheres (HGNs) which were conjugated with antibody, specifically targeting HER2 cancer markers overexpressed in breast cancer cells (MCF-7). Stronger and better homogeneous scattering was achieved compared to silver nanoparticles. HGNs provided highly specific and homogeneous contrast agents for cancer cell imaging [181]. SERS based PEGylated AuNPs were designed for *in vivo* tumor targeting and detection [182]. Malachite green, a Raman reporter molecule was adsorbed onto the surface of the gold nanoparticles (60 nm). It was then PEGylated to add an outer layer.

The contrast imaging obtained from these AuNPs were 200 times more superior than that of quantum dots and other types of optical contrasts. It was shown that a SERS microscope detected functionalized AuNPs which were subcutaneously injected into the flank of a mouse. Through passive targeting mechanism by EPR effects, SERS AuNPs can be transported to tumor cells. Active targeting mechanism entails tumor targeting proteins/peptides-functionalized nanoparticles. The conjugation of single-chain variable fragment (ScFv) antibody, as a targeting ligand on SERS AuNPs, allowed for active tracking of cancer cells in animal models. Epidermal growth factor receptor (EGFR) which is overexpressed in many types of tumors is recognized by the ScFv antibody. PEGylated AuNPs function as both optical and electromagnetic probes. Therefore, detailed investigations have been performed for gaining insights into the effects of nanoparticle size and surface coating on tissue targeting and biodistribution [182].

Naked AuNPs, obtained by laser ablation synthesis in solution, are assembled as highly efficient dual MRI and SERS substrates. For example, gold nanoparticles are functionalized with: (i) a naphthalocyanine reporter (ii) a functionalized MRI contrast agent and (iii) a dodecane tetraacetic acid (DOTA) PEG polymer—all loaded with Gd(III) MRI agent. MRI and SERS *ex vivo* and *in vivo* studies entailed exploiting the plasmonic property of the nanosystem for use in localized hyperthermia as well as simultaneously monitoring the progress of the treatment through MRI imaging [183].

4.1.9. Ultrasound

Ultrasound is usually performed at an acoustic frequency range of 25–100 MHz. For visualization of anatomical structures, intravascularities, ophthalmic features and skin imaging, high frequency ultrasound waves are utilized. Ultrasound provides a real-time, low-cost and non-toxic method of diagnosis. However, a severe limitation of this modality is the decrease in penetration capacity with increased spatial resolution. Therefore, there is an immediate requirement to develop technologies capable of enhancing the efficacy of ultrasound contrast agents for deep tissue penetration.

Metallic nanoparticles (5–100 nm diameters) are widely employed as molecular contrast agents for diverse imaging modalities. AuNPs are well known for their relative safety and surface plasmon absorption property. However, currently there is no ultrasound imaging system clinically available for accommodating the small size of the

nanoparticles for achieving a high spatial resolution [184].

In order to maximize diagnosis and therapy efficacy, ultrasound is combined with other modalities. For example, polydopamine-modified poly(lactic-co-glycolic acid) coated AuNPs hybrid capsules (AuNPs/PDA/PLGA), of 725 nm average size, have been developed for ultrasound imaging and high intensity focused ultrasound (HIFU) therapy applications [185]. Using ultrasound locally and non-invasively, pathogenic cells are destroyed in HIFU treatment. Utilizing gelatin phantom samples carrying gold nanocages with fluorescent dye, a controlled release was accomplished inside the HIFU focal volume. Tarapacki et al. investigated therapeutic effects of ultrasound-microbubbles along with PEGylated gold nanorod laser therapy on breast cancer cells. The therapeutic outcome was additive with the combination [186].

For *in vivo* monitoring of mesenchymal stem cells (MSC) tagged with gold nanotracers (20 nm), Nam et al. used ultrasound-guided photoacoustic imaging (US/PA). For stem cell-based therapeutics imaging and tracking of *in vivo* stem cells is critical. After immobilizing in a PEGylated fibrin gel, MSCs labelled with gold nanoparticles were intramuscularly injected in the lower limb of the Lewis rat. Ultrasound imaging provided anatomical details and photoacoustic imaging offered information on localization of AuNPs in cells [187].

4.2. Dual and multimodal imaging technique

Functionalized gold nanoparticles are gaining considerable prominence as effective probes toward the development of multifunctional nanoparticles for diagnosis and therapy. Designing a single contrast agent with multifaceted imaging and treatment capabilities still remains a major hurdle. Multi-functional contrast agents can be advantageous for imaging various modalities like single photon emission computed tomography (SPECT), positron emission tomography (PET), fluorescence imaging (FI), X-ray computed tomography (X-ray CT) and magnetic resonance imaging (MRI).

Biocompatible and tumor specific polymeric magneto-gold fluorescent nanoparticles (MGFs-LyP-1), consisting of extremely small iron oxide gold (Fe_3O_4 -Au) nanoparticles and NIR active fluorescent polymers, were developed for multimodal imaging using a solvent-mediated approach. These AuNPs simultaneously serve as T1 and T2-MRI/CT/NIR fluorescence bio-imaging agents for *in vivo* tumor targeting. Without affecting cell proliferation and differentiation functions, these gold nanoparticles of small size, display high accumulation in tumor cells and show optimal cytocompatibility for prolonged monitoring [188]. Using the bio-mineralization process and a bovine serum albumin (BSA) template, Xu et al. synthesized an imaging agent consisting of gold and gadolinium oxide nanoparticles (denoted as AuGds). AuGds were also conjugated with folic acid (FA) to produce FA-AuGds nanoparticles for specifically targeting folate receptors on keratin-forming (KB) tumor cells. These nanoparticles were used for optical, CT and MR imaging of xenografted tumors *in vivo*. The AuGds are biocompatible and showed rapid renal clearance and did not show any *in vivo* tissue toxicity [189]. Gold nanoparticles that have been used for cancer diagnosis and various other diseases are shown in Table 4. Dual mode or multimodal imaging is essential for accurate disease detection. The advantages include accurate tumor targeting with greater resolution. Examples of multimodal imaging involves fluorescence imaging (FI) and computed tomography (CT) with X-ray or magnetic resonance imaging (MRI).

4.2.1. Optical imaging and computed tomography

Silica coated gold nanoparticles with a thrombin activatable fluorescence peptide was developed by Kwon et al. for imaging and diagnosis of thrombosis utilizing both micro-computed tomography and near-infrared fluorescence (NRIF). Accumulation of gold nanoparticles in the thrombus was size dependent [190].

Table 4
Gold nanoparticles in diagnostic applications (part 1).

Imaging modality	Type of gold nanoparticles	Characteristics	Application	Ref.
Photoacoustic (PA)	EGCG conjugated gold nanoparticles	Spherical nanoparticles 20–40 nm in diameter. Mesotheliomas with gold nanoparticle tagging have stronger photoacoustic signals.	Circulating tumor cell detection	[122]
	Gold nanostars	Dual plasmonic gold nanostars (DPGNS) demonstrated ability for single node diagnosis and treatment due to their longer wavelength, which allows for more detailed imaging and therapy.	Tumor detection	[262]
	Gold nanoshells	External diameter of 38.7 nm, whereas the shell thickness is 4.5 nm. The probe targets the aortic arch and aortas <i>ex vivo</i> .	Atherosclerosis plaques detection	[138]
	Gold nanotripods (Anisotropic hybrid nanoparticles)	Particle size was less than 20 nm. Intravenous injection of cyclic (RGDfC) peptide conjugated Au-tripods (RGD-Au-tripods) to U87MG glioma tumor-bearing mice resulted in nearly threefold greater PA imaging contrasts in tumors than the blocking group.	Tumor detection	[145]
	Gold nanocages	Particle size was about 7 nm. In a rat model, SLNs harboring gold nanocages were detected with high contrast as deep as 33 mm below the skin surface.	Lymph node imaging	[263]
	Stimuli-responsive gold nanoparticles	AuNPs (10.7 nm) accumulated in cancer cells and amplified the signal twice as much as the control <i>in vivo</i> .	Tumor detection	[139]
SPECT	Gold nanoparticles doped with ¹⁹⁹ Au	Spherical nanoparticles having a particle size of 17.6 ± 0.9 nm and a sphere shape. In a rat xenograft model of TNBC and its metastases, gold nanoparticles conjugated with DAPTA can be utilized as a (CCR5)-targeted nanoprobe for the sensitive and specific detection of TNBC and its metastases.	Triple negative breast cancer cell (TNBC) detection	[142]
	Gold nanoparticles conjugated with Annexin V and ^{99m} Tc	Gold nanoparticles were with uniform size (30.2 ± 2.9 nm). The probe specially and efficiently targeted apoptotic macrophages and maintained inside the macrophages.	Atherosclerosis plaques detection	[264]
	¹⁹⁸ Au- and ¹⁹⁹ Au labelled graphene oxide nanoparticles	Nanoparticles (29–45 nm) 4 h intravenous post-injection, tumor uptake was rapid and high (tumor to muscle uptake ratio of 167 after 4 h). This resulted in successful tumor imaging.	Fibrosarcoma tumor detection	[143]
PA/Ultrasound	MAGE antibody conjugated gold nanoparticles	Polymeric multifunctional nanoparticle probes composed of melanoma-associated antigens-gold- liquid perfluorocarbon (perfluorinated hexane/PFH nanoparticles (MAGE-Au-PFH-NPs) were determined to be 354.27 ± 23.31 nm. <i>In vivo</i> , the targeted group's photoacoustic signal was greater and persisted longer than the untargeted groups. The nanoprobe's photoacoustic signal was enhanced <i>in vitro</i> by incorporating AuNPs.	Melanoma detection	[265]
Imaging modalities	Type of AuNPs	Results	Application	Ref.
X-ray CT	GA capped- AuNPs	Glucosammonium formate ionic liquid as a reductant GA as a stabilizer. Highly stable in different physiological media, non-toxic and good contrast properties.	Stability studies	[152]
	PAMAM conjugated AuNRs	Citrate as stabilizer and reducing agent. Strong X-ray absorption; Good hemocompatibility and non-cytotoxicity.	<i>In vitro</i> detection of cancer cells; <i>in vivo</i> imaging of mice blood pools	[266]
	UM-A9 Ab conjugated AuNPs	Seed mediated growth. Specific contrast images in head and neck cancer cells	Cancer cells	[157]
	GA-AuNPs	THPAL as reducing agent. Dose of 85 mg kg^{-1} body weight \rightarrow Hounsfield unit (HU) increase \rightarrow Enhanced contrast images in juvenile swine's liver and spleen after injection.	Models for molecular imaging of human organs	[159]
	Sulphydrated PEG conjugated Au nanocrystals	Citrate as stabilizer and reducing agent. Biocompatibility; Stable imaging immediately and up to 24 h after injection; clear tumor vascular structures in mice.	Tumor detection	[155]
FI + X-ray CT	BBN-AuNPs	Conjugated BBN-AuNPs demonstrated decreased reticuloendothelial system (RES) organ uptake while increasing uptake at tumor sites.	Prostate, breast, and small-cell lung cancer detection.	[156]
	FA-AuNCs-SiO ₂ nanoprobe	Excellent biocompatibility, active targeting of human gastric carcinoma FR (+) (MGC-803) cells and <i>in vivo</i> gastrointestinal cancer tissues with a diameter of 5 mm in nude mice models.	Cancer cells	[161]
	AuNPs-loaded phantoms	Detect AuNPs at depths acceptable for 3D <i>in vivo</i> investigations on small animals.	Tumor detection	[162]
MRI	MMP-Glycol chitosan-AuNPs	Glycol Chitosan as reducing and stabilizing agent. Good contrasted images of the tumor and recovery of fluorescence.	Tumor detection	[163]
	DNA-GdAuNPs	Citrate is used as a stabilizer and reducing agent. Improved T1 relaxivity and good cell uptake were observed in HeLa and NIH 3T3 cancer cell labeling experiments.	Cancer cells	[168]
SERS	ScFv Ab conjugated PEG AuNPs	Citrate as stabilizer and reducing agent. Targeting cancer cells and xenograft tumors in animal models via passive and active targeting.	Tumor, cancer	[182]
Ultrasound	AuNPs/PLGA hybrid capsules	<i>Ex vivo</i> and <i>in vivo</i> ultrasound-guided HIFU therapy with MAPP is shown to be very effective in ablation of rabbit VX2 xenograft tumors.	Xenograft tumor detection	[185]
FI + MRI + CT	PEG-coated gold nanorod	Ultrasound and microbubbles; Laser thermal therapy on breast cancer cells.	Breast cancer cells	[186]
	Gold cluster and gadolinium oxide	Target folate receptors on KB tumor cells with high specificity.	Tumor cells	[189]

Abbreviation: *Gum Arabic stabilized Au nanoparticles (GA-AuNP), Gold nanorods (AuNR), AuNPs conjugated with gastrin-releasing peptide (GRP) receptor-avid bombesin (BBN), Matrix metalloproteinase (MMP)-sensitive peptide conjugated Glycol chitosan (MMP-Glycol chitosan-AuNP), Deoxythymidine oligonucleotides bearing Gd(III) chelates conjugated AuNP (DNA-GdAuNP) (Amine-terminated fifth-generation poly(amidoamine) (PAMAM); Polydopamine-modified poly(lactic-co-glycolic acid) (AuNPs/PLGA) hybrid capsules, high intensity focused ultrasound (HIFU).

4.2.2. CT and photoacoustic imaging

Katti and Viator et al. demonstrated the novel use of cinnamon coated gold nanoparticles, a very good CT/photoacoustic contrast agent for cancer diagnosis. Cinnamon phytochemical coating onto gold nanoparticles plays a key role in the internalization of gold nanoparticles in cancer cells. Cinnamon coated gold nanoparticles accumulation in lungs enables its use as a lung imaging agent. Cinnamon coated gold nanoparticles were also utilized as a photoacoustic imaging contrast agent for *in vitro* tumor detection [191].

4.2.3. Photoacoustic flowmetry with optical reflectance

Optical absorption is correlative to the number of nanoparticles inside the tumor cells. Hence development of gold nanoparticles which will internalize selectively in tumor cells will be critical. In prostate cancer (PC-3) cells, epigallocatechin gallate (EGCG) conjugated gold nanoparticles (EGCG-AuNPs) selectively internalize with strong photoacoustic signals. Furthermore, EGCG conjugated gold nanoparticles are synthesized following a green process. In order to induce the optical contrast for the detection of non-pigmented tumor cells such as breast, prostate and lung cancers, gold nanoparticles with specific-receptor mediated internalization can be employed [122]. Hainfeld et al. have demonstrated photoacoustic response from PC-3 cells which allowed detection of single cells under flowmetry [150].

4.2.4. X-ray microscopy and fluorescence imaging

Huang et al. demonstrated a solution to high spatial resolution requirement by utilizing gold nanoparticle contrast agent for 3D X-ray and fluorescence imaging of brain tumor microvasculature. They concluded that glioma cells can be identified at inoculation sites in mice brain and subsequent development of gliomas can be followed. Full details of tumor microvasculature and leakage of nanoparticles into brain tumor areas can be detected with this technique as well [192].

5. Applications of gold nanoparticles in therapy

Biosynthesized gold nanoparticles are advantageous in treatment because of their inherent biocompatibility and facile preparations [41–45]. Their bioconjugation chemistry allows the development of tumor targeted nano probes. Gold nanoparticles exhibit enhanced absorption, tunable scattering of electromagnetic radiation and biocompatibility [41–45]. Further, gold nanoparticles can be engineered to have small sizes, both for core and hydrodynamic diameters, thus allowing penetration via porous vasculature and irregular tumor microenvironment (EPR effect) [11,193–199]. Various attributes of gold nanoparticles, as elaborated above, have opened up applications of

various types of gold nanoparticles as nanomedicine agents against viral and bacterial diseases as well as for treating cancer, retinal neovascularization, restenosis, and diabetes (Fig. 19a) etc. [194,195,200, 201].

5.1. Functionalized gold nanoparticles in drug delivery

The versatile surface chemistry of biocompatible gold nanoparticles has facilitated the development of innovative drug delivery systems for use in molecular imaging and therapy of various diseases. Surface chemistry of gold nanoparticles allow for efficient loading of DNA or RNA onto nanoparticulate surfaces via strong and biocompatible covalent interactions [45,46]. Recently, Gold nanoparticles functionalized with cationic dendrimers have shown efficacy as effective delivery agents for RNA delivery [46,47]. Folic acid conjugated gold nanoparticles were incorporated on to poly(amidoamine) dendrimers. Such nano-constructs have demonstrated excellent biocompatibility and surface chemistry to incorporate mRNA, because the polymer coating provides protection for mRNA within the cellular environment against RNases [46,47]. Recently, functionalized and biocompatible gold nanoparticles have found utility toward folate targeting to achieve enhanced receptor-mediated endocytosis, in breast tumor, MCF-7 cells, as evidenced through the receptor competition assays [48]. Recently, biocompatible gold nanorods materials functionalized with an FDA approved targeted monoclonal antibody drug Ramucirumab (Ab) have been investigated for their efficacy in delivering the drug effectively to gastric cancer (GC). This innovative gold nano-based drug delivery approach has shown optimal site specificity of the antibody drug enhancing the recognition, uptake and tumor specific accumulation under *in vitro* and *in vivo* conditions. It is important to recognize that this gold nano-formulation showed tumor cell specific induction of cell death in GC cells with no collateral damage to normal gastric cells [49].

Tumor specific targeting abilities of cancer drug functionalized gold nanoparticles is proving to be highly effective in alleviating debilitating effects of adverse toxicity and drug resistance of standard FDA approved chemotherapeutics [43,50–52]. Gold nanoparticles, because of their innate surface reactivity, have proven to be effective delivery vehicles for multiple cancer therapy drugs [44]. Investigations have shown that bleomycin and doxorubicin can be anchored on gold nanoparticulate surface simultaneously—thus opening new opportunities on capitalizing multiple mechanisms of therapeutic actions. Such multifaceted approaches provide distinct possibilities of reducing development of cancer drug resistance, while site specificity would reduce systemic drug toxicity—all aimed at achieving significant improvement in therapeutic efficacy of FDA approved chemotherapeutic agents [43,44,50–52].

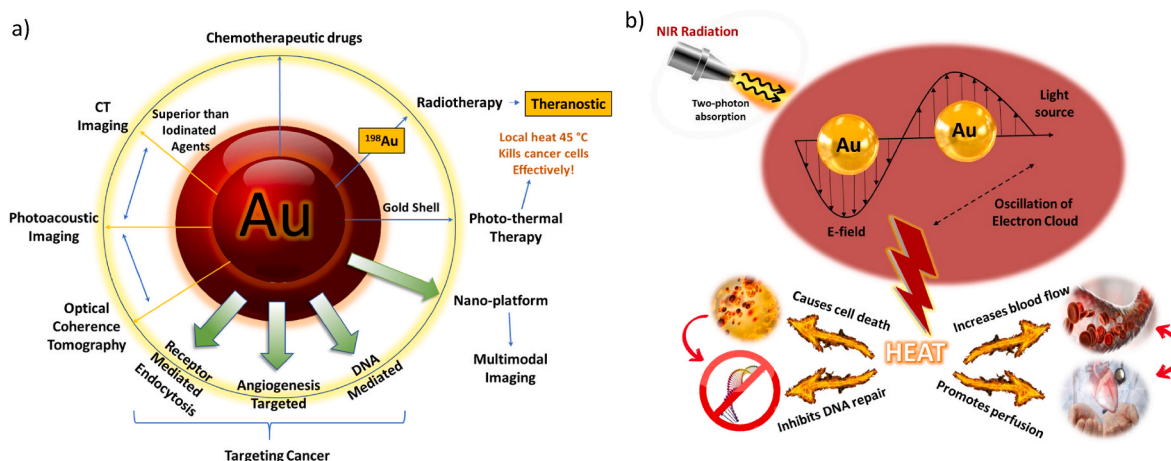


Fig. 19. Multifunctionality of Gold Nanoparticles a) Applications of AuNPs, and b) Photothermal therapy mechanism of AuNPs for targeted localized heating in cancer therapy. (For interpretation of the references to color in this figure legend, the reader is referred to the Web version of this article.)

5.2. Gold nanoparticles in photothermal therapy

Photothermal therapy (PTT) exploits the conversion of photon energy into thermal energy using laser exposure of photothermal sensitizers in the overall pursuit of inducing hyperthermia. Hyperthermia involves subjecting tissue(s) to thermal heat in the temperature range of 41–47 °C for several minutes. Tumors can be selectively and specifically exposed to hyperthermia for total obliteration and eradication in this temperature range due to their reduced heat-tolerance because of strong blood supply compared to normal tissue.

Laser therapy is a non-invasive procedure through an optical source that allows the emission of high-monoenergetic photons radiation in a narrow beam. Effective applications of Lasers in tumor eradication was first documented in 1965 [196]. Laser irradiation of nanoparticles (NPs) sensitize them to produce plasmon resonance (PR) effects as the NPs absorb and scatter light causing localized heating. This process creates irreversible cellular damage [197]. For nanoparticle sensitizers, absorption is preferred near infrared region (NIR) between 750 and 2500 nm to improve light penetration depth into deep tissues, since the intensity enhances the second-harmonic generation and anisotropic two-photon absorption (Fig. 19b). The range is therapeutically useful until 1200 nm [198]. Noble metal nanoparticles have attracted significant attention due to their enhanced absorption cross-sections. Therefore, AuNPs have received paramount importance for the possible applications in effective photothermal therapy with minimal damage to the surrounding healthy tissues [36,197].

The efficiency of NPs for PTT is mainly attributed to the size, shape, and physiochemical properties of nanoparticles. Eustis et al. delineated how optical properties and resonance of AuNPs differ by changing nanoparticles from nanospheres of 15–30 nm to nanorods of 2.5–7.5 aspect ratio (AR) [199]. It has also been shown that gold nanorods are more powerful in PTT destruction than gold nanospheres. NPs should be considered based on the application need in terms of cellular internalization and also based on the production complexity (which is affected by the shape) [36]. As an eco-friendly approach, Fazal et al., synthesized anisotropic AuNPs using a cocoa extract, it was found that the extract served a dual role as a reducing and stabilizing agent [202]. These AuNPs were investigated against epidermoid carcinoma cell lines and results revealed that irradiated AuNPs exhibited localized effective heating for photothermal cancer therapy.

Katti and Gamal-Eldeen et al. have performed detailed investigations for gaining insights on AuNPs conjugated with GA matrix composed of polysaccharides and glycoproteins to yield GA-AuNPs as effective probes for use in PTT. They examined the effects of GA-AuNPs on early stages of diethylnitrosamine (DEN)-induced preneoplastic lesions (PNLs) in the liver of BALB/c mice [36] and chemically-induced *in vivo* lung cancer models [7]. They have investigated the cytotoxicity and phototoxicity of GA-AuNPs in hepatic cell line. Their results have shown that there was no cytotoxicity neither by GA nor GA-AuNPs in the absence of laser exposure and NIR conditions. However, the laser irradiation induced collective photothermal effects resulting in extensive apoptotic cell death attributed to GA-AuNPs nanoparticulate assemblage. The mechanism has been rationalized in terms of the extrinsic apoptotic program since apoptosis was accompanied by a significant increase in the levels of cell death receptor 5 (DR5) and caspase-3 upon GA-AuNPs treatment. The results conclude invoking the interaction between the arabinogalactan in GA and asialoglycoprotein receptors of hepatocytes intensified the observed apoptosis.

Photothermal therapy is highly beneficial as an adjuvant modality in combination with other therapies including chemotherapy, gene regulation and immunotherapy for enhanced antitumor effects and reduced side effects of anticancer drugs. Salem et al. assessed the effectiveness of chitosan-coated 5-fluorouracil (5-FU)-Au nanocomposites combined with PTT as a multimodal cancer treatment method. The half maximal inhibitory concentration (IC₅₀) of drug-loaded NPs was found to be half of the free drug in absence of laser irradiation. Within 20 min of laser

exposure, the 5-FU-Au nanocomposites performed highly efficient photothermal conversion which showed a seven-fold decrease in the IC₅₀ value [203].

5.3. Gold nanoparticles in chemotherapy

Numerous types of cancers initially show response to chemotherapy, but a vast majority of tumors develop resistance in due course. Since cancer has instinctive characteristics such as innate ability to avoid cell death, metastasis and invasion; it is too complicated and challenging to treat within the tumor microenvironment (TME) especially through the approved chemotherapeutic agents [204]. Extensive investigations have shown promise on the utility of functionalized gold nanoparticles due to their ability to selectively target tumor cells and in tandem reducing the toxic off target side effects to healthy cells.

In the green synthesis of AuNPs, as elaborated in previous sections, biomass or extracts of various plants act as reducing agents. Gold nanoparticulate surface serve as efficient phytochemical carrier, which often serve as effective cancer therapy nanomedicine agents. The anticancer mechanisms of gold nanoparticles in terms of their interactions with tumor cells is represented in Fig. 20 [205]. The applications of AuNPs within the realms of green nanotechnology have encompassed delivery of doxorubicin [206], rifampicin [207], paclitaxel [208], and N-acetylcarnosine (NAC) [209].

Biosynthesized gold nanoparticles have been studied extensively for cancer treatment (Table 5) [210,211]. Potential therapeutic effects of AuNPs on A549 lung cancer cells have been evaluated by Castro-Aceituno et al. (2017). *Pleuropterus multiflorus*, an endemic oriental medicinal plant was used in the synthesis of AuNPs. These AuNPs were found to be non-cytotoxic to both normal keratinocytes and lung cancer cells for up to 100 mg/mL [212]. Syed, biosynthesized AuNPs using thermophilic fungus *Humicola* spp. extracellularly and used doxorubicin-conjugated nanoparticles for cytotoxicity, biodistribution and bioconjugation studies [206]. Since AuNPs are stabilized by secreted fungal proteins and peptide phytochelatin, it is presumed that they are capable of targeting multiple-receptors such as luteinizing hormone-releasing hormone (LHRH), epidermal growth factor receptor (EGFR) and EpCAM.

On the antimicrobial/antibiotic fronts, cationic and hydrophobic functionalized AuNPs were found to effectively inhibit the growth of clinical multidrug-resistant microorganisms [methicillin-resistant *Staphylococcus aureus* (MRSA), vancomycin-resistant *Enterococci* (VRE), extended-spectrum β -lactamase (ESBLs), *Klebsiella pneumoniae* carbapenemase (KPC) and gram-positive bacteria] [213,214]. Antibacterial and antifungal activity of novel AuNPs against oral pathogens was suggested by Emmanuel et al., AuNPs were synthesized using *Justicia glauca* (aqueous leaf extract). The broad-spectrum antimicrobial efficacy was boosted by coating NPs with antibiotics. These AuNPs showed

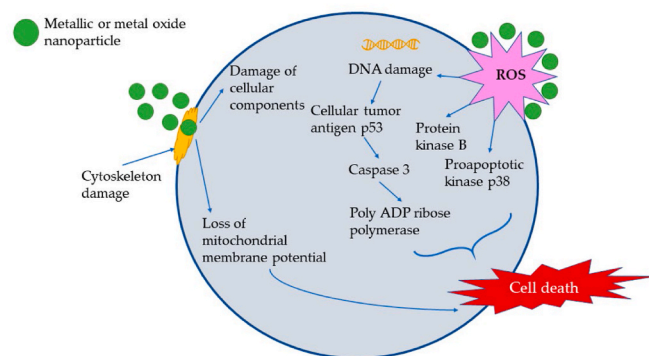


Fig. 20. Possible mechanisms of anticancer activity of AuNPs. (Adapted from Fierascu et al. [203], distributed under the terms of the Creative Commons CC-BY license).

Table 5
Applications of biosynthesized gold nanoparticles and toxicity concerns on various targets.

Nanoparticle	Size	Surface Modification	Application	Target	Toxicity Concerns for AuNPs	References
CAO-AuNPs	35 ± 8 nm	High negatively charged surface, CAO as a stabilizing and capping agent around the surface. Zeta potential of −20 mV	Anti-tumor activity	Human colon cancer, human breast cancer	No significant toxicity on HUVEC (human umbilical vein endothelial cells)	[267]
AuNPs by <i>Enterococcus</i> spp.	6–13 nm	–	Anticancer activity	Liver and lung cancer (HepG2 and A549 cell lines)	–	[211]
<i>Pleuropterus multiflorus</i> (PM-AuNPs)	104.8 nm	–	Anticancer activity	Lung cancer (A549 cell line)	No significant toxicity evaluated on HaCaT (normal keratinocyte) cell line	[212]
Colloidal AuNPs by <i>Justicia glauca</i>	32.5 ± 0.3 nm	Antibiotic coat	Antibacterial and antifungal activity	Oral pathogens	–	[214]
NAC loaded AuNPs by <i>Coccinia grandis</i> bark extract.	20 nm	–	Cataract treatment	L929 fibroblast cell line	Encapsulation of NAC into AuNPs did not show cytotoxicity against fibroblast cells	[209]
AuNPs by <i>Saccharomyces cerevisiae</i>	13 ± 1 nm	–	Anticancer activity	Ehrlich ascites carcinoma cells	No toxicity on normal cells observed	[193]
Anisotropic AuNPs by cocoa extract	150 ± 20 nm	Polyphenol coating. Zeta potential of −50 ± 8 mV	Photothermal ablation by femtolaser irradiation X-ray CT imaging	A431 human epidermoid carcinoma cell line	(–) Laser irradiation on untreated cells. No cytotoxicity for 100 µg/mL AuNPs + no laser irradiation. However, a slight reduction (~80%) in cell viability for 200 µg/mL AuNPs was observed for L929 and NIH-3T3 healthy cells	[202]
AuNPs by <i>Tricholoma crassum</i>	2–22 nm	Capped by natural proteins	Antimicrobial effectiveness against bacteria, fungi, and pathogenic microorganisms that are multidrug resistant Gene delivery for cancer cells	<i>Agrobacterium tumefaciens</i> strain LBA4404 and <i>E. coli</i> strain DH5α <i>Magnaporthe oryzae</i> spores Sarcoma 180 cancer cells Hepatocellular carcinoma	The maximum hemolytic activity detected for human erythrocytes at high nanoparticle solution concentrations (up to 20 g/mL) was less than 8%, indicating extremely minimal blood toxicity. (–) Laser irradiation with GA (9.0–57.7 µg/mL), GA-AuNPs (1.6–8.6 µg/mL), and GA (57.7 µg/mL) did not result in cell death in HepG2 cells.	[268]
GA-AuNPs	The core size: 21 ± 6 nm hydrodynamic size: 78 ± 4 nm	Capped by natural proteins	Photothermal suppression of hepatocarcinogenesis produced by lasers through activation of the extrinsic apoptotic pathway and inhibition of inflammation.	Hepatocellular carcinoma	(–) Laser irradiation with GA (9.0–57.7 µg/mL), GA-AuNPs (1.6–8.6 µg/mL), and GA (57.7 µg/mL) did not result in cell death in HepG2 cells.	[36]
AuNPs by <i>Humicola</i> spp.	18–24 nm	Capped by natural proteins	Anticancer, anti-angiogenesis	MDA-MB-231 human breast cancer cell line and NIH3T3 mouse embryonic fibroblast cell line.	Although nanoparticles are nontoxic to both normal (NIH3T3 mouse embryonic fibroblast) and malignant (MDA-MB-231 human breast carcinoma) cell lines at doses up to 50 µg/mL, they may be utilized confidently in targeted drug delivery systems.	[206]
AuNPs using chitosan	50 nm for drug loaded NPs	Negative charge on the surface	Antimicrobial activity	Gram positive bacteria (<i>B. subtilis</i>) and gram-negative bacteria (<i>Pseudomonas aeruginosa</i>).	–	[207]
GA- ¹⁹⁸ AuNPs	Hydrodynamic size of 85 nm	GA Coating	Anticancer activity	Prostate Cancer	No evidence of systemic harm has been detected over extended periods of time in toxicological studies employing standard dosages of radiation.	[39,218, 222]
EGCG- ¹⁹⁸ AuNPs	Hydrodynamic size of 65 ± 5 nm	EGCG coating	Anticancer activity	Selective affinity for Lam 67R receptors, which are overexpressed in prostate, colorectal, and a variety of other human cancers	Leakage into the blood is minimal/none. Overall health status, body weight, and blood parameters of mice treated with EGCG- ¹⁹⁸ AuNP demonstrate	[223]

(continued on next page)

Table 5 (continued)

Nanoparticle	Size	Surface Modification	Application	Target	Toxicity Concerns for AuNPs	References
MGF- ¹⁹⁸ AuNPs	Hydrodynamic size of 55 ± 1 nm	MGF coating	Anticancer activity	Selective affinity towards Lam 67R receptors, which are overexpressed in prostate, colorectal, and a variety of other human cancers	that radiotherapy is both effective and well tolerated. No signs of systemic toxicity.	[65]
Bimetallic (Au–Ag) NPs with <i>O. basilicum</i> , <i>Moringa oleifera</i> leaf and flower Extracts	21 ± 12 nm for the leaf formed bimetallic (Au–Ag) NPs 25 ± 9.63 nm for the flower formed bimetallic (Au–Ag) NPs.	–	Antidiabetic phytonanotherapy Antibacterial activity	Type Vi-B from porcine pancreas Against <i>S. aureus</i> , <i>E. coli</i> , <i>P. aeruginosa</i> , and <i>Bacillus subtilis</i>	–	[269]
Au NPs using chitosan	Hydrodynamic size of 100–500 nm	Positively charged amino groups on the surface of Au NPs	5-fluorouracil (5-FU) dosages are being reduced as a result of chemotherapy and photothermal treatment.	Hepatocellular carcinoma cells (HepG2)	–	[203]

*AuNP: gold nanoparticle, CAO: Carrageenan oligosaccharide, EGCG: Epigallocatechin gallate, GA: Gum Arabic, MGF: Mangiferin, NAC: N-acetylcarnosine, PM: *Pleuropterus multiflorus*.

antimicrobial activity ranging from 14 to 17 mm against *M. luteus*, *S. aureus*, *S. mutans*, *L. acidophilus*, *E. coli*, *P. aeruginosa*, *S. cerevisiae* and *C. albicans* [214]. Wang et al. (2018) synthesized gold nanoparticles using *Coccinia grandis* bark extract encapsulated them with N-acetylcarnosine (NAC) drug molecules for the treatment of senile cataracts [209].

5.4. Radioactive gold nanoparticles in cancer therapy

Radioactive gold nanoparticles have shown tremendous new opportunities toward the creation of next generation nanoradiopharmaceuticals for diagnostic, therapeutic and theranostic applications. Targeted radioactive gold NPs, homed into tumor masses, are capable of destroying tumor cells/tissues selectively with excellent efficacy causing minimal/no damage to surrounding healthy cells [215]. Radionuclide pharmaceuticals provide very high biological effects attributed by the delivery of highly potent forms of radiation directly to tumor cells and masses for cancer therapy. Radioactive nanoparticles facilitate radiation-induced ionizations, excitations, chemical transmutations, nuclear recoil, and local charge effects. Moreover, radioactive nanoparticles can emit γ photons, X-ray photons, and energetic negatrons/positrons utilized in cancer therapy with real-time imaging and therapeutic monitoring outcome capabilities.

For example, ¹⁹⁸Au exhibits β energy emission ($\beta_{\max} = 0.96$ MeV) and half-life ($t_{1/2} = 2.7$ days) that are highly suitable for destroying tumors at cellular levels [216]. ¹⁹⁸Au nanoparticles (¹⁹⁸AuNPs) exhibit a tissue penetration depth of up to 11 mm (equivalent to 1100 cell diameters), therefore ¹⁹⁸AuNPs are powerful in destroying tumor cells within this 11 mm range, yet short enough for minimal collateral damage [217]. ¹⁹⁸AuNPs derived Auger electron cascades offer substantial impacts on cancer therapy. The burst of low-energy electrons attributed by the electron emission due to the transient atoms decay results in extremely localized energy deposition (106–109 cGy) in a region of cubic nanometers surrounding the decay position. Immediate vicinity of the decay from ¹⁹⁸Au will be irradiated by these electrons as this process is significantly important for localized tumor therapeutic effects. Katti et al. have pioneered extensive investigations demonstrating compelling clinical evidence on the therapeutic effectiveness of using functionalized ¹⁹⁸AuNPs in the treatment of cancers in mice and dogs (as tumors in dogs mimic human cancers) [27,30,65,67,156,218].

There are several hypotheses on how and why engineered radioactive gold nanoparticles can serve as targeted radioactive probes with facile drug passage for use in a variety of cancer therapy modalities. One

hypothesis encompass: (1) Exploiting the leaky and porous tumor microenvironment, intrinsically therapeutic radioactive ¹⁹⁸AuNPs with low hydrodynamic size (85–100 nm) can be engineered to take advantage of EPR effects for uniform distribution, thus allowing tumor dosimetry to be uniform; (2) Radioactive ¹⁹⁸Au has an advantageous β energy emission ($\beta_{\max} = 0.96$ MeV) and half-life ($t_{1/2} = 2.7$ days) for effective destruction of tumor mass [38,217,219]. A tissue penetration depth range of 11 mm (up to 1100 cells diameter) is very efficient in overcoming tumor therapy obstacles resulting from suboptimal dosing of chemotherapeutics not reaching the tumor site efficiently [9,220]. Given the possibility of non-uniform distribution of ¹⁹⁸AuNPs within tumor sites, the penetration depth range and proximity of β rays (up to 11 mm in tissues or up to 1100 cell diameters) would still be efficient to cover the entire tumor mass, providing a novel therapeutic modality for the treatment of a variety of cancers.

In continued efforts toward finding new biocompatible gold compounds, a new family of trigonal and tetrahedral gold compounds functionalized with biocompatible water-soluble hydroxymethyl phosphine ligands was created by Katti and colleagues [221]. These biocompatible gold compounds exhibited wide antitumoral properties against tumors (breast, lung, non-Hodgkin's lymphoma, pancreatic, and prostate tumors) and various debilitating diseases which include osteoarthritis and Parkinson's diseases established through comprehensive preclinical *in vivo* investigations in mice, tumor-bearing dogs and most recently in human clinical trials [11].

In the context of prostate tumor therapy especially for patients in advanced disease stages, surgical removal is not an option. In such cases, localized therapy using radiation has a lot of potential offering significant benefits to patient population. Localized therapy utilizing β - or α -emitting radiation would be beneficial for the total eradication of micrometastatic disease. Radioactive ¹⁹⁸AuNPs in the size ranging from 30 to 100 nm, provide an attractive clinical therapeutic platform for targeted and localized treatment due to their high internalization into the tumor via tumor vasculature (typical diameter of 4–9 μ m). ¹⁹⁸AuNPs can readily be functionalized with tumor-specific ligands to enhance and facilitate their selective uptake within tumor cells. Therefore, tumor specific ligand(s)-functionalized radioactive gold NPs offer unparalleled advantages, as their size is suitable for effective permeation and retention effects (EPR), while tumor specific conjugation of proteins/peptides would enhance tumor selectivity and uptake to clinically significant levels. We discuss in the following sections specific examples showing results from extensive preclinical investigations on the utility of

^{198}Au NPs as effective nano-radiopharmaceuticals for use in oncology.

5.4.1. Gum Arabic functionalized ^{198}Au nanoparticles (GA- ^{198}Au NPs)

Acacia plant derived Gum arabic (GA) protein has found excellent utility in the synthesis and stabilization of AuNPs. It encapsulates AuNPs, thus providing excellent *in vitro* and *in vivo* stability. GA functionalized ^{198}Au NPs exhibit a hydrodynamic size of 85 nm which is optimum for efficient permeation across tumoral membrane through EPR and endocytosis mechanisms. When GA- ^{198}Au NPs were administered intratumorally into prostate tumor bearing xenografts in mice, *in vivo* investigations demonstrated that over 80% of retention of ^{198}Au therapeutic dose remained within the tumors with concurrent tumor retention over extended periods. Investigations on therapeutic efficacy and effectiveness of GA-functionalized ^{198}Au NPs in radiotherapy, intratumoral administration of single doses of GA- ^{198}Au NPs, resulted in a significant reduction (>85%) of the tumor volume when compared to control animal groups treated with saline. For extended periods of time, these investigations revealed no indications of systemic toxicity from the GA- ^{198}Au NPs, as elucidated through toxicological investigations using biological effective doses of radiotherapy [38,215,218,222].

5.4.2. Epigallocatechin gallate (EGCG) functionalized ^{198}Au nanoparticles (EGCG- ^{198}Au NPs)

Epigallocatechin gallate (EGCG) is a polyphenol found in abundance in tea. Due to its electron rich (or strong antioxidant) properties, this phytochemical serves as a powerful reducing agent to transform gold salt (HAuCl_4) into the EGCG encapsulated corresponding gold nanoparticles (EGCG-AuNPs) [27,65,67,218]. Pioneering investigations of Katti et al. have shown the dual role of EGCG in reduction and stabilization, through effective capping of gold nano-particulate surface, by synthesizing tumor specific EGCG-AuNPs. EGCG is well-known for its specific affinity towards Lam 67R receptors, which are overexpressed in a variety of human cancers, including prostate, colorectal, and a variety of other malignancies [67]. As a result, when EGCG-AuNPs are incubated with prostate tumor cells, derived from human prostate cancer (PC-3), they are internalized into PC-3 cells through the vacuoles and cytoplasm without entering the nucleus. The quantification of gold content in PC-3 cells using neutron activation analysis (NAA) and dark field microscopy, as well as extensive receptor blocking experiments, revealed that EGCG- ^{198}Au NPs are internalized into PC-3 cells through Lam 67 receptor-mediated endocytosis (RME). The AuNPs are found inside tumor cells, demonstrating excellent *in vivo* stability of EGCG-AuNPs. Extensive *in vivo* investigations on EGCG- ^{198}Au NPs tumor retention were conducted in mice bearing prostate tumor xenografts. In comparison to GA- ^{198}Au NPs, EGCG- ^{198}Au NPs demonstrated superior absorption of therapeutic payload inside tumors with minimal/no lymphatic leakage into the blood (only 0.06% ID/g at 24 h).

EGCG- ^{198}Au NPs showed excellent (94%) tumor retention over 24 h. Tumor specific EGCG- ^{198}Au NPs had an improved biodistribution compared to the non-specific GA- ^{198}Au NPs. Following a single intratumor injection of EGCG- ^{198}Au NPs, a substantial decrease in tumor volume (80%) was observed after a month, with minimal/no uptake in non-target organs. The tumors from the treatment group (EGCG- ^{198}Au NPs) were mostly necrotic, indicating significant tumor cell-kill and therapeutic effectiveness [67]. The tolerability of EGCG- ^{198}Au NPs *in vivo* was established by monitoring the body weight and blood parameters in both treated and control groups of mice. These results indicate that EGCG- ^{198}Au NPs nanomedicine radiotherapy is both effective and well tolerated. The selectivity of EGCG- ^{198}Au NPs for prostate cancer cells is a critical advantage of this approach because it showed effective treatment and stabilization of the primary disease thus suppressing/eliminating secondary morbidity. Therefore, EGCG- ^{198}Au NPs injected intratumorally is an effective new therapeutic approach in treating prostate and other solid tumors [67,215].

5.4.3. Mangiferin (MGF) functionalized ^{198}Au nanoparticles (MGF- ^{198}Au NPs)

Mangiferin (MGF), a glucose functionalized xanthonoid found abundantly in mango peel, acts as an effective reducing agent by injecting electrons for the production of stable MGF-AuNPs with tumor specific characteristics. MGF's ability to create an *in vitro* and *in vivo* stable corona around gold nanoparticles has resulted in the industrial scale production of therapeutic MGF-AuNPs. Detailed investigations by Katti et al. have shown that MGF-AuNPs exhibit specificity to laminin receptors overexpressed in many cancers, such as prostate, colorectal, pancreatic and breast cancers. The development of the corresponding radioactive MGF- ^{198}Au NPs has been recently achieved giving a multi-purpose theranostic system that can be used both for treatment and diagnosis of cancers. ^{198}Au emits both therapeutic beta emissions and diagnostic gamma rays for quantification of gold inside the tumors. Because of the high specificity of MGF-AuNPs toward laminin receptors, high tumor accumulation can be achieved. *In vivo* investigations in tumor bearing animals have revealed that over 80% of the dose injected intratumorally was retained within prostate tumors (PC-3) with minimal/no lymphatic drainage of radioactivity into non-target organs. Overall, a 5-fold reduction of tumor volume has been observed after three weeks of treatment as compared to untreated control groups [9]. Overall, MGF- ^{198}Au NPs nanomedicine agent showed significantly higher tumor retention when compared to GA- ^{198}Au NPs and EGCG- ^{198}Au NPs nanomedicine agents, presumably due to the glucose structural motif of MGF. Glucose moiety in MGF-AuNPs, targets tumors more than the normal cells, due to the efficient glycolysis pathway in all tumors.

Therefore, nanomedicine agents with MGF architecture (such as MGF-AuNPs) offer new opportunities in the development of therapeutic agents for treating prostate and other cancers. It may be noted that the currently available standard of care, through brachytherapy, which relies on radioactive brachytherapy seeds of 50–500 μm in size suffers from severe limitations due to limited efficacy and safety. Tumor vasculature allows porosity in the 10–500 nm range and the large size of brachy seeds fail to penetrate the tumor membrane. This causes leakage of seeds into non-target organs creating systemic radiotoxicity. MGF- ^{198}Au NPs, with a hydrodynamic size of 55 nm, can penetrate prostate tumors readily exhibiting a sufficiently high retention of therapeutic dose within tumors with minimal/lymphatic drainage in non-target organs. In addition, laminin receptor avidity of MGF-AuNPs, as discussed above, serve as an additional advantage in achieving tumor specificity of MGF-AuNPs for its effective use in oncological applications.

5.5. Laminin receptor-avid nanotherapeutic EGCG-AuNPs to prevent restenosis

As an alternative to drug-coated stents, EGCG-AuNPs can be rapidly internalized into smooth muscle cells (SMCs) and endothelial cells (ECs) through laminin receptor-mediated endocytosis (RME). This was supported by detailed toxicity profiles and specific affinity for SMCs and ECs—thus making EGCG-AuNPs an attractive candidate as a new therapeutic agent for treating cardiovascular diseases [223].

Many engineered AuNPs including EGCG-AuNPs have been discovered for use in various therapeutic applications [27,37,39,65,67,156,224]. Polyphenolic EGCG, obtained from tea extract have anti-thrombotic, anti-inflammatory and antioxidant properties [225,226]. EGCG-AuNPs are readily internalized by RME crossing the hydrophobic barrier of cell membranes [223]. Laminin receptors are expressed on ECs and SMCs within arterial walls [227]. Therefore, laminin receptor specific EGCG-AuNPs have the potential for use in effective repairs of vascular injuries—in this way, neointimal hyperplasia and restenosis caused by oxidative stress are substantially reduced, and the treatment of these conditions is greatly improved [223].

5.6. Gold nanoparticles in X-ray therapy

Dose amplification of X-ray therapeutic doses present huge clinical benefits. This has been demonstrated by encapsulation of tissue mimics on gold foil before X-ray therapy. Radiation dose amplification by a factor of 100 could be achieved in an environment of tissue-equivalent polymethylmethacrylate (PMMA) near to the surface of a thin metallic gold foil [71,72]. Dosimetry calculations indicated that a dose of 100 mGy delivered by 80 kV X-rays resulted in a frequency at an implanted gold surface equivalent to the frequency gained with a dose of about 4.5 Gy of ^{60}Co γ rays in homogeneous PMMA. This indicates that AuNPs have a substantially greater surface area to volume ratio and may exhibit improved dosimetry. The use of poly ^{198}Au radioactive gold dendrimer composite NPs (size 10–29 nm) for targeted radiopharmaceutical dose distribution to tumor masses has been reported [228]. Numerous studies have shown that a single intratumoral injection of 22 nm-sized NPs providing a dose of 74 μCi (after 8 days), reduced tumor volumes significantly by 45% in comparison with untreated groups [38].

The dose enhancement factor (DEF) is used to quantify the effect of AuNPs on radiotherapy efficiency amplification. The DEF of AuNPs is the ratio of the radiation dose absorbed by cancer cells in the presence of AuNPs to the dose absorbed in the absence of AuNPs [72,229]. Additionally, this effect may vary depending on the concentrations and properties of AuNPs, as well as their position inside the cell [72].

6. Toxicity of gold nanoparticles

Gold nanoparticles have great potential for imaging and therapy of cancers, inflammatory, cardiovascular, and ocular diseases. The current and the tremendous future utility of functionalized gold nanoparticles in various biomedical applications necessitates detailed investigations aimed at understanding the systemic toxicity of a myriad gold nanoparticles. As a result, substantial animal studies are required to provide insight into dose limits and establish safe concentrations of gold nanoparticles for application *in vivo*. [230].

Metallic gold's biosafety is well established, and it has been utilized *in vivo* since the 1950s. Functionalized AuNPs exhibit dose dependent toxicity profiles [231]. According to research conducted on different plant-derived metallic nanoparticles, cytotoxicity was dependent on time and dose. Irrespective of the type of cancer cell, biosynthesized silver nanoparticles were more lethal than gold nanoparticles synthesized by the same plants (*Plumbago zeylanica*, *Commelina nudiflora*, and *Cassia auriculata*). The majority of research have indicated that the cytotoxicity of AuNPs is highly dependent on their size and shape. It is discovered that cytotoxicity is inversely related to size. When gold nanoparticles were reduced in size, the LD_{50} or IC_{50} values decreased proportionately. The cellular response to gold nanoparticles is size dependent. Pan et al. (2007), for example, demonstrated that AuNPs with the smallest size measured (1.4 nm) had the greatest toxicity when compared to AuNPs with sizes up to 15 nm. This confirmed that the toxicity of nanoparticles is size and ligand dependent [230,232].

Metallic nanoparticles produced by plant-mediated synthesis were predominantly spherical or quasi-spherical in shape, with a mean lethal dose of 1–20 g/mL. Other forms of nanoparticles (triangular, hexagonal, and rods) were less effective. When employed in therapy, powerful anti-cancer medicines have the potential to destroy not only cancer cells but also normal healthy cells [232]. Metallic nanoparticles, derived from the mango peel, Genipa Americana fruit and night jasmine flowers, showed no cytotoxic effects, thus opening up new opportunities for the use of these and related phytochemicals from plants as drug-delivery carriers for various drug development applications [230].

Dong et al. established the cytotoxicity of AuNCs stabilized with bovine serum albumin (BSA) utilizing three tumor cell lines and two normal cell lines. This research indicated that adding free BSA to BSA-AuNCs solutions may reduce cytotoxicity, suggesting that BSA can protect cells from harm. The AuNCs showed varying degrees of

cytotoxicity against various cells, which may account for gold nanoparticle's apparent toxicity within a specific concentration range [233]. Dhar et al. investigated the oral toxicity of gellan gum synthesized gold nanoparticles (GG-AuNPs). Subacute 28-day oral toxicity studies in rats were used to determine the toxicity of GG-AuNPs. After subacute delivery of GG-AuNPs to rats, no haematological or biochemical abnormalities were observed, suggesting that these AuNPs were well-tolerated for a 28 day period [234].

Surapaneni et al. investigated the molecular mechanisms behind the cytotoxicity of differently charged AuNPs in triple negative breast cancer (TNBC) cells. Cell toxicity assays revealed that the surface potential of AuNPs had an effect on several epigenetic alterations. Furthermore, negatively charged AuNPs triggered a gradual death process in MDA-MB-231 cells, while positively charged AuNPs resulted in an abrupt cell death [235]. It is well established that the liver is the primary site of gold nanoparticles (AuNPs) accumulation in humans. Paino et al. took advantage of this by utilizing human hepatoma (HepG2) cells as *in vitro* toxicological models. Healthy cells are less susceptible to DNA damage than cancer cells are. The findings indicate that gold nanoparticles interact with HepG2 cells and human peripheral blood mononuclear cells (PBMCs) and may potentially show *in vitro* gene and cytotoxicity at very low doses [236].

Zhang et al. investigated the *in vivo* cytotoxicity of AuNPs with a diameter of 13.5 nm in mice. Over a 14 to 28-day period, the authors examined animal survival, weight, hematological, morphology, and $\mu\text{g}/\text{organ}$ index at various concentrations (137.5–2200 μg). The data suggested that AuNPs posed no substantial toxicity at low doses, even after they degraded *in vivo* over time. Increasing the concentration of AuNPs, on the other hand, resulted in weight reduction, but no statistically significant difference was found. Additionally, among the three different administration routes, oral and intraperitoneal injections were found to be highly toxic, while tail vein injection was the least toxic [231].

Once within the body, AuNPs interact with a variety of biological molecules, including proteins, lipids, polysaccharides, and nucleic acids. Plasma proteins are able to interact with AuNPs resulting in a protein corona, which has an effect on the biodistribution and availability of AuNPs in various organs and tissues. The interaction of AuNPs with proteins may alter the AuNP's and protein's inherent characteristics. Notably, the interaction can induce a variety of physiological changes, including changes in the conformation of bound proteins, complement activation, blood clotting, and protein aggregation. The cellular effects of AuNPs are the result of the synergistic combinations of various factors, including dose, duration of exposure, and the characteristics of nanoparticles, such as surface chemistry, surface charge, size, functionalization, and shape, as well as the protein corona [237].

Both the safety profile and therapeutic efficacy of AuNPs are critical for their biomedical applications. Current studies have significantly increased our knowledge of the biological effects of AuNPs; however, detailed investigations about the mechanisms remain necessary. Complexity in nanoparticle characteristics, cell types, tumor microenvironments, and physical factors all influence cell-nanoparticle interactions, which has a direct effect on toxicity and effectiveness. To develop a reasonable design of nanomaterials in the future, it is necessary to gain a better understanding of the systemic interaction of gold nanoparticles with proteins. Moreover, appropriate analytical techniques are critical for deciphering how AuNPs affect the structures and physiological functions of proteins and cells, as well as their fate *in vivo*. It is essential to employ state-of-the-art techniques, such as single-cell analysis, to forecast possible risks to cells [237].

7. Conclusions

The coverage of subject matter in this review embodies recent and cutting-edge advances in Green Nanotechnology, especially as they relate to important implications in diagnostic and therapeutic nanomedicine. The overarching theme of Green Nanotechnology, as

discussed in several sections, emphasizes the need to embrace green technological processes to reduce the continuous carbon foot print and global warming consequences. The specific types of gold nanoparticles, derived through Green Nanotechnology, as discussed elaborately provide how nanotechnology of gold can deliver a paradigm shift in the way diagnosis and therapy of cancer and various other diseases would be performed in the near future. In particular, this review covers the chemistry, physics, engineering and various fascinating scientific aspects of gold nanoparticles and relate those specific properties to deliver medical applications. This review unequivocally outlines the power of plant kingdom, through a plethora of high-antioxidant phytochemicals, on how those electrons from plants can be used to synthesize and stabilize phytochemicals-encapsulated nanoparticles for various medical applications. The tremendous diversity of the plant kingdom will, in the future, translate into widespread applicability of Green Nanotechnology to sectors beyond the field of Medicine.

Declaration of competing interest

The authors declare no conflict of interests.

Acknowledgements

This work has been carried out within the Erasmus Mundus Joint Master Degree “Nanomedicine for Drug Delivery” (NANOMED EMJMD) and financially supported by the Education, Audiovisual and Culture Executive Agency (EACEA) of the European Commission and is part of the Erasmus Programme. The authors P. Çakilkaya, U. Farooq, H. Genedy, N. Kaeokhamloed, H. Phan, R. Rezwan and G. Tezcan thank Prof. K. Andrieux, Prof. S. Antimisari, Prof. C. Caramella, Dr C. Roques, Dr E. Roger and Prof. M. C. Venier-Julienne who co-lead the training programme of NANOMED EMJMD. We also acknowledge all the logistical support from the Institute of Green Nanotechnology, University of Missouri, Columbia, USA. Prof. Kattesh V. Katti thanks International Atomic Energy Agency (IAEA), Vienna, Austria, and the University of Missouri, Institute of Green Nanotechnology, for support.

Appendix A. Supplementary data

Supplementary data to this article can be found online at <https://doi.org/10.1016/j.jddst.2022.103256>.

References

- [1] J. Tollefson, Earth is warmer than it's been in 125,000 years, says Landmark Climate Report, *Nature* 596 (5) (2021) 171–172, <https://doi.org/10.1038/d41586-021-01518-8>.
- [2] S. Modi, et al., Recent trends in fascinating applications of nanotechnology in allied health sciences, *Crystals* 12 (1) (2022), <https://doi.org/10.3390/cryst12010039>.
- [3] A. Barhoum, et al., Review on natural, incidental, bioinspired, and engineered nanomaterials: history, definitions, classifications, synthesis, properties, market, toxicities, risks, and regulations, *Nanomaterials* 12 (2) (2022) 177, <https://doi.org/10.3390/nano12020177>.
- [4] M. Gupta, K. Seema, in: K. Pal (Ed.), *Living Nano-Factories: an Eco-Friendly Approach towards Medicine and Environment BT - Bio-Manufactured Nanomaterials: Perspectives and Promotion*, Springer International Publishing, Cham, 2021, pp. 95–124.
- [5] T. Tangthong, et al., Water-soluble chitosan conjugated DOTA-bombesin peptide capped gold nanoparticles as a targeted therapeutic agent for prostate cancer, *Nanotechnol. Sci. Appl.* 14 (Mar. 2021) 69–89, <https://doi.org/10.2147/NSA.S301942>.
- [6] K.V.K.M. Khoobchandani, et al., Prostate tumor therapy advances in nuclear medicine: green nanotechnology toward the design of tumor specific radioactive gold nanoparticles, *J. Radioanal. Nucl. Chem.* 318 (3) (2018) 1737–1747, <https://doi.org/10.1007/s10967-018-6320-4>.
- [7] A.M. Gamal-Eldeen, et al., Gum Arabic-encapsulated gold nanoparticles for a non-invasive photothermal ablation of lung tumor in mice, *Biomed. Pharmacother.* 89 (2017) 1045–1054, <https://doi.org/10.1016/j.biopha.2017.03.006>.
- [8] M. Khoobchandani, et al., New approaches in breast cancer therapy through green nanotechnology and nano-ayurvedic medicine - pre-clinical and pilot human clinical investigations, *Int. J. Nanomed.* 15 (Jan. 2020) 181–197, <https://doi.org/10.2147/IJN.S219042>.
- [9] A.Y. Al-Yasiri, et al., Mangiferin functionalized radioactive gold nanoparticles (MGF-198AuNPs) in prostate tumor therapy: green nanotechnology for production; in vivo tumor retention and evaluation of therapeutic efficacy, *Dalton Trans.* 46 (42) (Oct. 2017) 14561–14571, <https://doi.org/10.1039/c7dt00383h>.
- [10] V.C. Thihe, et al., Development of resveratrol-conjugated gold nanoparticles: interrelationship of increased resveratrol corona on anti-tumor efficacy against breast, pancreatic and prostate cancers, *Int. J. Nanomed.* 14 (2019) 4413–4428, <https://doi.org/10.2147/ijn.s204443>.
- [11] M. Khoobchandani, et al., Green nanotechnology of MGF-AuNPs for immunomodulatory intervention in prostate cancer therapy, *Sci. Rep.* 11 (1) (2021) 16797, <https://doi.org/10.1038/s41598-021-96224-8>.
- [12] N.R.S. Sibuyi, V.C. Thihe, K. Panjtan-Amiri, M. Meyer, K.V. Katti, Green synthesis of gold nanoparticles using acai berry and elderberry extracts and investigation of their effect on prostate and pancreatic cancer cells, *BJGP Open* 8 (2021) 1–8, <https://doi.org/10.1177/1849543521995310>.
- [13] M.J. Eckelman, J.B. Zimmerman, P.T. Anastas, Toward green nano, *J. Ind. Ecol.* 12 (3) (Oct. 2008) 316–328, <https://doi.org/10.1111/j.1530-9290.2008.00043.x>.
- [14] A. DeViero Kreuder, et al., A method for assessing greener alternatives between chemical products following the 12 principles of green chemistry, *ACS Sustain. Chem. Eng.* 5 (4) (Apr. 2017) 2927–2935, <https://doi.org/10.1021/acssuschemeng.6b02399>.
- [15] A. McWilliams, *Nanodevices and Nanomachines: the Global Market*, vol. 11, 2018.
- [16] Williams Nanocomposites NANO21H Report Overview.Pdf.”.
- [17] T. Tangthong, et al., Bombesin peptide conjugated water-soluble chitosan gallate—a new nanopharmaceutical architecture for the rapid one-pot synthesis of prostate tumor targeted gold nanoparticles, *Int. J. Nanomed.* 16 (October) (2021) 6957–6981, <https://doi.org/10.2147/IJN.S327045>.
- [18] M. Khoobchandani, K.K.V. Katti, A.R. Karikachery, V.C. Thihe, P.L.R. Bloebaum, K.K.V. Katti, *Targeted Phytochemical-Conjugated Gold Nanoparticles In Cancer Treatment*, Biotechnol, Springer International Publishing, 2019.
- [19] P. Singh, S.K. Yadav, M. Kuddus, in: S. Ahmed, W. Ali (Eds.), *Green Nanomaterials for Wastewater Treatment BT - Green Nanomaterials: Processing, Properties, and Applications*, Springer Singapore, Singapore, 2020, pp. 227–242.
- [20] R. Dhinra, et al., Sustainable nanotechnology: through green methods and life-cycle thinking, *Sustainability* 2 (10) (Oct. 2010) 3323–3338, <https://doi.org/10.3390/su2103323>.
- [21] J.J. Cao, Y. Huang, Q. Zhang, Ambient air purification by nanotechnologies: from theory to application, *Catalysts* 11 (11) (2021) 1–41, <https://doi.org/10.3390/catal1111276>.
- [22] S.Z. Mat Isa, R. Zainon, M. Tamal, State of the art in gold nanoparticle synthesis via pulsed laser ablation in liquid and its characterisation for molecular imaging: a review, *Materials* 15 (3) (2022) 875, <https://doi.org/10.3390/ma15030875>.
- [23] M.H. Hussain, et al., Synthesis of various size gold nanoparticles by chemical reduction method with different solvent polarity, *Nanoscale Res. Lett.* 15 (2020) 140–150.
- [24] M. Sengani, A.M. Grumazescu, V.D. Rajeswari, Recent trends and methodologies in gold nanoparticle synthesis – a prospective review on drug delivery aspect, *Open 2* (July) (Oct. 2017) 37–46, <https://doi.org/10.1016/j.onano.2017.07.001>.
- [25] E.V. Soares, H.M.V.M. Soares, Harmful effects of metal(loid) oxide nanoparticles, *Appl. Microbiol. Biotechnol.* 105 (4) (2021) 1379–1394, <https://doi.org/10.1007/s00253-021-11124-1>.
- [26] A. Zambre, et al., CHAPTER 6:green nanotechnology – a sustainable approach in the nanorevolution, in: *Sustainable Preparation of Metal Nanoparticles*, 2012, pp. 144–156.
- [27] R. Shukla, et al., Soybeans as a phytochemical reservoir for the production and stabilization of biocompatible gold nanoparticles, *Small* 4 (9) (Sep. 2008) 1425–1436, <https://doi.org/10.1002/sml.200800525>.
- [28] A. Vágó, G. Szakacs, G. Sáfrán, R. Horvath, B. Pécz, I. Lagzi, One-step green synthesis of gold nanoparticles by mesophilic filamentous fungi, *Chem. Phys. Lett.* 645 (Oct. 2016) 1–4, <https://doi.org/10.1016/j.cplett.2015.12.019>.
- [29] N. González-Ballesteros, S. Prado-López, J.B. Rodríguez-González, M. Lastra, M. C. Rodríguez-Argüelles, Green synthesis of gold nanoparticles using brown algae *Cystoseira baccata*: its activity in colon cancer cells, *Colloids Surf. B Biointerfaces* 153 (Oct. 2017) 190–198, <https://doi.org/10.1016/j.colsurf.2017.02.020>.
- [30] V. Kattumuri, et al., Gum Arabic as a phytochemical construct for the stabilization of gold nanoparticles: in vivo pharmacokinetics and X-ray-contrast-imaging studies, *Small* 3 (2) (Feb. 2007) 333–341, <https://doi.org/10.1002/sml.200600427>.
- [31] N. Chanda, R. Shukla, K. V Katti, R. Kannan, *Gastrin Releasing Protein Receptor Specific Gold Nanorods : Breast and Prostate Tumor Avid Nanovectors for Molecular Imaging* 2009, 2009.
- [32] S.K. Nune, et al., Green nanotechnology from tea: phytochemicals in tea as building blocks for production of biocompatible gold nanoparticles, *J. Mater. Chem.* 19 (19) (Oct. 2009) 2912–2920, <https://doi.org/10.1039/B822015H>.
- [33] R. Kannan, et al., (12) United States Patent vol. 2, 2012, 12.
- [34] K. V Katti, M.O. Us, E. Boote, M.I. Us, R. Kannan, *Stabilized Gold Nanoparticle and Contrast Agent*, 2017.
- [35] R. Kannan, et al., Nanocompatible chemistry toward fabrication of target-specific gold nanoparticles, *J. Am. Chem. Soc.* 128 (35) (Sep. 2006) 11342–11343, <https://doi.org/10.1021/ja063280c>.

- [36] A.M. Gamal-Eldeen, et al., Photothermal therapy mediated by gum Arabic-conjugated gold nanoparticles suppresses liver preneoplastic lesions in mice, *J. Photochem. Photobiol. B Biol.* 163 (2016) 47–56, <https://doi.org/10.1016/j.jphotobiol.2016.08.009>.
- [37] K.K.V.K. Katti, et al., Green nanotechnology from cumin phytochemicals: generation of biocompatible gold nanoparticles, *Int. J. Green Nanotechnol. Biomed.* 1 (1) (Aug. 2009) B39–B52, <https://doi.org/10.1080/19430850902931599>.
- [38] R. Kannan, et al., Functionalized radioactive gold nanoparticles in tumor therapy, *Wiley Interdiscip. Rev. Nanomedicine Nanobiotechnology* 4 (1) (2012) 42–51, <https://doi.org/10.1002/wnan.161>.
- [39] N. Chanda, et al., An effective strategy for the synthesis of biocompatible gold nanoparticles using cinnamon phytochemicals for phantom CT imaging and photoacoustic detection of cancerous cells, *Pharm. Res.* 28 (2) (Oct. 2011) 279–291, <https://doi.org/10.1007/s11095-010-0276-6>.
- [40] M. Khoobchandani, A. Zambre, K.V.K. Katti, C. Lin, K.V.K. Katti, Green nanotechnology from brassicaceae: development of broccoli phytochemicals – encapsulated gold nanoparticles and their applications, *Nanomedicine* (2013), <https://doi.org/10.1177/1943089213509474>.
- [41] S.K. Nune, et al., Nanoparticles for biomedical imaging, *Expert Opin. Drug Deliv.* 6 (11) (Nov. 2009) 1175–1194, <https://doi.org/10.1517/17425240903229031>.
- [42] S. Ahmed, S. Annu, Ikram, S. Yudha S, Biosynthesis of gold nanoparticles: a green approach, *J. Photochem. Photobiol. B Biol.* 161 (Oct. 2016) 141–153, <https://doi.org/10.1016/j.jphotobiol.2016.04.034>.
- [43] Z. Yang, et al., The applications of gold nanoparticles in the diagnosis and treatment of gastrointestinal cancer, *Front. Oncol.* 11 (2022) 1–12, <https://doi.org/10.3389/fonc.2021.819329>, January.
- [44] M.U. Farooq, et al., Gold nanoparticles-enabled efficient dual delivery of anticancer therapeutics to HeLa cells, *Sci. Rep.* 8 (1) (2018) 1–12, <https://doi.org/10.1038/s41598-018-21331-y>.
- [45] P.P.P. Kumar, D.K. Lim, Gold-polymer nanocomposites for future therapeutic and tissue engineering applications, *Pharmaceutics* 14 (1) (2022), <https://doi.org/10.3390/pharmaceutics14010070>.
- [46] F. Palombarini, et al., Self-assembling ferritin-dendrimer nanoparticles for targeted delivery of nucleic acids to myeloid leukemia cells, *J. Nanobiotechnol.* 19 (1) (2021) 1–12, <https://doi.org/10.1186/s12951-021-00921-5>.
- [47] L.S. Mbatia, F. Maiyo, A. Daniels, M. Singh, Dendrimer-coated gold nanoparticles for efficient folate-targeted mRNA delivery in vitro, *Pharmaceutics* 13 (6) (2021), <https://doi.org/10.3390/pharmaceutics13060900>.
- [48] C. Joseph, A. Daniels, S. Singh, M. Singh, Histidine-tagged folate-targeted gold nanoparticles for enhanced transgene expression in breast cancer cells in vitro, *Pharmaceutics* 14 (1) (2022), <https://doi.org/10.3390/pharmaceutics14010053>.
- [49] L. Fan, W. Wang, Z. Wang, M. Zhao, Gold nanoparticles enhance antibody effect through direct cancer cell cytotoxicity by differential regulation of phagocytosis, *Nat. Commun.* 12 (1) (2021) 1–13, <https://doi.org/10.1038/s41467-021-26694-x>.
- [50] A. Ayub, S. Wettig, An overview of nanotechnologies for drug delivery to the brain, *Pharmaceutics* 14 (2) (2022), <https://doi.org/10.3390/pharmaceutics14020224>.
- [51] J. Kadhoda, A. Aghanejad, B. Safari, J. Barar, S.H. Rasta, S. Davaran, Aptamer-conjugated gold nanoparticles for targeted paclitaxel delivery and photothermal therapy in breast cancer, *J. Drug Deliv. Sci. Technol.* 67 (2022) 102954, <https://doi.org/10.1016/j.jddst.2021.102954>.
- [52] M. Yafout, A. Ousaid, Y. Khayati, and I. S. El Otmani, “Gold nanoparticles as a drug delivery system for standard chemotherapeutics: a new lead for targeted pharmacological cancer treatments,” *Sci. African*, vol. 11, 2021, doi: 10.1016/j.sciaf.2020.e00685.
- [53] Q. Gao, J. Zhang, J. Gao, Z. Zhang, H. Zhu, D. Wang, Gold nanoparticles in cancer theranostics, *Front. Bioeng. Biotechnol.* 9 (April) (2021) 1–20, <https://doi.org/10.3389/fbioe.2021.647905>.
- [54] S.M. van de Looij, E.R. Hebel, M. Viola, M. Hembury, S. Oliveira, T. Vermonden, Gold nanoclusters: imaging, therapy, and theranostic roles in biomedical applications, *Bioconjugate Chem.* 33 (1) (2022) 4–23, <https://doi.org/10.1021/acs.bioconjchem.1c00475>.
- [55] N. Chanda, et al., Radioactive gold nanoparticles in cancer therapy: therapeutic efficacy studies of GA-198 AuNP nanoconstruct in prostate tumor – bearing mice, *Nanomed. Nanotechnol. Biol. Med.* 6 (2) (2010) 201–209, <https://doi.org/10.1016/j.nano.2009.11.001>.
- [56] V.G. Kravets, A.V. Kabashin, W.L. Barnes, A.N. Grigorenko, Plasmonic surface lattice resonances: a review of properties and applications, *Chem. Rev.* 118 (12) (2018) 5912–5951, <https://doi.org/10.1021/acs.chemrev.8b00243>.
- [57] V. Turzhitsky, et al., Spectroscopy of scattered light for the characterization of micro and nanoscale objects in biology and medicine, *Appl. Spectrosc.* 68 (2) (2014) 133–154, <https://doi.org/10.1366/13-07395>.
- [58] X. Huang, M.A. El-Sayed, Gold nanoparticles: optical properties and implementations in cancer diagnosis and photothermal therapy, *J. Adv. Res.* 1 (1) (Oct. 2010) 13–28, <https://doi.org/10.1016/j.jare.2010.02.002>.
- [59] V. Amendola, R. Pilot, M. Frascioni, O.M. Maragò, M.A. Iatì, Surface plasmon resonance in gold nanoparticles: a review, *J. Phys. Condens. Matter* 29 (20) (Oct. 2017) 203002, <https://doi.org/10.1088/1361-648X/aa60f3>.
- [60] P.-L.L. Lam, W.-Y.Y. Wong, Z. Bian, C.-H.H. Chui, R. Gambari, Recent advances in green nanoparticulate systems for drug delivery: efficient delivery and safety concern, *Nanomedicine* 12 (4) (Oct. 2017) 357–385, <https://doi.org/10.2217/nmm-2016-0305>.
- [61] D. Cabuzu, A. Cirja, R. P. A.M. P. A.M. Grumezescu, Biomedical applications of gold nanoparticles, *Curr. Top. Med. Chem.* 15 (16) (Oct. 2015) 1605–1613.
- [62] N. Mahhngam, et al., Targeted therapy of tumour microenvironment by gold nanoparticles as a new therapeutic approach, *J. Drug Target.* (Jan. 2022) 1–17, <https://doi.org/10.1080/1061186X.2022.2032095>.
- [63] R. Zhao, J. Xiang, B. Wang, L. Chen, S. Tan, Recent advances in the development of noble metal NPs for cancer therapy, *Bioinorgan. Chem. Appl.* 2022 (2022) 2444516, <https://doi.org/10.1155/2022/2444516>.
- [64] M. Kenchegowda, et al., Smart nanocarriers as an emerging platform for cancer therapy: a review, *Molecules* 27 (1) (Dec. 2021) 146, <https://doi.org/10.3390/molecules27010146>.
- [65] S.K. Nune, et al., Green nanotechnology from tea: phytochemicals in tea as building blocks for production of biocompatible gold nanoparticles, *J. Mater. Chem.* 19 (19) (Oct. 2009) 2912–2920, <https://doi.org/10.1039/B822015H>.
- [66] R.A. Petros, J.M. DeSimone, Strategies in the design of nanoparticles for therapeutic applications, *Nat. Rev. Drug Discov.* 9 (8) (Oct. 2010) 615–627, <https://doi.org/10.1038/nrd2591>.
- [67] R. Shukla, et al., Laminin receptor specific therapeutic gold nanoparticles (198AuNP-EGCG) show efficacy in treating prostate cancer, *Proc. Natl. Acad. Sci. Unit. States Am.* 109 (31) (Jul. 2012) 12426–12431, <https://doi.org/10.1073/pnas.1121174109>.
- [68] R. Society, The Bakerian Lecture: Experimental Relations of Gold (and Other Metals) to Light Author (S): Michael Faraday Source, vol. 147, *Philosophical Transactions of the Royal Society of London*, 2018, pp. 145–181, 147 (1857), pp 145- Published by: Royal Society Stable URL 1857.
- [69] J. Kimling, M. Maier, B. Okenve, V. Kotaidis, H. Ballot, A. Plech, Turkevich Method for Gold Nanoparticle Synthesis Revisited, vol. 95, 2006, pp. 15700–15707.
- [70] G. Frens, Controlled nucleation for the regulation of the particle size in monodisperse gold suspensions, *Nat. Phys. Sci.* 241 (1973) 20–22, <https://doi.org/10.1038/physci241020a0>.
- [71] R. Shukla, V. Bansal, M. Chaudhary, A. Basu, R.R. Bhonde, M. Sastry, Biocompatibility of gold nanoparticles and their endocytotic fate inside the cellular compartment, *A Microscopic Overview* 25 (2005) 10644–10654.
- [72] K. Haume, et al., Gold nanoparticles for cancer radiotherapy: a review, *Cancer Nanotechnol* (2016), <https://doi.org/10.1186/s12645-016-0021-x>.
- [73] M. Brust, M. Walker, D. Bethell, D.J. Schiffrin, R. Whyman, Synthesis of Thiol-Derivatised Gold Nanoparticles in, 2000, pp. 801–802.
- [74] V. Patil, R.B. Malvankar, M. Sastry, Role of particle size in individual and competitive diffusion of carboxylic acid derivatized colloidal gold particles in thermally evaporated fatty amine films, *Langmuir* 15 (4) (1999) 8197–8206.
- [75] B. Verlag, et al., A Colloidal Gold Prepared with Ultrasonics, 1980, pp. 472–473.
- [76] J. Turkevich, P.C. Stevenson, J. Hillier, A study of the nucleation and growth processes in the synthesis of colloidal gold, *Discuss. Faraday Soc.* 11 (1951) 55–75, <https://doi.org/10.1039/DF9511100055>.
- [77] H.M.E. Azzazy, M.M.H. Mansour, T.M. Samir, R. Franco, Gold nanoparticles in the clinical laboratory: principles of preparation and applications, *Clin. Chem. Lab. Med.* 50 (2) (2012) 193–209, <https://doi.org/10.1515/cclm.2011.732>.
- [78] C. Deraedt, et al., Sodium borohydride stabilizes very active gold nanoparticle catalysts, *Chem. Commun.* 50 (91) (2014) 14194–14196, <https://doi.org/10.1039/c4cc05946h>.
- [79] A. Sharma, B.P. Singh, A.K. Gathania, Synthesis and characterization of dodecanethiol-stabilized gold nanoparticles, *Indian J. Pure Appl. Phys.* 52 (2) (2014) 93–100.
- [80] P. Dobrowolska, A. Krajewska, M. Gajda-Raczka, B. Bartosiewicz, P. Nyga, B. J. Jankiewicz, Application of turkevich method for gold nanoparticles synthesis to fabrication of SiO₂@Au and TiO₂@Au core-shell nanostructures, *Materials* 8 (6) (2015) 2849–2862, <https://doi.org/10.3390/ma8062849>.
- [81] K. Zabetakis, W.E. Ghann, S. Kumar, M.C. Daniel, Effect of high gold salt concentrations on the size and polydispersity of gold nanoparticles prepared by an extended Turkevich-Frens method, *Gold Bull* 45 (4) (2012) 203–211, <https://doi.org/10.1007/s13404-012-0069-2>.
- [82] N. Chanda, et al., Bombesin Functionalized Gold Nanoparticles Show In Vitro and In Vivo Cancer Receptor Specificity, 2010, <https://doi.org/10.1073/pnas.1002143107>.
- [83] R. Kannan, K.K. Katti, (12) United States Patent, vol. 2, 2012, 12.
- [84] K.V.K.M. Khoobchandani, V.C.T.A.Y. Al, Y.K.K. Katti, S.K.L.T.M. Sakr, Prostate tumor therapy advances in nuclear medicine: green nanotechnology toward the design of tumor specific radioactive gold nanoparticles, *J. Radioanal. Nucl. Chem.* 318 (3) (2018) 1737–1747, <https://doi.org/10.1007/s10967-018-6320-4>.
- [85] P. Agarwal, R. Gupta, N. Agarwal, Advances in synthesis and applications of microalgal nanoparticles for wastewater treatment, *J. Nanotechnol.* 2019 (2019), <https://doi.org/10.1155/2019/7392713>.
- [86] M. Ovais, A.T. Khalil, M. Ayaz, I. Ahmad, S.K. Nethi, S. Mukherjee, Biosynthesis of metal nanoparticles via microbial enzymes: a mechanistic approach, *Int. J. Mol. Sci.* 19 (12) (2018) 1–20, <https://doi.org/10.3390/ijms19124100>.
- [87] P. Khandel, S.K. Shahi, Mycogenic nanoparticles and their bio-prospective applications: current status and future challenges, *J. Nanostructure Chem.* 8 (4) (2018) 369–391, <https://doi.org/10.1007/s40097-018-0285-2>.
- [88] G. Gahlawat, A.R. Choudhury, A review on the biosynthesis of metal and metal salt nanoparticles by microbes, *RSC Adv* 9 (23) (2019) 12944–12967, <https://doi.org/10.1039/c9ra10483b>.
- [89] X. Fang, Y. Wang, Z. Wang, Z. Jiang, M. Dong, Microorganism assisted synthesized nanoparticles for catalytic applications, *Energies* 12 (2019), <https://doi.org/10.3390/en12010190>, 1.
- [90] K.B. Narayanan, N. Sakthivel, Colloids and Surfaces A: physicochemical and Engineering Aspects Facile green synthesis of gold nanostructures by NADPH-dependent enzyme from the extract of *Sclerotium rolfsii*, *Colloids Surfaces A*

- Physicochem. Eng. Asp. 380 (1–3) (2011) 156–161, <https://doi.org/10.1016/j.colsurfa.2011.02.042>.
- [91] S. Roy, T. Kumar, G. Prasad, U. Basu, Microbial biosynthesis of nontoxic gold nanoparticles, *Mater. Sci. Eng. B* 203 (2016) 41–51, <https://doi.org/10.1016/j.mseb.2015.10.008>.
- [92] X. Ma, Biosynthesis of Gold Nanoparticles by the Extreme Bacterium *Deinococcus Radiodurans* and an Evaluation of Their Antibacterial Properties, 2016, pp. 5931–5944.
- [93] P. Mukherjee, et al., *Verticillium Sp.* And Surface Trapping of the Gold Nanoparticles Formed **, vol. 19, 2001, pp. 3585–3588.
- [94] J.D. Obayemi, Y.T.D.G. Etuk-udo, Biosynthesis of Gold Nanoparticles and Gold/Prodigiosin Nanoparticles with *Serratia marcescens* Bacteria, 2017, <https://doi.org/10.1007/s12649-016-9734-7>.
- [95] M.H. M. C.G. Joshi, A. Danagoudar, J. Poyya, A.K. Kudva, D. Bl, Biogenic synthesis of gold nanoparticles by marine endophytic fungus- *Cladosporium cladosporioides* isolated from seaweed and evaluation of their antioxidant and antimicrobial properties, *Process Biochem* 63 (September) (2017) 137–144, <https://doi.org/10.1016/j.procbio.2017.09.008>.
- [96] M. Ali, H. Forootanfar, Colloids and Surfaces B: biointerfaces Biosynthesis and characterization of gold nanoparticles produced by laccase from *Paraconiomyrium variabile*, *Colloids Surf. B Biointerfaces* 87 (1) (2011) 23–27, <https://doi.org/10.1016/j.colsurfb.2011.04.022>.
- [97] K.S.U. Suganya, et al., Blue green alga mediated synthesis of gold nanoparticles and its antibacterial effect against Gram positive organisms, *Mater. Sci. Eng. C* 47 (2015) 351–356, <https://doi.org/10.1016/j.msec.2014.11.043>.
- [98] S.A. Kumar, Y. Peter, J.L. Nadeau, Facile biosynthesis, separation and conjugation of gold nanoparticles to doxorubicin, *Nanotechnology* 19 (2008), <https://doi.org/10.1088/0957-4484/19/49/495101>.
- [99] V.R.R.V.R. Rai, Actinomycetes mediated synthesis of gold nanoparticles from the culture supernatant of *Streptomyces griseoruber* with special reference to catalytic activity, *3 Biotech* 7 (5) (2017) 1–7, <https://doi.org/10.1007/s13205-017-0930-3>.
- [100] R. Bhambure, M. Bule, N. Shaligram, M. Kamat, R. Singhal, Extracellular biosynthesis of gold nanoparticles using *Aspergillus Niger* – its characterization and stability, *Chem. Eng. Technol.* 32 (7) (2009) 1036–1041, <https://doi.org/10.1002/ceat.200800647>.
- [101] P. Williams, A. Sorribas, M.-J.R. Howes, Natural products as a source of Alzheimer's drug leads, *Nat. Prod. Rep.* 28 (1) (Jan. 2011) 48–77, <https://doi.org/10.1039/c0np00027b>.
- [102] M. Noruzi, D. Zare, D. Davoodi, A rapid biosynthesis route for the preparation of gold nanoparticles by aqueous extract of cypress leaves at room temperature, *Spectrochim. Acta Part A Mol. Biomol. Spectrosc.* 94 (2012) 84–88, <https://doi.org/10.1016/j.saa.2012.03.041>.
- [103] D. Philip, Rapid green synthesis of spherical gold nanoparticles using *Mangifera indica* leaf, *Spectrochim. Acta Part A Mol. Biomol. Spectrosc.* 77 (4) (2010) 807–810, <https://doi.org/10.1016/j.saa.2010.08.008>.
- [104] J.K. Andeani, H. Kazemi, S. Mohsenzadeh, A. Safavi, Biosynthesis of gold nanoparticles using dried flowers extract of *Achillea wilhelmsii* plant, *Dig J Nanomater Bios* 6 (3) (2011) 1011–1017.
- [105] M.V. Sujitha, S. Kannan, Green synthesis of gold nanoparticles using Citrus fruits (Citrus limon, Citrus reticulata and Citrus sinensis) aqueous extract and its characterization, *Spectrochim. Acta Part A Mol. Biomol. Spectrosc.* 102 (2013) 15–23, <https://doi.org/10.1016/j.saa.2012.09.042>.
- [106] K. Gopinath, S. Gowri, V. Karthika, A. Arumugam, Green synthesis of gold nanoparticles from fruit extract of *Terminalia arjuna*, for the enhanced seed germination activity of *Gloriosa superba*, *J. Nanostructure Chem.* 4 (3) (2014) 115, <https://doi.org/10.1007/s40097-014-0115-0>.
- [107] S. Ghosh, et al., *Gnidia glauca* flower extract mediated synthesis of gold nanoparticles and evaluation of its chemocatalytic potential, *J. Nanobiotechnol.* 10 (1) (2012) 17, <https://doi.org/10.1186/1477-3155-10-17>.
- [108] R.K. Das, N. Gogoi, U. Bora, Green synthesis of gold nanoparticles using *Nyctanthes arborescens* flower extract, *Bioproc. Biosyst. Eng.* 34 (5) (2011) 615–619, <https://doi.org/10.1007/s00449-010-0510-y>.
- [109] K.B. Narayanan, N. Sakthivel, Coriander leaf mediated biosynthesis of gold nanoparticles, *Mater. Lett.* 62 (30) (2008) 4588–4590, <https://doi.org/10.1016/j.matlet.2008.08.044>.
- [110] J.Y. Song, H.-K.K. Jang, B.S. Kim, Biological synthesis of gold nanoparticles using *Magnolia kobus* and *Diopyros kaki* leaf extracts, *Process Biochem* 44 (10) (2009) 1133–1138, <https://doi.org/10.1016/j.procbio.2009.06.005>.
- [111] R. Shukla, N. Chanda, A. Zambre, A. Upendran, K. Katti, R.R. Kulkarni, Laminin Receptor Specific Therapeutic Gold Efficacy in Treating Prostate Cancer, 2012, pp. 1–6, <https://doi.org/10.1073/pnas.1121174109>.
- [112] M. Aslam, L. Fu, M. Su, K. Vijayamohan, V.P. Dravid, Novel one-step synthesis of amine-stabilized aqueous colloidal gold nanoparticles, *J. Mater. Chem.* 14 (12) (2004) 1795–1797.
- [113] A. Bacic, et al., Structural classes of arabinogalactan-proteins, in: *Cell and Developmental Biology of Arabinogalactan-Proteins*, Springer, 2000, pp. 11–23.
- [114] A.V. Kabashin, M. Meunier, C. Kingston, J.H.T. Luong, Fabrication and characterization of gold nanoparticles by femtosecond laser ablation in an aqueous solution of cyclodextrins, *J. Phys. Chem. B* 107 (19) (2003) 4527–4531, <https://doi.org/10.1021/jp034345q>.
- [115] V.G. Kumar, et al., Facile green synthesis of gold nanoparticles using leaf extract of anti-diabetic potent *Cassia auriculata*, *Colloids Surf. B Biointerfaces* 87 (1) (2011) 159–163, <https://doi.org/10.1016/j.colsurfb.2011.05.016>.
- [116] K. Leonard, B. Ahmmad, H. Okamura, J. Kurawaki, In situ green synthesis of biocompatible ginseng capped gold nanoparticles with remarkable stability, *Colloids Surf. B Biointerfaces* 82 (2) (2011) 391–396, <https://doi.org/10.1016/j.colsurfb.2010.09.020>.
- [117] C.-C. Wu, D.-H. Chen, Facile green synthesis of gold nanoparticles with gum Arabic as a stabilizing agent and reducing agent, *Gold Bull* 43 (4) (2010) 234–240, <https://doi.org/10.1007/BF03214993>.
- [118] C.J. Murphy, et al., Gold nanoparticles in biology: beyond toxicity to cellular imaging, *Acc. Chem. Res.* 41 (2008), <https://doi.org/10.1021/ar800035u>, 12.
- [119] S. Ahn, S.Y. Jung, S.J. Lee, Gold nanoparticle contrast agents in advanced X-ray imaging technologies, *Molecules* 18 (5) (2013) 5858–5890, <https://doi.org/10.3390/molecules18055858>.
- [120] N. Goswami, Z. Luo, X. Yuan, D.T. Leong, J. Xie, Engineering gold-based radiosensitizers for cancer radiotherapy, *Mater. Horizons* 4 (5) (2017) 817–831, <https://doi.org/10.1039/C7MH00451F>.
- [121] F. Lu, T.L. Doane, J.J. Zhu, C. Burda, Gold nanoparticles for diagnostic sensing and therapy, *Inorg. Chim. Acta* 393 (2012) 142–153, <https://doi.org/10.1016/j.ica.2012.05.038>.
- [122] D.R. McCormack, K. Bhattacharyya, R. Kannan, D. Ph, K. Katti, D. Ph, Enhanced Photoacoustic Detection of Melanoma Cells Using Gold Nanoparticles, vol. 338, March, 2011, pp. 333–338, <https://doi.org/10.1002/lsm.21060>.
- [123] E. Boote, et al., Gold nanoparticle contrast in a phantom and juvenile swine: models for molecular imaging of human organs using X-ray computed tomography, *Acad. Radiol.* 17 (4) (2010) 410–417, <https://doi.org/10.1016/j.acra.2010.01.006>.
- [124] R. Shukla et al., “Photoacoustic Detection of Circulating Prostate, Breast and Pancreatic Cancer Cells Using Targeted Gold Nanoparticles: Implications of Green Nanotechnology in Molecular Imaging,” p. 3.
- [125] S. Her, D.A. Jaffray, C. Allen, Gold nanoparticles for applications in cancer radiotherapy: mechanisms and recent advancements, *Adv. Drug Deliv. Rev.* 109 (2017) 84–101, <https://doi.org/10.1016/j.addr.2015.12.012>.
- [126] M. Saravanan, et al., Emerging antineoplastic biogenic gold nanomaterials for breast cancer therapeutics: a systematic review, *Int. J. Nanomed.* 15 (2020) 3577–3595, <https://doi.org/10.2147/IJN.S240293>.
- [127] M. Sivasubramanian, S. Ramasamy, S. Muthupandian, H. Barabadi, A. Ramaswamy, Emerging Theragnostic Metal-Based Nanomaterials to Combat Cancer, 2021, pp. 317–334.
- [128] S. Muthupandian, et al., Emerging Theranostic Silver and Gold Nanobiomaterials for Breast Cancer: Present Status and Future Prospects, 2021, pp. 439–456.
- [129] H. Barabadi, et al., Emerging theranostic gold nanomaterials to combat lung cancer: a systematic review, *J. Cluster Sci.* (Jul. 2020), <https://doi.org/10.1007/s10876-019-01650-4>.
- [130] H. Barabadi, et al., Emerging Theranostic Gold Nanomaterials to Combat Colorectal Cancer: A Systematic Review, Nov. 2019, <https://doi.org/10.1007/s10876-019-01681-x>.
- [131] M. Saravanan, H. Barabadi, H. Vahidi, Chapter 5 - green nanotechnology: isolation of bioactive molecules and modified approach of biosynthesis, in: C. Patra, I. Ahmad, M. Ayaz, A.T. Khalil, S. Mukherjee, C.T. Ovais (Eds.), *Micro and Nano Technologies*, Elsevier, 2021, pp. 101–122.
- [132] H. Barabadi, et al., Green nanotechnology-based gold nanomaterials for hepatic cancer therapeutics: a systematic review, *Iran. J. Pharm. Res.* 19 (3) (2020) 3–17, <https://doi.org/10.22037/ijpr.2020.113820.14504>.
- [133] H. Barabadi, et al., Emerging antineoplastic gold nanomaterials for cervical cancer therapeutics: a systematic review, *J. Cluster Sci.* 31 (6) (2020) 1173–1184, <https://doi.org/10.1007/s10876-019-01733-2>.
- [134] B. Wang, et al., Plasmonic intravascular photoacoustic imaging for detection of macrophages in atherosclerotic plaques, *Nano Lett* 9 (6) (2009) 2212–2217, <https://doi.org/10.1021/nl801852e>.
- [135] A.J. Mieszawska, W.J.M.M. Mulder, Z.A. Fayad, D.P. Cormode, Multifunctional gold nanoparticles for diagnosis and therapy of disease, *Mol. Pharm.* 10 (3) (2013) 831–847, <https://doi.org/10.1021/mp3005885>.
- [136] S. Raveendran, H.T. Lim, T. Maekawa, M. Vadakke Matham, D. Sakthi Kumar, Gold nanocages entering into the realm of high-contrast photoacoustic ocular imaging, *Nanoscale* 10 (29) (2018) 13959–13968, <https://doi.org/10.1039/c8nr02866d>.
- [137] W. Li, X. Chen, Gold nanoparticles for photoacoustic imaging, *Nanomedicine* (2015), <https://doi.org/10.2217/nnm.14.169>.
- [138] L. Rouleau, et al., VCAM-1-targeting gold nanoshell probe for photoacoustic imaging of atherosclerotic plaque in mice, *Contrast Media Mol. Imaging* (2013), <https://doi.org/10.1002/cmmi.1491>.
- [139] J. Song, et al., ‘smart’ gold nanoparticles for photoacoustic imaging: an imaging contrast agent responsive to the cancer microenvironment and signal amplification: via pH-induced aggregation, *Chem. Commun.* (2016), <https://doi.org/10.1039/c6cc03100e>.
- [140] X. Li, et al., 99mTc-Labeled multifunctional low-generation dendrimer-entrapped gold nanoparticles for targeted SPECT/CT dual-mode imaging of tumors, *ACS Appl. Mater. Interfaces* 8 (31) (2016) 19883–19891, <https://doi.org/10.1021/acsami.6b04827>.
- [141] Q. Chen, et al., Targeted CT/MR dual mode imaging of tumors using multifunctional dendrimer-entrapped gold nanoparticles, *Biomaterials* (2013), <https://doi.org/10.1016/j.biomaterials.2013.03.009>.
- [142] Y. Zhao, et al., Gold nanoparticles doped with (199) Au atoms and their use for targeted cancer imaging by SPECT, *Adv. Healthc. Mater.* 5 (8) (2016) 928–935, <https://doi.org/10.1002/adhm.201500992>.
- [143] K.C.L. Black, W.J. Akers, G. Sudlow, B. Xu, R. Laforest, S. Achilefu, Dual-radiolabeled nanoparticle SPECT probes for bioimaging, *Nanoscale* (2015), <https://doi.org/10.1039/c4nr05269b>.

- [144] Y. Fazaeli, O. Akhavan, R. Rahighi, M.R. Aboudzadeh, E. Karimi, H. Afarideh, In vivo SPECT imaging of tumors by 198Au-labeled graphene oxide nanostructures, *Mater. Sci. Eng. C* (2014), <https://doi.org/10.1016/j.msec.2014.09.019>.
- [145] K. Cheng, et al., Construction and validation of nano gold tripods for molecular imaging of living subjects, *J. Am. Chem. Soc.* 136 (9) (2014) 3560–3571, <https://doi.org/10.1021/ja412001e>.
- [146] Y. Wang, et al., Evaluating the pharmacokinetics and in vivo cancer targeting capability of au nanocages by positron emission tomography imaging, *ACS Nano* 6 (7) (2012) 5880–5888, <https://doi.org/10.1021/nn300464r>.
- [147] C.S. Kim, D. Ingato, P.W. Smith, Z. Chen, Y.J. Kwon, Stimuli - disassembling gold nanoclusters for diagnosis of early stage oral cancer by optical coherence tomography, *Nano Converge* (2018), <https://doi.org/10.1186/s40580-018-0134-5>.
- [148] H. Lusic, M.W. Grinstaff, X-ray-computed tomography contrast agents, *Chem. Rev.* 113 (3) (Mar. 2013) 1641–1666, <https://doi.org/10.1021/cr200358s>.
- [149] P.C. Chen, S.C. Mwakwari, A.K. Oyelere, Gold nanoparticles: from nanomedicine to nanosensing, *Nanotechnol. Sci. Appl.* 1 (Nov. 2008) 45–65.
- [150] J.F. Hainfeld, H.M. Smilowitz, M.J. O'Connor, F.A. Dilmanian, D.N. Slatkin, Gold nanoparticle imaging and radiotherapy of brain tumors in mice, *Nanomedicine* 8 (10) (2013) 1601–1609, <https://doi.org/10.2217/nnm.12.165>.
- [151] R. Meir, et al., Nanomedicine for cancer immunotherapy: tracking cancer-specific T-cells in vivo with gold nanoparticles and CT imaging, *ACS Nano* 9 (6) (Jun. 2015) 6363–6372, <https://doi.org/10.1021/acs.nano.5b01939>.
- [152] P. Iranpour, M. Ajamian, A. Safavi, N. Iranpour, A. Abbaspour, S. Javanmardi, Synthesis of highly stable and biocompatible gold nanoparticles for use as a new X-ray contrast agent, *J. Mater. Sci. Mater. Med.* 29 (5) (Apr. 2018) 48, <https://doi.org/10.1007/s10856-018-6053-5>.
- [153] R. Meir, R. Popovtzer, Cell tracking using gold nanoparticles and computed tomography imaging, *Wiley Interdiscip. Rev. Nanomed. Nanobiotechnol.* 10 (2) (Mar. 2018), e1480, <https://doi.org/10.1002/wnan.1480>.
- [154] L. Torrisi, N. Restuccia, I. Paterniti, Gold nanoparticles by laser ablation for X-ray imaging and protontherapy improvements, *Recent Pat. Nanotechnol.* 12 (1) (Feb. 2018) 59–69, <https://doi.org/10.2174/1872210511666170609093433>.
- [155] Q.-Y. Cai, et al., Colloidal gold nanoparticles as a blood-pool contrast agent for X-ray computed tomography in mice, *Invest. Radiol.* 42 (12) (2007) 797–806, <https://doi.org/10.1097/RLL.0b013e31811ecdcd>.
- [156] N. Chanda, et al., Bombesin functionalized gold nanoparticles show in vitro and in vivo cancer receptor specificity, *Proc. Natl. Acad. Sci. Unit. States Am.* 107 (19) (May 2010) 8760–8765, <https://doi.org/10.1073/pnas.1002143107>.
- [157] R. Popovtzer, et al., Targeted gold nanoparticles enable molecular CT imaging of cancer, *Nano Lett* 8 (12) (Dec. 2008) 4593–4596.
- [158] J.T. Au, et al., Gold nanoparticles provide bright long-lasting vascular contrast for CT imaging, *Am. J. Roentgenol.* 200 (6) (Jun. 2013) 1347–1351, <https://doi.org/10.2214/AJR.12.8933>.
- [159] E. Boote, et al., Gold nanoparticle contrast in a phantom and juvenile swine, *Acad. Radiol.* 17 (4) (Apr. 2010) 410–417, <https://doi.org/10.1016/j.acra.2010.01.006>.
- [160] M.A. Hahn, A.K. Singh, P. Sharma, S.C. Brown, B.M. Moudgil, Nanoparticles as contrast agents for in-vivo bioimaging: current status and future perspectives, *Anal. Bioanal. Chem.* 399 (1) (2011) 3–27, <https://doi.org/10.1007/s00216-010-4207-5>.
- [161] Z. Zhou, et al., Folic acid-conjugated silica capped gold nanoclusters for targeted fluorescence/X-ray computed tomography imaging, *J. Nanobiotechnol.* 11 (1) (2013) 16–23, <https://doi.org/10.1186/1477-3155-11-17>.
- [162] K. Ricketts, C. Guazzoni, A. Castoldi, A.P. Gibson, G.J. Royle, An x-ray fluorescence imaging system for gold nanoparticle detection, *Phys. Med. Biol.* 58 (21) (2013) 7841–7855, <https://doi.org/10.1088/0031-9155/58/21/7841>.
- [163] I.-C.C. Sun, et al., Tumor-targeting gold particles for dual computed tomography/optical cancer imaging, *Angew. Chem. Int. Ed.* 50 (40) (Sep. 2011) 9348–9351, <https://doi.org/10.1002/anie.201102892>.
- [164] R. Weissleder, U. Mahmood, Molecular imaging, *Radiology* 219 (2) (May 2001) 316–333, <https://doi.org/10.1148/radiology.219.2.r01ma19316>.
- [165] L. Luo, et al., Manganese-enhanced MRI optic nerve tracking: effect of intravitreal manganese dose on retinal toxicity, *NMR Biomed* 25 (12) (Dec. 2012) 1360–1368, <https://doi.org/10.1002/nbm.2808>.
- [166] L.M. De León-Rodríguez, A.F. Martins, M.C. Pinho, N.M. Rofsky, A.D. Sherry, Basic MR relaxation mechanisms and contrast agent design, *J. Magn. Reson. Imag.* 42 (3) (Sep. 2015) 545–565, <https://doi.org/10.1002/jmri.24787>.
- [167] C. Alric, et al., Gadolinium chelate coated gold nanoparticles as contrast agents for both X-ray computed tomography and magnetic resonance imaging, *J. Am. Chem. Soc.* 130 (18) (2008) 5908–5915, <https://doi.org/10.1021/ja078176p>.
- [168] F.J. Nicholls, M.W. Rotz, H. Ghuman, K.W. MacRenaris, T.J. Meade, M. Modo, DNA-gadolinium-gold nanoparticles for in vivo T1 MR imaging of transplanted human neural stem cells, *Biomaterials* 77 (Jan. 2016) 291–306, <https://doi.org/10.1016/j.biomaterials.2015.11.021>.
- [169] M.Y. Sha, H. Xu, S.G. Penn, R. Cromer, SERS nanoparticles: a new optical detection modality for cancer diagnosis, *Nanomedicine* 2 (5) (Oct. 2007) 725–734, <https://doi.org/10.2217/17435889.2.5.725>.
- [170] R.A. Halvorsen, P.J. Vikesland, Surface-enhanced Raman spectroscopy (SERS) for environmental analyses, *Environ. Sci. Technol.* 44 (20) (Oct. 2010) 7749–7755, <https://doi.org/10.1021/es101228z>.
- [171] R.H. Lahr, P.J. Vikesland, Surface-enhanced Raman spectroscopy (SERS) cellular imaging of intracellular biosynthesized gold nanoparticles, *ACS Sustain. Chem. Eng.* 2 (7) (Jul. 2014) 1599–1608, <https://doi.org/10.1021/sc500105n>.
- [172] C.C. Lai, C.Y. Wang, W.L. Liu, Y.T. Huang, P.R. Hsueh, Time to positivity of blood cultures of different *Candida* species causing fungaemia, *J. Med. Microbiol.* 61 (5) (2012) 701–704, <https://doi.org/10.1099/jmm.0.038166-0>.
- [173] A.M. Schwartzberg, T.Y. Oshiro, J.Z. Zhang, T. Huser, C.E. Talley, Improving nanoprobe using surface-enhanced Raman scattering from 30-nm hollow gold particles, *Anal. Chem.* 78 (13) (Jul. 2006) 4732–4736, <https://doi.org/10.1021/ac060220g>.
- [174] G. Yang, J. Nanda, B. Wang, G. Chen, D.T. Hallinan, Self-assembly of large gold nanoparticles for surface-enhanced Raman spectroscopy, *ACS Appl. Mater. Interfaces* 9 (15) (Apr. 2017) 13457–13470, <https://doi.org/10.1021/acsami.7b01121>.
- [175] X.-M. Qian, S.M. Nie, Single-molecule and single-nanoparticle SERS: from fundamental mechanisms to biomedical applications, *Chem. Soc. Rev.* 37 (5) (May 2008) 912, <https://doi.org/10.1039/b708839f>.
- [176] S. Penn, et al., Nanoplex™ biotags: near-IR excited, highly multiplexed nanoparticulate optical detection tags for diagnostic assays, in: 2007 NSTI Nanotechnol. Conf. Trade Show - NSTI Nanotech 2007, Tech. Proc., vol. 2, 2007, pp. 447–448.
- [177] M. Laudon, et al., NSTI Nanotech 2007 : 2007 NSTI Nanotechnology Conference and Trade Show, Santa Clara, May 20–24, 2007, Nano Science and Technology Institute, Boca Raton, FL, 2007.
- [178] L. Chen, et al., Surface-enhanced Raman scattering (SERS) active gold nanoparticles decorated on a porous polymer filter, *Appl. Spectrosc.* 71 (7) (Jul. 2017) 1543–1550, <https://doi.org/10.1177/0003702817703293>.
- [179] L. Zhang, C. Guan, Y. Wang, J. Liao, Highly effective and uniform SERS substrates fabricated by etching multi-layered gold nanoparticle arrays, *Nanoscale* 8 (11) (Mar. 2016) 5928–5937, <https://doi.org/10.1039/C6NR00502K>.
- [180] N. Leopold, et al., One step synthesis of SERS active colloidal gold nanoparticles by reduction with polyethylene glycol, *Colloids Surfaces A Physicochem. Eng. Asp.* 436 (2013) 133–138, <https://doi.org/10.1016/j.colsurfa.2013.05.075>.
- [181] S. Lee, et al., Surface-enhanced Raman scattering imaging of HER2 cancer markers overexpressed in single MCF7 cells using antibody conjugated hollow gold nanospheres, *Biosens. Bioelectron.* 24 (7) (2009) 2260–2263, <https://doi.org/10.1016/j.bios.2008.10.018>.
- [182] X. Qian, et al., In vivo tumor targeting and spectroscopic detection with surface-enhanced Raman nanoparticle tags, *Nat. Biotechnol.* 26 (1) (Jan. 2008) 83–90, <https://doi.org/10.1038/nbt1377>.
- [183] L. Litti, et al., A SERRS/MRI multimodal contrast agent based on naked Au nanoparticles functionalized with a Gd(III) loaded PEG polymer for tumor imaging and localized hyperthermia, *Nanoscale* 10 (3) (Jan. 2018) 1272–1278, <https://doi.org/10.1039/c7nr07398d>.
- [184] S. Mallidi, et al., Ultrasound-based imaging of nanoparticles: from molecular and cellular imaging to therapy guidance, in: 2009 IEEE International Ultrasonics Symposium, Sep. 2009, pp. 27–36, <https://doi.org/10.1109/ULTSYM.2009.5441484>.
- [185] X. Wang, et al., Au-nanoparticle coated mesoporous silica nanocapsule-based multifunctional platform for ultrasound mediated imaging, cytolysis and tumor ablation, *Biomaterials* 34 (8) (Mar. 2013) 2057–2068, <https://doi.org/10.1016/j.biomaterials.2012.11.044>.
- [186] C. Tarapacki, R. Karshafian, Enhancing laser therapy using PEGylated gold nanoparticles combined with ultrasound and microbubbles, *Ultrasonics* 57 (Mar. 2015) 36–43, <https://doi.org/10.1016/j.ultras.2014.10.015>.
- [187] S.Y. Nam, L.M. Ricles, L.J. Suggs, S.Y. Emelianov, In vivo ultrasound and photoacoustic monitoring of mesenchymal stem cells labeled with gold nanotracers, *PLoS One* 7 (5) (May 2012), e37267, <https://doi.org/10.1371/journal.pone.0037267>.
- [188] G. Wang, K. Qian, X. Mei, A theranostic nanoplatfrom: magneto-gold@fluorescence polymer nanoparticles for tumor targeting: T1 & T2-MRI/CT/NIR fluorescence imaging and induction of genuine autophagy mediated chemotherapy, *Nanoscale* 10 (22) (Jun. 2018) 10467–10478, <https://doi.org/10.1039/c8nr02429d>.
- [189] C. Xu, Y. Wang, C. Zhang, Y. Jia, Y. Luo, X. Gao, AuGd integrated nanoprobe for optical/MRI/CT triple-modal in vivo tumor imaging, *Nanoscale* 9 (13) (Mar. 2017) 4620–4628, <https://doi.org/10.1039/c7nr01064h>.
- [190] S.P. Kwon, et al., Thrombin-activatable fluorescent peptide incorporated gold nanoparticles for dual optical/computed tomography thrombus imaging, *Biomaterials* 150 (2018) 125–136, <https://doi.org/10.1016/j.biomaterials.2017.10.017>.
- [191] J.A. Viator, et al., Gold nanoparticle mediated detection of prostate cancer cells using photoacoustic flowmetry with optical reflectance, *J. Biomed. Nanotechnol.* 6 (2) (2010) 187–191, <https://doi.org/10.1166/jbnn.2010.1105>.
- [192] P. Huang, et al., Biodegradable gold nanovesicles with an ultrastrong plasmonic coupling effect for photoacoustic imaging and photothermal therapy, *Angew. Chem. Int. Ed.* 52 (52) (2013) 13958–13964, <https://doi.org/10.1002/anie.201308986>.
- [193] Y.A. Attia, Y.E. Farag, Y.M.A. Mohamed, A.T. Hussien, T. Youssef, Photo-extracellular synthesis of gold nanoparticles using Baker's yeast and their anticancer evaluation against Ehrlich ascites carcinoma cells, *New J. Chem.* 40 (11) (Oct. 2016) 9395–9402, <https://doi.org/10.1039/C6NJ01920J>.
- [194] R. Hu, K.-T. Yong, I. Roy, H. Ding, S. He, P.N. Prasad, Metallic nanostructures as localized plasmon resonance enhanced scattering probes for multiplex dark-field targeted imaging of cancer cells, *J. Phys. Chem. C* 113 (7) (Feb. 2009) 2676–2684, <https://doi.org/10.1021/jp8076672>.
- [195] D.B. Chithrani, M. Dunne, J. Stewart, C. Allen, D.A. Jaffray, Cellular uptake and transport of gold nanoparticles incorporated in a liposomal carrier, *Nanomed.*

- Nanotechnol. Biol. Med. 6 (1) (Feb. 2010) 161–169, <https://doi.org/10.1016/j.nano.2009.04.009>.
- [196] J.P. Minton, C.D. Moody, J.R. Dearman, W.B. McKnight, A.S. Ketcham, AN evaluation OF the physical response OF malignant tumor implants to pulsed laser radiation, *Surg. Gynecol. Obstet.* 121 (1965) 538–544.
- [197] Z.-Z.J. Lim, J.-E.J. Li, C.-T. Ng, L.-Y.L. Yung, B.-H. Bay, Gold nanoparticles in cancer therapy, *Acta Pharmacol. Sin.* 32 (8) (2011) 983–990, <https://doi.org/10.1038/aps.2011.82>.
- [198] X. Huang, W. Qian, I.H. El-Sayed, M.A. El-Sayed, The potential use of the enhanced nonlinear properties of gold nanospheres in photothermal cancer therapy, *Laser Surg. Med.* 39 (9) (Oct. 2007) 747–753, <https://doi.org/10.1002/lsm.20577>.
- [199] S. Eustis, M.A. el-Sayed, M.A. El-sayed, M. Kasha, M.A. el-Sayed, Why gold nanoparticles are more precious than pretty gold : noble metal surface plasmon resonance and its enhancement of the radiative and nonradiative properties of nanocrystals of different shapes, *Chem. Soc. Rev.* 35 (3) (Mar. 2006) 209–217, <https://doi.org/10.1039/b514191e>.
- [200] A.R. Kirtane, M. Verma, P. Karandikar, J. Furin, R. Langer, G. Traverso, Nanotechnology approaches for global infectious diseases, *Nat. Nanotechnol.* 16 (4) (2021) 369–384, <https://doi.org/10.1038/s41565-021-00866-8>.
- [201] G. Yang, S. Chen, J. Zhang, Bioinspired and biomimetic nanotherapies for the treatment of infectious diseases, *Front. Pharmacol.* 10 (Jul. 2019) 751, <https://doi.org/10.3389/fphar.2019.00751>.
- [202] S. Fazal, A. Jayasree, S. Sasidharan, M. Koyakutty, S. V Nair, D. Menon, Green synthesis of anisotropic gold nanoparticles for photothermal therapy of cancer, *ACS Appl. Mater. Interfaces* 6 (2014) 8080–8089, <https://doi.org/10.1021/am500302t>.
- [203] D.S. Salem, M.A. Sliem, M. El-Sesy, S.A. Shouman, Y. Badr, Improved chemo-photothermal therapy of hepatocellular carcinoma using chitosan-coated gold nanoparticles, *J. Photochem. Photobiol. B Biol.* 182 (Oct. 2018) 92–99, <https://doi.org/10.1016/j.jphotobiol.2018.03.024>.
- [204] S. Valastyan, R.A. Weinberg, Tumor metastasis: molecular insights and evolving paradigms, *Cell* 147 (2) (Oct. 2011) 275–292, <https://doi.org/10.1016/j.cell.2011.09.024>.
- [205] I. Fierascu, C.I. Fierascu, I.R. Brazdis, M.A. Baroi, T. Fistos, C.R. Fierascu, Phytosynthesized metallic nanoparticles—between nanomedicine and toxicology. A brief review of 2019's findings, *Materials* 13 (3) (2020), <https://doi.org/10.3390/ma13030574>.
- [206] A. Syed, Extracellular biosynthesis of monodispersed gold nanoparticles, their characterization, cytotoxicity assay, biodistribution and conjugation with the anticancer drug doxorubicin, *J. Nanomed. Nanotechnol.* 4 (1) (2012) 1–6, <https://doi.org/10.4172/2157-7439.1000156>.
- [207] S. Malathi, M.D. Balakumaran, P.T. Kalaichelvan, S. Balasubramanian, Green synthesis of gold nanoparticles for controlled delivery, *Adv. Mater. Lett.* 4 (12) (2013) 933–940, <https://doi.org/10.5185/amlett.2013.5477>.
- [208] J.D. Gibson, B.P. Khanal, E.R. Zubarev, Paclitaxel-functionalized gold nanoparticles, *J. Am. Chem. Soc.* 129 (37) (Sep. 2007) 11653–11661, <https://doi.org/10.1021/ja075181k>.
- [209] Y. Wang, R. Xia, H. Hu, T. Peng, Biosynthesis, characterization and cytotoxicity of gold nanoparticles and their loading with N-acetylcarnosine for cataract treatment, *J. Photochem. Photobiol. B Biol.* 187 (2018) 180–183, <https://doi.org/10.1016/j.jphotobiol.2018.08.014>, July.
- [210] C. Krishnaraj, P. Muthukumaran, R. Ramachandran, M.D. Balakumaran, P. T. Kalaichelvan, Acalypha indica Linn: biogenic synthesis of silver and gold nanoparticles and their cytotoxic effects against MDA-MB-231, human breast cancer cells, *Biotechnol. Reports* 4 (Dec. 2014) 42–49, <https://doi.org/10.1016/j.btre.2014.08.002>.
- [211] S. Rajeshkumar, Anticancer activity of eco-friendly gold nanoparticles against lung and liver cancer cells, *J. Genet. Eng. Biotechnol.* 14 (1) (2016) 195–202, <https://doi.org/10.1016/j.jgeb.2016.05.007>.
- [212] V. Castro-Aceituno, et al., Pleuropteris multiflorus (Hasuo) mediated straightforward eco-friendly synthesis of silver, gold nanoparticles and evaluation of their anti-cancer activity on A549 lung cancer cell line, *Biomed. Pharmacother.* 93 (2017) 995–1003, <https://doi.org/10.1016/j.biopha.2017.07.040>.
- [213] J. Li, et al., Synergetic approach for simple and rapid conjugation of gold nanoparticles with oligonucleotides, *ACS Appl. Mater. Interfaces* 6 (19) (Oct. 2014) 16800–16807, <https://doi.org/10.1021/am504139d>.
- [214] R. Emmanuel, M. Saravanan, M. Ovais, S. Padmavathy, Z.K. Shinwari, P. Prakash, Antimicrobial efficacy of drug blended biosynthesized colloidal gold nanoparticles from Justicia glauca against oral pathogens: a nanoantibiotic approach, *Microb. Pathog.* 113 (October) (2017) 295–302, <https://doi.org/10.1016/j.micpath.2017.10.055>.
- [215] K. V Katti, Renaissance of nuclear medicine through green nanotechnology: functionalized radioactive gold nanoparticles in cancer therapy—my journey from chemistry to saving human lives, *J. Radioanal. Nucl. Chem.* 309 (1) (2016) 5–14, <https://doi.org/10.1007/s10967-016-4888-0>.
- [216] W. Shen, et al., The potential clinical applications of radionuclide labeled/doped gold-based nanomaterials, *Radiat. Med. Prot.* 1 (4) (2020) 186–195, <https://doi.org/10.1016/j.radmp.2020.11.001>.
- [217] B. Seniwai, V.C. Thihe, S. Singh, T.C.F. Fonseca, L. Freitas de Freitas, Recent advances in brachytherapy using radioactive nanoparticles: an alternative to seed-based brachytherapy, *Front. Oncol.* 11 (2021), <https://doi.org/10.3389/fonc.2021.766407>.
- [218] N. Chanda, et al., Radioactive gold nanoparticles in cancer therapy: therapeutic efficacy studies of GA-198AuNP nanoconstruct in prostate tumor-bearing mice, *Nanomed. Nanotechnol. Biol. Med.* 6 (2) (2010) 201–209, <https://doi.org/10.1016/j.nano.2009.11.001>.
- [219] K.C.L. Black, et al., Radioactive 198Au-doped nanostructures with different shapes for in vivo analyses of their biodistribution, tumor uptake, and intratumoral distribution, *ACS Nano* 8 (5) (2014) 4385–4394, <https://doi.org/10.1021/nn406258m>.
- [220] J. Jeon, Review of therapeutic applications of radiolabeled functional nanomaterials, *Int. J. Mol. Sci.* 20 (9) (2019), <https://doi.org/10.3390/ijms20092323>.
- [221] D.E. Berning, K.V. Katti, C.L. Barnes, W.A. Volkert, A.R. Ketrang, Chemistry in environmentally benign media. 7.(1) chelating hydroxymethyl-functionalized bisphosphines as building blocks to water-soluble and in-vitro-stable gold(I) complexes. Synthesis, characterization, and X-ray crystal structures of [Au{(HOH)(2)C(2)P, *Inorg. Chem.* 36 (13) (Jun. 1997) 2765–2769.
- [222] J.N. Bryan, et al., Gum Arabic-coated radioactive gold nanoparticles cause no short-term local or systemic toxicity in the clinically relevant canine model of prostate cancer, *Int. J. Nanomed.* 9 (October) (2014) 5001–5011, <https://doi.org/10.2147/IJN.S67333>.
- [223] M. Khoobchandani, K. Katti, A. Maxwell, W.P. Fay, K.V. Katti, Laminin receptor-avid nanotherapeutic EGCg-AuNPs as a potential alternative therapeutic approach to prevent restenosis, *Int. J. Mol. Sci.* 17 (3) (2016), <https://doi.org/10.3390/ijms17030316>.
- [224] M. Khoobchandani, A. Zambre, K. Katti, C.-H. Lin, K.V. Katti, Green nanotechnology from brassicaceae, *Int. J. Green Nanotechnol.* 1 (Jan. 2013), <https://doi.org/10.1177/1943089213509474>, 194308921350947.
- [225] S.M. Weakley, et al., Ginkgolide A-gold nanoparticles inhibit vascular smooth muscle proliferation and migration in vitro and reduce neointimal hyperplasia in a mouse model, *J. Surg. Res.* 171 (1) (Nov. 2011) 31–39, <https://doi.org/10.1016/j.jss.2011.03.018>.
- [226] M.-K. Yeh, et al., Improving anticancer efficacy of (-)-epigallocatechin-3-gallate gold nanoparticles in murine B16F10 melanoma cells, *Drug Des. Dev. Ther.* 8 (May 2014) 459, <https://doi.org/10.2147/DDDT.S58414>.
- [227] E.W. Holy, et al., Laminin receptor activation inhibits endothelial tissue factor expression, *J. Mol. Cell. Cardiol.* 48 (6) (Jun. 2010) 1138–1145, <https://doi.org/10.1016/j.yjmcc.2009.08.012>.
- [228] M.K. Khan, et al., Fabrication of {198Au0} radioactive composite nanodevices and their use for nanobrachytherapy, *Nanomed. Nanotechnol. Biol. Med.* 4 (1) (Mar. 2008) 57–69, <https://doi.org/10.1016/j.nano.2007.11.005>.
- [229] O.S. Muddineti, B. Ghosh, S. Biswas, Current trends in using polymer coated gold nanoparticles for cancer therapy, *Int. J. Pharm.* 484 (1–2) (Apr. 2015) 252–267, <https://doi.org/10.1016/j.ijpharm.2015.02.038>.
- [230] N.A. Hanan, et al., Cytotoxicity of plant-mediated synthesis of metallic nanoparticles: a systematic review, *Int. J. Mol. Sci.* 19 (2018), <https://doi.org/10.3390/ijms19061725>, 6.
- [231] X.D. Zhang, et al., Toxicologic effects of gold nanoparticles in vivo by different administration routes, *Int. J. Nanomed.* (2010), <https://doi.org/10.2147/IJN.S8428>.
- [232] Y. Pan, et al., Size-dependent cytotoxicity of gold nanoparticles, *Small Weinheim an der Bergstrasse Ger* 3 (11) (2007) 1941–1949, <https://doi.org/10.1002/sml.200>.
- [233] L. Dong, et al., Cytotoxicity of BSA-stabilized gold nanoclusters: in vitro and in vivo study, *Small* 11 (21) (2015) 2571–2581, <https://doi.org/10.1002/sml.201403481>.
- [234] S. Dhar, V. Mali, S. Bodhankar, A. Shiras, B.L.V. Prasad, V. Pokharkar, Biocompatible gellan gum-reduced gold nanoparticles: cellular uptake and subacute oral toxicity studies, *J. Appl. Toxicol.* 31 (5) (2011) 411–420, <https://doi.org/10.1002/jat.1595>.
- [235] S.K. Surapaneni, S. Bashir, K. Tikoo, Gold nanoparticles-induced cytotoxicity in triple negative breast cancer involves different epigenetic alterations depending upon the surface charge, *Sci. Rep.* 8 (1) (2018) 1–12, <https://doi.org/10.1038/s41598-018-30541-3>.
- [236] I.M.M. Paino, V.S. Marangoni, R. de C.S. de Oliveira, L.M.G. Antunes, V. Zucolotto, Cyto and genotoxicity of gold nanoparticles in human hepatocellular carcinoma and peripheral blood mononuclear cells, *Toxicol. Lett.* 215 (2) (2012) 119–125, <https://doi.org/10.1016/j.toxlet.2012.09.025>.
- [237] P. Wang, X. Wang, L. Wang, X. Hou, W. Liu, C. Chen, Interaction of gold nanoparticles with proteins and cells, *Sci. Technol. Adv. Mater.* 16 (3) (2015) 34610, <https://doi.org/10.1088/1468-6996/16/3/034610>.
- [238] R. Kumar, R. Ramani, D. Organisation, M. Sastry, Intracellular Synthesis of Gold Nanoparticles by a Novel Alkotolerant Actinomycetes , *Rhodococcus Species Intracellular Synthesis of Gold Nanoparticles by a Novel Alkalotolerant Actinomycete , Rhodococcus Species*, 2003, <https://doi.org/10.1088/0957-4484/14/7/323>, June 2014.
- [239] A. Ahmad, S. Senapati, M.I. Khan, R. Kumar, M. Sastry, Extracellular biosynthesis of monodisperse gold nanoparticles by a novel extremophilic actinomycete , *thermomonospora sp*, *Langmuir* 15 (2003) 3550–3553.
- [240] L. Du, E. Wang, Biosynthesis of Gold Nanoparticles Assisted by Escherichia coli DH5 a and its Application on Direct Electrochemistry of Hemoglobin, vol. 9, 2007, pp. 1165–1170, <https://doi.org/10.1016/j.elecom.2007.01.007>.
- [241] S. He, Z. Gua, Y. Zhang, S. Zhang, J. Wang, N. Gu, Biosynthesis of gold nanoparticles using the bacteria *Rhodospseudomonas capsulata*, *Mater. Lett.* 61 (2007) 3984–3987, <https://doi.org/10.1016/j.matlet.2007.01.018>.
- [242] Y. Nangia, N. Wangoo, N. Goyal, G. Shekhawat, C.R. Suri, A Novel Bacterial Isolate *Stenotrophomonas Maltophilia* as Living Factory for Synthesis of Gold Nanoparticles, vol. 7, 2009, pp. 1–7, <https://doi.org/10.1186/1475-2859-8-39>.

- [243] K. Kalishwaralal, et al., Colloids and Surfaces B : biointerfaces Biosynthesis of silver and gold nanoparticles using *Brevibacterium casei*, Colloids Surf. B Biointerfaces 77 (2) (2010) 257–262, <https://doi.org/10.1016/j.colsurfb.2010.02.007>.
- [244] P. Mukherjee, S. Senapati, Extracellular Synthesis of Gold Nanoparticles by the Fungus *Fusarium Oxysporum*, vol. 5, 2002, pp. 461–463.
- [245] A. Ahmad, S. Senapati, M.I. Khan, R. Kumar, M. Sastry, Extra-/intracellular biosynthesis of gold nanoparticles by an alkalotolerant fungus, *Trichothecium* sp., J. Biomed. Mater. Res. 1 (2005) 47–53, <https://doi.org/10.1166/jbn.2005.012>.
- [246] A. Mishra, S.K. Tripathy, R. Wahab, S. Jeong, Microbial Synthesis of Gold Nanoparticles Using the Fungus *Penicillium brevicompactum* and Their Cytotoxic Effects against Mouse Mayo Blast Cancer C 2 C 12 Cells, 2011, pp. 617–630, <https://doi.org/10.1007/s00253-011-3556-0>.
- [247] X. Zhang, et al., Colloids and Surfaces A : physicochemical and Engineering Aspects Biogenic synthesis of gold nanoparticles by yeast *Magnusiomyces ingens* LH-F1 for catalytic reduction of nitrophenols, Colloids Surfaces A Physicochem. Eng. Asp. 497 (2016) 280–285, <https://doi.org/10.1016/j.colsurfa.2016.02.033>.
- [248] A. Chauhan, et al., Fungus-mediated biological synthesis of gold nanoparticles : potential in detection of liver cancer, Int. J. Nanomed. 6 (2011) 2305–2319.
- [249] S.K. Das, C. Dickinson, F. Lafir, D.F. Brougham, E. Marsili, Synthesis, characterization and catalytic activity of gold nanoparticles biosynthesized with *Rhizopus oryzae* protein extract, Green Chem 14 (5) (2012) 1322–1334, <https://doi.org/10.1039/c2gc16676c>.
- [250] B. Sharma, D. Dhar, S. Hazra, L. Gogoi, Biosynthesis of gold nanoparticles using a freshwater green alga, *Prasiola crispata*, Mater. Lett. 116 (2014) 94–97, <https://doi.org/10.1016/j.matlet.2013.10.107>.
- [251] M. Esselen, S.W. Barth, Food-borne topoisomerase inhibitors: risk or benefit, in: *Advances in Molecular Toxicology*, vol. 8, Elsevier, 2014, pp. 123–171.
- [252] H. Wei, R. Bowen, Q. Cai, S. Barnes, Y. Wang, Antioxidant and antipromotional effects of the soybean isoflavone genistein, Proc. Soc. Exp. Biol. Med. 208 (1) (1995) 124–130, <https://doi.org/10.3181/00379727-208-43844>.
- [253] Y. Akiyama, S. Eda, K. Katō, K. Kato, Gum Arabic is a kind of arabinogalactan–protein, Agric. Biol. Chem. 48 (1) (1984) 235–237, <https://doi.org/10.1080/00021369.1984.10866126>.
- [254] M.E. Ebada, Cuminaldehyde: a potential drug candidate, J. Pharmacol. Clin. Res. 2 (2) (2017) 555585, <https://doi.org/10.19080/JPCR.2017.02.555585>.
- [255] H.-S. Lee, Cuminaldehyde: aldose reductase and α -glucosidase inhibitor derived from *Cuminum cyminum* L. seeds, J. Agric. Food Chem. 53 (7) (2005) 2446–2450, <https://doi.org/10.1021/jf048451g>.
- [256] R.K. Mohanty, S. Thennarasu, A.B. Mandal, Resveratrol stabilized gold nanoparticles enable surface loading of doxorubicin and anticancer activity, Colloids Surf. B Biointerfaces 114 (2014) 138–143, <https://doi.org/10.1016/j.colsurfb.2013.09.057>.
- [257] J.A. Baur, D.A. Sinclair, Therapeutic potential of resveratrol: the in vivo evidence, Nat. Rev. Drug Discov. 5 (6) (2006) 493, <https://doi.org/10.1038/nrd2060>.
- [258] A. Matkowski, P. Kus, E. Goralska, D. Wozniak, Mangiferin–a bioactive xanthonoid, not only from mango and not just antioxidant, Mini Rev. Med. Chem. 13 (3) (2013) 439–455. MPMC-EPUB-20121123-2 [pii].
- [259] X. Huang, H. Wu, X. Liao, B. Shi, One-step, size-controlled synthesis of gold nanoparticles at room temperature using plant tannin, Green Chem 12 (3) (2010) 395–399, <https://doi.org/10.1039/b918176h>.
- [260] A.V. Pereira, et al., Tannins obtained from medicinal plants extracts against pathogens: antimicrobial potential, Battle Against Microb. Pathog. Basic Sci. Technol. Adv. Educ. Programs, Formatex Res. Center, Badajoz 1 (2015) 228–235.
- [261] H. Mühlplfordt, The preparation of colloidal gold particles using tannic acid as an additional reducing agent, Cell. Mol. Life Sci. 38 (9) (1982) 1127–1128, <https://doi.org/10.1007/BF01955405>.
- [262] Y. Gao, et al., Multifunctional gold nanostar-based nanocomposite: synthesis and application for noninvasive MR-SERS imaging-guided photothermal ablation, Biomaterials (2015), <https://doi.org/10.1016/j.biomaterials.2015.05.004>.
- [263] K.H. Song, C. Kim, C.M. Cobley, Y. Xia, L.V. Wang, Near-infrared gold nanocages as a new class of tracers for photoacoustic sentinel lymph node mapping on a rat model, Nano Lett (2009), <https://doi.org/10.1021/nl802746w>.
- [264] X. Li, et al., Gold nanoparticles-based SPECT/CT imaging probe targeting for vulnerable atherosclerosis plaques, Biomaterials (2016), <https://doi.org/10.1016/j.biomaterials.2016.08.048>.
- [265] Q. Zhang, et al., Gold nanoparticles as a contrast agent for *in vivo* tumor imaging with photoacoustic tomography, Nanotechnology 20 (39) (Sep. 2009) 395102, <https://doi.org/10.1088/0957-4484/20/39/395102>.
- [266] C. Peng, et al., Facile formation of dendrimer-stabilized gold nanoparticles modified with diatrizoic acid for enhanced computed tomography imaging applications, Nanoscale 4 (21) (Nov. 2012) 6768–6778, <https://doi.org/10.1039/c2nr31687k>.
- [267] X. Chen, et al., Green synthesis of gold nanoparticles using carrageenan oligosaccharide and their in vitro antitumor activity, Mar. Drugs 16 (8) (2018) 277, <https://doi.org/10.3390/md16080277>.
- [268] A. Basu, et al., Evaluating the antimicrobial, apoptotic, and cancer cell gene delivery properties of protein-capped gold nanoparticles synthesized from the edible mycorrhizal fungus *Tricholoma crassum*, Nanoscale Res. Lett. 13 (2018), <https://doi.org/10.1186/s11671-018-2561-y>.
- [269] V. Malapermal, J.N. Mbatha, R.M. Gengan, K. Anand, Biosynthesis of Bimetallic Au-Ag Nanoparticles Using *Ocimum Basilicum* (L.) with Antidiabetic and Antimicrobial Properties, Oct. 2015.